

UCSF

UC San Francisco Electronic Theses and Dissertations

Title

Molecular Control of a Cell Cycle Event

Permalink

<https://escholarship.org/uc/item/9dd936bt>

Author

Lyons, Nicholas Anthony

Publication Date

2012

Peer reviewed|Thesis/dissertation

MOLECULAR CONTROL OF A CELL CYCLE EVENT

by

Nicholas Anthony Lyons

DISSERTATION

Submitted in partial satisfaction of the requirements for the degree of

DOCTOR OF PHILOSOPHY

in

BIOCHEMISTRY AND MOLECULAR BIOLOGY

in the

GRADUATE DIVISION

of the

UNIVERSITY OF CALIFORNIA, SAN FRANCISCO

ACKNOWLEDGEMENTS

Many people's paths have intersected mine and affected how I got to where I am today. First chronologically is of course my parents, Ken and Maureen, who not only gave me a good set of genes to become a scientist but also provided the best possible environment for those genes to be raised. Without their love and encouragement, I'm not sure how far I would have made it. I have had great scientific mentors too, and the greatest impact was made by Bob Malone when I was a naïve undergraduate. His close mentorship created a really good foundation for my future laboratory experience, and it was in his lab that I first realized what scientists *actually* do and how all the classes I had taken would in fact apply to my career. Bob's encouragement to shoot for the top is how I landed at UCSF (a school I didn't know I could get in to), and his love of teaching young scientists is something I plan to emulate when the tables are turned. The other major science mentor I've had is Dave Morgan, whose mentorship style meshes perfectly with my learning style. It has been here in his lab that I have experienced the most growth as a researcher, largely attributable to Dave's promotion of independence in his students. As stressful as it can be, learning to do things on one's own is the best way to really learn. It takes a lot of restraint for a PI to allow their lab to run this way, and it is one of Dave's qualities I will try to emulate myself. Lastly (and never leastly), I want to thank Ellen for all her help, feedback, encouragement, support, and most of all love. The future would be a lot more scary without her around, and I can't wait to see how the rest of our lives turn out.

Portions of this work have been published elsewhere, including Chapter 2 (Lyons and Morgan. (2011) *Mol. Cell* 42, 378-89.) and Chapter 3 (submitted to *Nat. Struct. Mol. Biol.*). The mass spectrometry presented in Chapter 3 was performed by Bryan Fonslow (with help from Jolene Dietrich), a great guy in the lab of John Yates III at Scripps.

MOLECULAR CONTROL OF A CELL CYCLE EVENT

Nicholas Anthony Lyons

ABSTRACT

Progression through the eukaryotic cell cycle occurs through an exact sequence of precisely coordinated events, culminating in the segregation of the duplicated copies of all the cellular components into two daughter cells. Crucial to the faithful execution of all the cellular events that must take place is the temporal separation of mutually exclusive enzyme activities. Controlling all these processes are a network of regulatory proteins, including a number of kinases and ubiquitin ligases, which ensure the proper sequence of events in every cycle. This thesis explores the control of one particular event in the cell cycle, establishment of sister-chromatid cohesion, using *Saccharomyces cerevisiae* as a model organism. Cohesion between chromatids is necessary to keep track of which pieces of DNA need to be separated to opposite daughter cells, and also has a function in the molecular recognition of readiness for anaphase. Cohesion establishment is restricted to S phase of a normal cycle and can be reactivated in metaphase upon DNA damage, but the basis for this regulation was unknown. I have found that the phosphorylation-mediated degradation of the cohesion-promoting protein Eco1 is responsible for the differential regulation of cohesion generation over time and in response to stress. Eco1 phosphorylation occurs by an interesting cascade of primed kinases: Cdk1 bound to B-type cyclins phosphorylates Eco1 at a site that creates a consensus motif for the kinase

Cdc7-Dbf4, whose activity in turn creates a consensus motif for Mck1, a homolog of the tumor-suppressor GSK-3. Only after all three kinases have phosphorylated Eco1 is it targeted for ubiquitination by SCF-Cdc4. This is because the substrate adapter Cdc4 only binds degrons with precisely-spaced diphosphates. The combination of all these factors is necessary to degrade Eco1 and shut off establishment of new cohesion, setting up a system in which inhibition of any one regulatory component (by cell cycle progression or DNA damage for instance) can initiate cohesion generation. This complex regulation reflects the depths to which evolutionary forces are capable of selecting, magnified by the importance of properly segregating the genetic material from which all the cell cycle machinery arise.

TABLE OF CONTENTS

Preface:

Acknowledgements	iii
Abstract	v
List of tables	viii
List of figures	ix

Chapter 1: 1

Introduction

Chapter 2: 8

Cdk1-Dependent Destruction of Eco1 Prevents Cohesion Establishment After S phase

Chapter 3: 53

Sequential Primed Kinases Create a Damage-Responsive Phosphodegron on Eco1 to Control Sister-Chromatid Cohesion

Chapter 4: 99

Conclusion

Bibliography 110

LIST OF TABLES**Chapter 2**

Table S1	52
----------	----

Chapter 3

Table S1	96
----------	----

Table S2	97
----------	----

LIST OF FIGURES

Chapter 1

Figure 1	7
----------	---

Chapter 2

Figure 1	41
----------	----

Figure 2	42
----------	----

Figure 3	43
----------	----

Figure 4	44
----------	----

Figure 5	45
----------	----

Figure 6	46
----------	----

Figure 7	47
----------	----

Supplemental Figure 1	48
-----------------------	----

Supplemental Figure 2	49
-----------------------	----

Supplemental Figure 3	49
-----------------------	----

Supplemental Figure 4	50
-----------------------	----

Supplemental Figure 5	51
-----------------------	----

Chapter 3

Figure 1	86
----------	----

Figure 2	87
----------	----

Figure 3	88
----------	----

Figure 4	89
Figure 5	90
Figure 6	91
Figure 7	92
Supplemental Figure 1	93
Supplemental Figure 2	95
Chapter 4	
Figure 1	107
Figure 2	108

CHAPTER 1: INTRODUCTION

The eukaryotic cell cycle is simply two things: duplication of all cellular content, followed by segregation of each duplicate copy to the daughter cells. Underlying this apparent simplicity is a vast regulatory network that ensures every process necessary to duplicate the cellular contents occurs in the correct time and space—every time.

A nice description of this comes from the book, *The Major Transitions in Evolution* (63), in which the cell cycle is described as “the organization of gene action in time”. This quote succinctly describes three key aspects of the cell cycle: “organization” refers to the regulatory network that organizes the myriad biochemical activities, or “gene actions”, required to duplicate a cell, which is complex enough to incorporate the fourth dimension, “time”, a feature commonly seen in systems like circadian rhythms and metazoan development.

Videos of cells going through the division cycle are impressive, displaying complicated cellular movements and coordinated behaviors at the microscopic scale. In fact, the cell cycle is a classic example (along with chemotaxis and apoptosis) of a collection of molecular actions that is easily anthropomorphized. Commonly used words in the field include “want”, “decide”, and “prepare”. Words like these are useful informally, but disguise the underlying truth: cells are essentially bags of highly concentrated chemicals. Confined within a lipid-based membrane are thousands of complex macromolecules interacting with each other chemically and physically. They do so in such a highly coordinated and organized way, however, that the molecular

interactions collectively produce emergent properties and complex behaviors to which we can ascribe human qualities.

A good illustration of the relationship between emergent properties and the biochemical components that produce them are photo mosaics. These are pictures made up of pixels that are themselves smaller pictures. On a large scale mosaics form one big image, but on closer inspection are in fact collections of smaller images—the smallest actual pixel size forms a picture that becomes a larger pixel for another picture. Photo mosaics therefore exist on two separate levels. Likewise, the cell cycle is a series of individual biochemical reactions (small pixels) that collectively produce events like the metaphase to anaphase transition (large pixels) that constitute the cycle. Like the mosaic, the cell cycle exists on two separate levels, and natural selection can act on both levels: the biochemical traits of an enzyme as well as the efficiency of progression through the events of the cycle.

A key requirement of these sorts of systems (photo mosaics and cell cycles) is the correct placement of each constituent component within the overall picture. Moving a pixel (small or large) from one area of the mosaic to another disrupts the coherence of the larger image—the eye is immediately drawn to the mistake. Likewise, a biochemical event occurring at an inappropriate time in the cell cycle (as in the work described in this thesis) disrupts the overall flow of the cycle and will thus be selected against over long enough time. Thus the individual macromolecule components of the cell cycle, while obviously important, are not the full story. Of equal importance is the context in which each biochemical reaction occurs. The operative word in the above quote, then, is “organization”: the vast regulatory network is what makes the cell cycle run by ensuring

that each molecular event is properly ordered in space and time. This is ultimately what my dissertation is about: elucidating the biochemical mechanisms that regulate cellular processes during the cell cycle.

Because this concept of regulation is so central to the cell cycle (and this thesis), I will further emphasize its importance with another analogy. The reported empirical formula of the human body is $H_{2.5E9}O_{9.7E8}C_{4.9E8}N_{4.7E7}P_{9.0E6}Ca_{8.9E6}K_{2.0E6}Na_{1.9E6}S_{1.6E6}Cl_{1.3E6}Mg_{3.0E5}Fe_{5.5E4}F_{5.4E4}Zn_{1.2E4}Si_{9.1E3}Cu_{1.2E3}B_{7.1E2}Cr_{98}Mn_{93}Ni_{87}Se_{65}Sn_{64}I_{60}Mo_{19}Co_{17}V$ (107). If all of these chemical elements were combined in the indicated stoichiometries, would it produce a human being? Of course not, but the real question is: what is the difference between the chemicals listed above and a human being? The difference is regulation—in the human, each element was put in the proper place at the proper time during development. Each atom had to be carefully ordered and controlled over the course of embryogenesis to produce such a complex organism from so simple a chemical formula.

A similar question can be posed with regard to the cell cycle: if you recapitulate every molecular process required to duplicate a cell *in vitro*, would the system cycle? Again no, but partly for the simple reason that many cell cycle events are mutually exclusive and must be kept separated in time (70). For example, DNA polymerase cannot be both primed for initiation (characterized by low levels of phosphorylation by Cdk1) and actively polymerizing DNA (high amount of Cdk1 phosphorylation); the two states are chemically incompatible. Similarly, as will be seen in Chapter 2 and 3 of this thesis, sister chromatids would never get linked together if separase were active during S phase to cleave all newly-established cohesion. The key is to temporally regulate opposing

activities, confining establishment activity to S phase and separase activity to anaphase. Thus, both the activity of enzymes and their proper coordination are essential for cell viability, and as a result there will be strong selection to increase its effectiveness, leading to the highly intricate control system seen today.

Since regulation of the diverse number of cellular states is so critical, the regulatory network behind it must be correspondingly complex. The cell cycle machinery can be loosely organized into tiers (Figure 1): “top-players”, such as Cdk1, coordinating the large-scale structure of the cycle; “executor” proteins like the anaphase-promoting complex and transcription factors are regulated by top-players and translate the regulatory information to the cellular processes; and finally the nuts and bolts, the chemical events themselves directly responsible for cell duplication, such as the cohesin ring. The arrangement is not strict, as many top-players also directly coordinate the biochemical machinery (33), and the regulation of executors by top-level regulators is often reciprocal. The activities of top-players oscillate with (and help cause) cell cycle phases, but can also respond to non-genetic inputs like extracellular signals and internal stress. The stress response is transmitted to lower executor proteins, which decode the information by altering their biochemical activities and can act as hubs of regulation onto which multiple signals converge. I will present data in this thesis supporting the role of Eco1 as an executor in the cohesion-generation pathway, integrating several top-level inputs from both the normal cell cycle and the response to DNA damage.

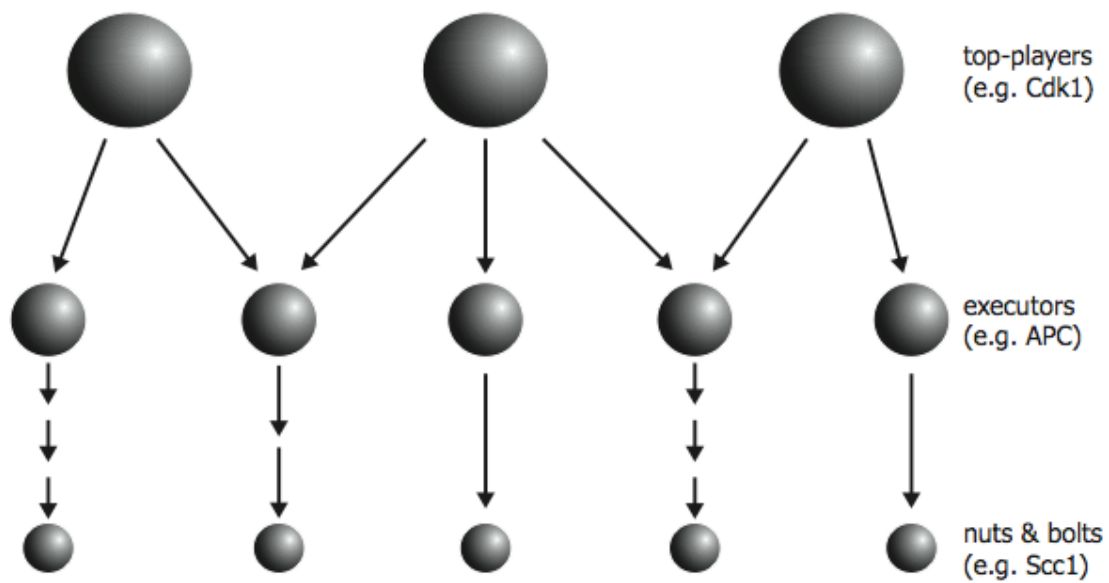
The structure of regulatory networks depicted in Figure 1 transmits signals from the top through multiple tiers to ultimately exert an effect on cellular behavior. The more tiers a signal passes through the more opportunities for different inputs to affect that

process, increasing the ability of the cell to adapt to environmental variation (for a great example, see the cohesion pathway, Chapter 4 Figure 1). Regulatory proteins are therefore highly modular, presumably facilitating the evolution of highly interconnected regulatory systems like the cell cycle and metazoan development.

How does the cell cycle regulatory system actually carry out this impressive degree of control? It turns out that every stage of the central dogma is subject to intense regulation: transcription, mRNA stability, translation, and post-translational modifications to protein activities (33,93,109), further illustrating the advantage of having multiple tiers responsive to different inputs. Regulation of the above stages is often accomplished by chemical modification of macromolecules, usually by covalent attachment of specific moieties (e.g. phosphates, acetyl groups, methyl groups, ubiquitins, fatty-acids, carbohydrates) to amino acids side chains. These chemical moieties are analogous to bits of information that are by themselves meaningless, but in the right context can be decoded into a change in cell physiology. Large-scale surveys of post-translational modifications, such as Cdk1-dependent phosphorylations (33), can give a broad indication of the types of processes affected by a certain enzyme, but merely knowing that a protein is chemically modified is not enough—more important is how that moiety is interpreted into a meaningful output. Unfortunately this step is much more labor-intensive, but deciphering the means by which top-level regulators convey specific information to the executor proteins has been the primary motivation behind my dissertation.

The specific process I have chosen in order to investigate how the cell cycle machinery achieves such a high level of organization is the establishment of sister-

chromatid cohesion in *Saccharomyces cerevisiae*. In Chapter 1, I demonstrate that generation of cohesion is limited to S phase of the cell cycle by phosphorylation-mediated degradation of the cohesion establishment factor Eco1. In Chapter 2 this is expanded upon to more fully flesh out the mechanisms of Eco1 phosphorylation and degradation, revealing an extremely complex degree of regulation that so far includes three separate kinases and precise substrate discrimination by a ubiquitin ligase. In all, these experiments establish Eco1 as a regulatory hub that integrates multiple inputs to precisely coordinate cohesion generation with global cellular events.

Figure 1

CHAPTER 2: CDK1-DEPENDENT DESTRUCTION OF ECO1 PREVENTS COHESION ESTABLISHMENT AFTER S PHASE

This chapter was previously published as reference (59) in the Bibliography.

SUMMARY

Accurate genome segregation depends on cohesion mechanisms that link duplicated sister chromatids, thereby allowing their tension-dependent biorientation in metaphase. In *Saccharomyces cerevisiae*, cohesion is established during DNA replication when Eco1 acetylates the cohesin subunit Smc3. Cohesion establishment is restricted to S phase of the cell cycle, but the molecular basis of this regulation is unknown. Here we show that Eco1 is negatively regulated by the protein kinase Cdk1. Phosphorylation of Eco1 after S phase targets it to SCF^{Cdc4} for ubiquitination and subsequent degradation. A nonphosphorylatable mutant of Eco1 establishes cohesion after DNA replication, suggesting that Cdk1-dependent phosphorylation of Eco1 is a key factor limiting establishment to S phase. We also show that deregulation of Eco1 results in chromosome separation defects in anaphase. We conclude that this regulatory mechanism helps optimize the level of sister chromatid cohesion, ensuring a robust and efficient anaphase.

INTRODUCTION

The accurate transfer of genetic information to the next generation is necessary for the propagation of life. Multiple mechanisms therefore exist in the cell division cycle to ensure proper duplication and segregation of chromosomes (70). Following DNA replication in S phase, sister chromatid pairs are bioriented on the mitotic spindle, with one sister attached to each pole. Biorientation requires a means of discerning which chromatids are sisters; a mechanism has therefore evolved to hold sister chromatids together from S phase to mitosis (73,76,111). When sister chromatid pairs are attached to microtubules from opposite poles, sister-chromatid cohesion resists the spindle forces pulling the chromatids apart. The resulting tension is used both to strengthen microtubule attachments and as a readout for the spindle assembly checkpoint, which delays anaphase until correct biorientation is achieved. When all chromosomes are correctly bioriented, sister-chromatid cohesion is removed, allowing sisters to separate and be pulled apart by the spindle.

Sister-chromatid cohesion depends primarily on a protein complex called cohesin. In *Saccharomyces cerevisiae*, the core components of this complex are Smc1, Smc3, Scc1/Mcd1, and Scc3 (73,76,111). Smc1 and Smc3 are large coiled-coil proteins of the highly conserved 'Structural Maintenance of Chromosomes' (SMC) family. These two subunits form a large ring structure that is linked tightly at one end by globular hinge domains, and at the other end by the Scc1 subunit, together with Scc3. At the onset of anaphase, cleavage of Scc1 by the protease separase opens the ring, resulting in cohesin dissociation and thus sister separation (113).

Sister-chromatid cohesion is achieved in two steps: cohesin loading and establishment. Beginning in G1 and continuing throughout the cell cycle, cohesin is constitutively loaded onto chromosomes by a poorly understood mechanism that requires the proteins Scc2 and Scc4 (12). Loaded cohesin appears to have a low affinity for chromosomes (22) and is thus unable to hold sister chromatids together. As the chromosomes are duplicated in S phase, sister chromatid cohesion is 'established' when a fraction of the loaded cohesin molecules is converted into a form that tightly links the newly formed sister chromatids, providing cohesion that can resist the forces of the spindle (91,108,112).

Among the many proteins known to be required for cohesion establishment, the best understood is the highly conserved acetyltransferase Eco1/Ctf7 (36,91,108). Eco1 promotes cohesion by acetylating the cohesin subunit Smc3 during S phase. Smc3 acetylation appears to counteract an 'anti-establishment' activity of the cohesin-associated proteins Wpl1/Rad61 and Pds5, as mutation of either of these proteins renders Eco1 non-essential for viability (83,84,100,115,128).

The establishment of cohesion is tightly regulated both spatially and temporally. In a normal cell cycle, establishment is strictly confined to S phase; cohesin loaded onto chromatin in a metaphase-arrested cell is not able to establish cohesion (26,112). The restriction of establishment to S phase is believed to depend in part on the recruitment of Eco1 to the replication fork by the processivity clamp PCNA (52,69,83). However, association with the replication fork cannot be the only factor limiting cohesion establishment, since certain mutants (such as *wpl1Δ*) are able to establish cohesion post-

replication (30), suggesting that the necessary components are present after S phase but are somehow inhibited.

Indeed, cohesion can also be established after S phase in cells experiencing DNA damage (95,96,116). Damage-induced cohesion is necessary for efficient DNA repair (90,96,114) and genetic evidence suggests that it might be established by acetylation of the Scc1 subunit of cohesin by Eco1, which antagonizes the inhibitory activity of Wpl1 (30). The S phase and damage acetylation marks appear to be distinct, as neither is able to compensate for loss of the other at the appropriate stage (30).

Despite its critical role in the control of sister chromatid cohesion, the regulation of Eco1 is largely unexplored. In HeLa cells, Esco1 and Esco2 are known to undergo post-translational changes during the cell cycle: chromatin-bound Esco1 is phosphorylated during mitosis, and Esco2 levels are reduced from G2 through the end of M phase (34). In *Xenopus laevis*, Eco1 and Eco2 are phosphorylated upon entry into mitosis, and Eco2 is ubiquitinated in late mitosis by the ubiquitin ligase APC^{Cdh1} (49). The functions of these regulatory events are not known. Intriguingly, over-expression of Eco1 allows yeast cells to establish cohesion in metaphase (116), suggesting that Eco1 activity is a limiting factor for post-replicative cohesion establishment, and that Eco1 is somehow inhibited after S phase.

The tight coupling of cohesion establishment to the cell cycle suggests that a cell cycle component regulates Eco1 activity. Indeed, yeast Eco1 is known to be a target of the cyclin-dependent kinase Cdk1, a key regulator of cell cycle progression (110), and mutations that reduce Cdk1 activity are synthetically lethal with an *eco1* mutation (8). However, mutation of the four Cdk1 consensus phosphorylation sites in Eco1 does not

affect cell viability or sensitivity to DNA-damaging agents (8), and thus the role of Cdk1 in Eco1 regulation is not clear.

Here, we demonstrate that Cdk1-dependent phosphorylation of Eco1 from late S phase through mitosis leads to its degradation. This helps limit the establishment of cohesion to S phase, as stabilization of Eco1, either through mutation of its Cdk1 sites or activation of the DNA damage pathway, permits ectopic establishment of cohesion in metaphase. Finally, we show that anaphase progression is defective in cells that fail to decrease Eco1 activity after S phase, illustrating the importance of this regulation for robust chromosome segregation.

RESULTS

Phosphorylation of Eco1 by Cdk1

Cdk1 has previously been implicated in Eco1 regulation *in vitro* (110) and in genetic studies (8). However, mutation of the four Cdk1 consensus phosphorylation motifs in Eco1 (the *ECO1-4A* mutant, see Figure S1A) has no apparent effect on cell viability or DNA damage sensitivity (8). Given that Eco1 activity is limiting in metaphase (116), when Clb-Cdk1 activity is highest, we speculated that Cdk1 phosphorylation is inhibitory and that Eco1-4A is therefore overactive. This could explain why *ECO1-4A* cells display no obvious phenotype, as overexpression of Eco1 has no detectable effect on viability (7). Also, overactive Eco1 might be genetically equivalent to *wpl1Δ*, which also has no viability defect (83,100).

According to these arguments, a constitutively phosphorylated form of Eco1 should be less active and therefore more likely to display a phenotype, since Eco1 is essential. In an attempt to test this, we constructed a ‘phosphomimic’ version of Eco1 in which the Cdk1 consensus sites were mutated to aspartate or glutamate (*ECO1-4D*) to imitate the negative charge of the phosphorylated state. This mutant, like *ECO1-4A*, displayed neither a loss of viability nor a genetic interaction with mutation of the spindle checkpoint (*mad2Δ*, Figure 1A), which is known to enhance the phenotype of Eco1 loss-of-function mutants (see Figure 1C below).

Development of a Phosphomutant Fusion Approach

Our negative results with the *ECO1-4D* mutant illustrate a common problem in the study of phosphoregulation: no amino acid substitution can perfectly mimic a phosphorylated residue. To address this problem, we developed a method for rapidly creating proteins that are constitutively phosphorylated (or dephosphorylated) *in vivo*. We modified the target substrate to include a kinase or phosphatase fused to the C-terminus (Figure 1B) to promote constant phosphorylation or dephosphorylation, respectively. To direct the phosphorylation of Cdk1 sites, we fused target proteins to the G1 cyclin Cln3, which recruits Cdk1. For the phosphatase fusion we used the mouse protein Cdc14B, a homolog of a yeast phosphatase, Cdc14, that is known to specifically dephosphorylate Cdk1 consensus motifs (24). To reduce the impact of ectopic regulation on the substrate, both fused proteins were truncated versions lacking localization and degradation motifs (24,72).

We designed the fusions to be attached to the end of a tandem affinity purification (TAP) tag, to provide a flexible linker between the substrate and enzyme. The availability of a library of yeast strains with every ORF tagged with a TAP tag (23) allows this fusion technique to be applied to any protein using the same DNA construct, facilitating the rapid creation of large numbers of different phosphomutants. In addition, to allow the study of lethal mutants, a *loxP-STOP-loxP* system with a galactose-inducible Cre recombinase was used to allow conditional generation of the protein fusions (Figure 1B; see more detailed diagram in Figure S1B).

In pilot experiments with numerous Cdk substrates, we found that cellular levels of substrate proteins were greatly reduced, to widely varying degrees, by the integration of the fusion construct, even prior to Cre induction of the fusion (data not shown). Although we were unable to solve this problem, we could control for the effects of protein levels by analysis of additional mutants: in the case of cyclin fusions, mutation of Cdk1 consensus phosphorylation sites in the substrate should reduce the phenotype, and for phosphatase fusions, the phenotype should be reduced by mutation of the catalytic cysteine, C314, in Cdc14B.

Constitutive Phosphorylation Inhibits Eco1 Function

We used the fusion technique to address the phosphoregulation of Eco1 by Cdk1. Fusion of the phosphatase Cdc14B to Eco1 (*ECO1-PPase*) had no effect on cell viability, while fusion to Cln3 (*ECO1-kinase*) caused a severe growth defect (Figure 1C). The kinase fusion, but not the phosphatase fusion, was expressed at very low levels (data not shown). Importantly, the viability defect in *ECO1-kinase* cells was reduced by mutation of the

four Cdk1 consensus phosphorylation sites in Eco1 (*ECO1-4A-kinase*), implying that the defect was due in part to the phosphorylation state of the fused substrate and not simply to nonspecific disruption of Eco1 function or abundance.

The growth defect of the *ECO1-kinase* strain was also reduced by deletion of *WPL1*, mutation of which is known to rescue loss-of-function mutants such as the temperature-sensitive mutant *eco1-G211D* (*eco1-1*, Figure 1C) (83). This result, along with the observation that the kinase fusion is heterozygous recessive (Figure 1C), suggested that the constitutively phosphorylated form of Eco1 is inactive. Indeed, *ECO1-kinase* cells phenocopied the metaphase arrest seen in *eco1-1* cells (Figure 2A). This metaphase accumulation was reduced by mutation of the four Cdk1 sites in Eco1, *wpl1Δ*, or heterozygosity (Figure 2A). The arrest was due to activation of the spindle checkpoint, as *ECO1-kinase mad2Δ* double mutants lacking a functional checkpoint did not arrest and were synthetically sick (Figures 1C, 2A), indicative of a cohesion loss mutant (91).

To directly test the effect of phosphorylation on Eco1 cohesion establishment activity, we performed sister chromatid cohesion assays using a *ura3::lacO₂₅₆, GFP-LacI* strain, which contains a GFP dot at a specific chromosomal locus. In a metaphase arrest, properly joined sister chromatids display a single GFP focus, while loss of cohesion results in two separate foci. *ECO1-kinase* cells showed a marked loss of cohesion, to the same extent as *eco1-1* cells at the restrictive temperature (Figure 2B). This effect was rescued by mutation of the four phosphorylation sites or deletion of *WPL1*. Interestingly, *wpl1Δ* did not rescue the loss of cohesion in *eco1-1* cells at the restrictive temperature (Figure 2B), as seen in previous studies with *eco1Δ* cells (83,84,100), perhaps indicating that *WPL1* deletion does not fully compensate for a severe loss of *ECO1* function, and

that the kinase fusion retains a low level of activity. Consistent with this possibility, deletion of *WPL1* rescued the metaphase arrest in *eco1-1* cells at a permissive temperature (Figure 2A), where Eco1-1 possesses a small amount of acetyltransferase activity (84).

All *ECO1-kinase* phenotypes were absent in the *ECO1-4D* mutant, demonstrating the usefulness of the fusion technique for uncovering effects that cannot be detected using traditional phosphomimics.

Cdk1 Phosphorylates Eco1 *in vivo*

Our results suggest that Eco1 function in the cell is inhibited by phosphorylation at one or more of its four Cdk1 consensus sites. We next confirmed that these sites are targets of Cdk1 *in vitro* and *in vivo*. As in our previous work (56,110), we found that purified Eco1 is phosphorylated *in vitro* by purified complexes of Cdk1 with the S-phase cyclin Clb5 or the M-phase cyclin Clb2 (Figure 3A). This phosphorylation was abolished by the 4A mutations, indicating that Cdk1 phosphorylates one or more of these sites *in vitro*.

Eco1 was phosphorylated at equivalent rates by Clb2-Cdk1 and Clb5-Cdk1, after normalization for activity toward a general substrate, histone H1 (Figure 3A). Because the intrinsic activity of Clb5-Cdk1 is ten-fold lower than that of Clb2-Cdk1 (56), normalization for general activity requires the use of at least ten-fold more Clb5-Cdk1 protein. Thus, Eco1 behaves like a general Cdk1 substrate that is expected to be poorly phosphorylated in S phase by Clb5-Cdk1 and more effectively phosphorylated by Clb2-Cdk1 in mitosis.

We next confirmed that the Cdk1 sites on Eco1 are phosphorylated *in vivo*. We found that Eco1 from metaphase cells, but not from G1 cells, displayed a mobility shift on an SDS-PAGE gel supplemented with a phosphate-binding reagent (Figure 3B) (41). This shift was abolished in the *ECO1-4A* mutant, demonstrating that Eco1 in mitotic cells is phosphorylated at one or more of the Cdk1 consensus sites.

Studies of additional point mutants revealed that the phosphate-dependent gel mobility shift was not affected by mutation to alanine of the first two Cdk1 sites in the Eco1 sequence (*ECO1-2A-1*; see Figure S1A) but was abolished by mutation of the nearby third and fourth sites (*ECO1-2A-2*) (Figure 3C). Thus, the mobility shift is caused by phosphorylation at the third and/or fourth sites. Given that phosphorylation does not always result in mobility shifts, these results do not rule out phosphorylation at the first two sites; indeed, results discussed below clearly support phosphorylation at these sites.

Phosphorylation Promotes Eco1 Degradation

We noticed that the steady-state levels of Eco1-4A and 2A proteins in metaphase were higher than those of the wild-type protein (Figures 3B, C), suggesting that phosphorylation causes a decrease in Eco1 abundance. If so, Eco1 levels should drop at cell cycle stages where Cdk1 activity is high. Indeed, there is previous evidence that Eco1 levels oscillate in the cell cycle (7,108). To address whether these oscillations are due to phosphorylation by Cdk1, we measured Eco1 and Eco1-4A levels in cells progressing synchronously through the cell cycle (Figure 3D). Upon release from a G1 arrest, levels of wild-type Eco1 rose slightly at the G1/S transition and dropped in late S phase through mitosis. Entry into S phase was accompanied by partial phosphorylation, which became

more complete as Clb2 levels rose just before mitosis. This timing of phosphorylation is consistent with the biochemical data above (Figure 3A). Levels of Eco1 declined as peak mitotic Clb2 levels were reached. Eco1-4A levels did not oscillate but simply accumulated throughout the time course, suggesting that phosphorylation by Clb2-Cdk1 promotes the decrease in Eco1 levels after S phase.

ECO1 mRNA levels oscillate slightly during the cell cycle, peaking in early S phase (93). It was therefore possible that oscillations in Eco1 protein levels are due in part to variations in transcription rates. However, cells in which the *ECO1* promoter was replaced with that of the constitutively-transcribed *CYCI* gene still showed a difference in protein levels between asynchronous and metaphase-arrested cultures, and this difference depended on the presence of Cdk1 sites (Figure S2). Thus, cell cycle variation in Eco1 levels depends primarily on post-transcriptional mechanisms.

We next tested whether phosphorylation affects Eco1 stability. We measured the half-life of Eco1 in metaphase-arrested cells, using cycloheximide to inhibit new protein synthesis (Figure 4A). Wild-type Eco1 was rapidly degraded in metaphase-arrested cells, with a half-life of about 20 minutes. Eco1-4A was greatly stabilized, demonstrating that degradation depends on phosphorylation by Cdk1. Inhibition of the proteasome also stabilized Eco1 (Figure 4B), implying that phosphorylated Eco1 is targeted for destruction by the proteasome.

Based on our kinase assays *in vitro* (Figure 3A), together with the correlation between Clb2 levels and the decline in Eco1 levels during the cell cycle (Figure 3D), we propose that the primary regulator of Eco1 abundance is the Clb2-Cdk1 complex (and perhaps complexes of Cdk1 with the other late cyclins Clb1, 3, and 4). Our results with

Eco1-2A mutants further suggest that Eco1 must be phosphorylated at multiple sites to be degraded. Interestingly, gel mobility shifts in our cell cycle experiments indicate that Eco1 is partially phosphorylated starting at the beginning of S phase, long before it is degraded. It seems likely that this partial phosphorylation is catalyzed by the relatively low activity of Clb5-Cdk1 and is not sufficient for degradation. Consistent with this possibility, the Eco1-2A-1 mutant is stabilized despite undergoing a mobility shift (Figure 3C), indicating that phosphorylation of the third and/or fourth Cdk1 sites causes a mobility shift without causing degradation. The degradation of Eco1 therefore resembles that of the Cdk inhibitor Sic1, which is degraded only when phosphorylated at multiple sites (71).

Eco1 Destruction Depends on SCF^{Cdc4}

The interplay of phosphorylation and ubiquitin-mediated degradation is a common theme in cell cycle regulation. For instance, many Cdk1 substrates are also substrates of the ubiquitin ligase SCF, a modular complex that employs F-box adaptor subunits to target different substrates for ubiquitination (122). The only F-box protein essential for cell cycle regulation in budding yeast is Cdc4, which is required for the ubiquitination of the Cdk1 inhibitors Sic1 and Far1, the DNA replication factor Cdc6, and the transcription factor Swi5 (38). Although SCF^{Cdc4} activity is constant throughout the cell cycle, it is only known to recognize phosphorylated substrates, allowing protein destruction to be coordinated with cell cycle events.

Because Eco1 degradation requires both phosphorylation and proteasome activity (Figure 4A, 4B), we hypothesized that Eco1 is an SCF substrate. We initially attempted

to measure Eco1 half-life in temperature-sensitive SCF mutants, but found that Eco1 is intrinsically thermolabile independent of its phosphorylation state (Figure S3). We therefore constructed a strain in which *CDC4* was placed under the control of the dextrose-repressible *GALS* promoter, allowing us to conditionally turn off SCF^{Cdc4} activity. When we arrested cells in metaphase and shut off *CDC4* expression, Eco1 was stabilized to a similar degree as Eco1-4A (Figure 4C). Phosphorylated Eco1 accumulated in the presence of MG132 and in a *CDC4* shutoff (Figure 4D), consistent with the model of phosphorylation-mediated degradation. The increased abundance of Eco1 in the absence of Cdc4 was not due to an indirect effect caused by stabilization of the Cdk1 inhibitor Sic1, as Eco1 was equally stabilized and phosphorylated when *CDC4* was shut off in a *sic1Δ* background (Figure 4D). Our earlier finding that degradation requires multiple phosphorylation sites (Figure 3C) is also consistent with Eco1 being a substrate of SCF^{Cdc4}, as recognition of many Cdc4 substrates requires multiple phosphates (27,71).

Nuclear Localization of Eco1 Enhances Its Degradation

Eco1 is known to interact during S phase with the DNA replication clamp PCNA, and this interaction depends on a PCNA-interacting motif ('PIP box', QxKL; Figure S1A) near the N-terminus of Eco1 (69). Deletion of the N-terminal 32 residues (*eco1-Δ32*, Figure 5A), including the PIP box, was previously shown to abolish the PCNA interaction and cause an increase in Eco1 levels (69). To investigate further the role of the N-terminal region in protein stability, we tested the effects of a series of mutations in this region. Mutations of the N-terminus are lethal (Figure S4) (69), so experiments were performed in a suppressing *wpl1Δ* background, which does not affect Eco1 stability or

localization (data not shown). Deletion of the N-terminal 32 residues resulted in complete protein stabilization, consistent with the previous study, while deletion of just the PIP box (*eco1- Δ PIP*) conferred partial stabilization (Figure 5B).

We wondered what other features of the N-terminus might be contributing to degradation. Using a recently developed method (46), we found that residues 4-36 of Eco1 contain a potential bipartite nuclear localization signal (NLS; Figure 5A, S1A). To verify this, we deleted the first 13 residues of Eco1, comprising half of the predicted NLS (*eco1- Δ 13*), and examined its subcellular localization. While Eco1, Eco1-4A and Eco1- Δ PIP all appeared constitutively nuclear, Eco1- Δ 32 and Eco1- Δ 13 were present in both the cytoplasm and nucleus (Figure 5C). This localization defect was rescued by addition of an ectopic NLS (from the SV40 Large T antigen) to the N-terminus of these mutants (*NLS-eco1- Δ 32* and *NLS-eco1- Δ 13*; Figure 5C). The ectopic NLS also rescued the lethality of the *eco1- Δ 13* mutation (Figure S4), demonstrating that Eco1 nuclear localization is essential for viability.

Deletion of just the NLS (the Eco1- Δ 13 mutant) stabilized the protein to the same extent as Eco1- Δ 32 (Figure 5B). Attachment of the SV40 NLS to Eco1- Δ 13 and Eco1- Δ 32 restored the normal rapid rate of degradation (Figure 5B), suggesting that the stability of these mutants is due entirely to their localization defect. We also tested whether deletion of the PIP box, which contains basic residues within the NLS, has a subtle effect on localization despite appearing mostly nuclear. Addition of an ectopic NLS to Eco1- Δ PIP decreased its stability (Figure 5B), implying that this mutant does have a slight localization defect and that binding to PCNA is not contributing significantly to Eco1 destruction. Both *eco1- Δ 32* and *eco1- Δ PIP* mutants are inviable

(Figure S4) and are not rescued by forcing nuclear localization with the SV40 NLS. This shows that PCNA binding is essential beyond the contribution of the PIP box residues to subcellular localization, as suggested previously (69).

The dependence of Eco1 degradation on nuclear localization is consistent with Eco1 being a substrate of SCF^{Cdc4}, as Cdc4 is entirely nuclear (6,79). Consistent with this, all N-terminal mutants displayed a gel mobility shift in a metaphase arrest, and this shift depended on their Cdk1 sites (Figure 5D). Thus, the stabilization conferred by these mutants is downstream of Cdk1 phosphorylation, likely at the level of SCF recognition.

Eco1 Degradation Prevents Post-Replication Cohesion Establishment

We hypothesized that the degradation of Eco1 upon Cdk1 phosphorylation provides an explanation for previous evidence that limited Eco1 activity prevents cohesion establishment after S phase (116). Cells expressing the nonphosphorylatable Eco1 mutant should therefore be competent to establish cohesion even after DNA replication. To test this, we assayed cohesion establishment in metaphase-arrested cells by modifying a previously published approach (Figure 6A) (116) to avoid the use of high temperatures, due to Eco1 thermolability (Figure S3). In this assay, cells establish cohesion in S phase with a version of Scc1 containing a TEV protease recognition site (Scc1-TEV) and are then arrested in metaphase with nocodazole. Expression of wild-type Scc1 (without a TEV site) is then induced, followed by induction of TEV protease to dissolve pre-established S phase cohesion, leaving only the metaphase-expressed cohesin to hold sister chromatids together. The readout for establishment of cohesion is the same as that used in Figure 2B: GFP-tagged chromosomes appearing as one or two foci.

In otherwise wild-type cells, which cannot establish new cohesion in metaphase, induction of TEV resulted in an increased frequency of chromatid separation (Figure 6B). Strikingly, we found that cells expressing Eco1-4A were able to establish cohesion in a metaphase-arrested cell, to the same extent as a *wpl1* Δ positive control (30) and dependent on the expression of metaphase cohesin. These results demonstrate that Cdk1 activity towards Eco1 helps limit the establishment of cohesion after replication.

DNA Damage Stabilizes Eco1

Double-strand DNA breaks are known to trigger cohesion establishment outside of S phase (95,96,116). Given that the reactivation of cohesion establishment after damage depends on Eco1 (116), we wondered whether DNA damage affects Eco1 stability. Indeed, Eco1 levels were markedly increased in cells treated with the DNA damaging agents 4-nitroquinoline 1-oxide (4-NQO, a UV mimetic), zeocin (which generates DNA breaks), or the ribonucleotide reductase inhibitor hydroxyurea (HU, which induces replication stress) (Figure 6C). Analysis of Eco1 half-life confirmed that Eco1 was dramatically stabilized in HU-arrested cells (Figure 6D).

This stabilization occurred despite the fact that DNA damage triggers a mitotic arrest with high Clb2-Cdk1 activity. Indeed, we found that Eco1 was extensively phosphorylated at Cdk1 sites in damage arrests (Figure 6C). Thus, Eco1 is stabilized after DNA damage despite being phosphorylated at the destabilizing Cdk1 sites. We conclude that upon DNA damage, ubiquitination of phospho-Eco1 by SCF is somehow prevented, thereby allowing the establishment of new, replication-independent cohesion.

Excess Cohesion in *ECO1-4A* Cells Leads to Anaphase Defects

Our studies reveal a mechanism that appears to limit the establishment of excess sister-chromatid cohesion by reducing Eco1 activity after S phase, a mechanism that can also be circumvented when extra cohesion is desirable (i.e. after DNA damage). We next sought to understand the importance of this mechanism by determining whether Eco1-4A, by generating excess cohesion, causes defects in sister chromatid behavior during anaphase.

If Eco1-4A generates excess cohesion, then anaphase defects might occur in cells with a reduced ability to remove cohesin. However, we found that there is only a minor genetic interaction between the *ECO1-4A* mutation and a temperature-sensitive separase mutant (*esp1-2*) at the permissive temperature (Figure 7A). Thus, the low separase activity in these cells seems sufficient to remove any increased cohesion in *ECO1-4A* cells. We next hypothesized that a spindle checkpoint delay would allow *ECO1-4A* cells to accumulate higher levels of cohesion that are less readily removed by separase. Indeed, we observed a subtle but reproducible synthetic defect in *esp1-2 ECO1-4A* cells growing in the presence of the spindle poison benomyl (Figure 7A).

Although *ECO1-4A* cells appear normal in crude assessments of colony growth, we wanted to use a more refined approach to test the possibility that these cells exhibit anaphase defects that do not result in gross viability problems. Our approach was to use a single-cell microscopy assay to measure the synchrony of sister chromatid separation (32). This method employs a yeast strain with *lacO* arrays at two loci, *TRP1* and *URA3*, 12 and 35 kilobases from the centromeres of chromosomes IV and V, respectively (note that this is a different strain from that used in our previous studies; see supplemental

experimental procedures for details). Expression of LacI-GFP in these cells generates GFP foci on two different chromosomes, and the time between the separation of the two chromosomes provides an indication of the synchrony of sister chromatid separation. Our previous work indicated that this method provides a useful measure of the rates of separase activation and cohesin cleavage (32).

In a wild-type background, the two GFP foci separated almost simultaneously during anaphase, with a mean time of about 5 seconds between chromatid separation events (Figures 7B, S5). A hypomorphic mutant of separase (*esp1-2*) increased the mean time between separations by over an order of magnitude (Figure 7B, S5), presumably because a decreased rate of cohesin cleavage prolongs anaphase, resulting in greater differences in the time at which each sister pair is separated.

Most importantly, *ECO1-4A* cells showed a significant four-fold increase in the average time between chromatid separation events (Figure 7B). This increased average resulted from a skewing of the distribution of separation times towards longer intervals (Figure S5). We observed many *ECO1-4A* cells in which the second chromosome separated well over 40 seconds after the first, a phenomenon that was also seen in *esp1-2* but never in wild-type cells. These data are consistent with the idea that unregulated Eco1 activity leads to excess cohesion, which delays but does not completely disrupt anaphase progression.

A combination of *ECO1-4A* and *esp1-2* mutations resulted in a severe loss of anaphase synchrony, with chromosome separation times on the scale of minutes (Figures 7B, S5). We observed many *ECO1-4A esp1-2* cells in which neither chromosome had separated but both were repeatedly pulled back and forth between poles, possibly

reflecting the initiation of late anaphase spindle dynamics prior to full cleavage of cohesin. Thus, despite the near-normal growth of *ECO1-4A esp1-2* cells on plates (Figure 7A), the timing and robustness of sister chromatid separation is clearly compromised, illustrating that proper cohesion regulation is important for the precise coordination of anaphase events.

DISCUSSION

The cycle of sister chromatid cohesion is tightly woven into the fabric of the cell division cycle. In this study we demonstrate the direct regulation of cohesion establishment by the master cell cycle regulator Cdk1. Our results suggest that Clb2-Cdk1-dependent phosphorylation of Eco1 from late S phase to mitosis targets nuclear Eco1 for ubiquitination by SCF^{Cdc4} and subsequent degradation by the proteasome. This reduces the amount of Eco1 acetyltransferase activity below some threshold required to establish cohesion, which, together with reduced *ECO1* transcription in G1 (93), prevents the establishment of new cohesion until DNA replication occurs in S phase of the next cell cycle. In cells containing a nonphosphorylatable Eco1, or upon activation of the DNA damage response, Eco1 is stabilized and cohesion can be established in metaphase.

The regulation of cohesion establishment, like that of all critical processes, is a finely tuned balance of opposing positive and negative influences. In this case, the acetyltransferase activity of Eco1 during DNA replication facilitates the establishment of

sister chromatid cohesion. In metaphase, however, Cdk1 kinase activity inhibits Eco1, allowing the anti-establishment activities of Wpl1 and Pds5 to predominate, thus preventing establishment after replication. By modulating the positive input (establishment), Cdk1 helps generate a level of chromosomal cohesion that is optimal for efficient sister chromatid separation in anaphase.

We uncovered the regulation of Eco1 by Cdk1 using a new method of creating constitutively phosphorylated mutants. Linking Cdk1 to Eco1 (via Cln3) inhibited Eco1 function, greatly reducing cell viability. Significantly, *ECO1-4D* did not mimic the phosphorylated state, revealing the usefulness of the fusion technique for detecting phenotypes that are not seen with traditional phosphomimics. The effect of Cdk1 phosphorylation on the majority of its substrates is unknown; the technique presented here, combined with previously created yeast library strains (23) and the recent identification of hundreds of Cdk1 substrates (33,110), could facilitate a better understanding of the role of Cdk1 in regulating cell cycle events.

Eco1 undergoes an interesting pattern of phosphorylation by Cdk1 over the cell cycle (Figure 3D). Given that Eco1 is not a Clb5-specific substrate (Figure 3A) (56), the phosphorylation seen in early S phase is likely to be incomplete. This partial phosphorylation might not be sufficient for degradation, given that Cdc4 only has appreciable affinity for multiply phosphorylated substrates. Instead, early phosphorylation by Clb5-Cdk1 may prime Eco1 to be rapidly phosphorylated when Clb2 activity rises in late S phase. It is also possible that phosphorylated Eco1 exists in S phase cells because some other mechanism prevents its degradation at that stage of the cell cycle.

In a cell experiencing double-strand DNA breaks (DSBs), new cohesion aids DNA repair and is established by the reactivation of Eco1 (90,96,114,116). This appears to occur by two separate mechanisms: the stabilization of Eco1 (Figure 6D) and the phosphorylation of Scc1 by Chk1 (29). Either mechanism is sufficient to establish cohesion in metaphase independent of DNA damage signaling (Figure 6B) (30). Once the mechanism of Eco1 stabilization in damage is elucidated, it will be possible to test whether stabilization, like Scc1 phosphorylation (29), is necessary for establishment of damage-induced cohesion. Interestingly, we found that Eco1 is stabilized not only after induction of DSBs, but also following inhibition of DNA replication with hydroxyurea (Figure 6D). Perhaps Eco1 stabilization facilitates cohesion establishment upon removal of replication stress.

The substrate of Eco1 during S phase is the Smc3 subunit of cohesin, whereas damage-induced Eco1 activity is thought to target the Scc1 subunit (30). It is likely that Eco1-4A also targets Scc1, since the metaphase cohesion that results from *ECO1* overexpression depends on lysines in Scc1, not Smc3 (30), and does not promote excess Smc3 acetylation (7). Mechanisms therefore exist to focus Eco1 activity on Smc3 in S phase and on Scc1 thereafter. The molecular basis of this selectivity is not known, although it seems likely that other factors, such as the replication fork or mitotic chromatin structure, influence the choice of targets. Structural changes in cohesin or cohesin-associated factors throughout the cell cycle are also possible. Interestingly, acetylation of Smc3 in S phase can occur even when Eco1 levels are severely reduced (10) or when replication is delayed until late S phase (4), possibly due to a high local concentration of Eco1 at the replication fork. Scc1 acetylation, on the other hand, is more

sensitive to enzyme concentration, as the degradation promoted by Cdk1 in mitosis is sufficient to prevent cohesion establishment at this stage.

Given that excess cohesion establishment activity is not grossly detrimental to yeast cell viability, why has an intricate system evolved to inhibit it? Since cells establish new genome-wide cohesion upon DNA damage, the cohesion removal system has likely developed a tolerance to some excess cohesion. This could be achieved by an excess of separase activity, for example. Indeed, we found that a reduction in separase activity (the *esp1-2* mutation) had little effect on the viability of *ECO1-4A* cells (Figure 7A).

However, we did observe defects in *ECO1-4A esp1-2* cells delayed in mitosis by the spindle checkpoint, suggesting that separase activity becomes limiting when *ECO1-4A* cells accumulate too much cohesion during a metaphase delay. Moreover, we observed a loss of sister separation synchrony in *ECO1-4A* cells that was greatly enhanced when *ECO1-4A* was combined with a separase mutation. Yeast cells have therefore evolved both an excess of separase activity and a mechanism to temporally inhibit cohesion establishment to ensure robust and efficient cohesion removal at the onset of anaphase.

The regulatory mechanism we uncovered might be conserved in other eukaryotes. Vertebrate homologs of Eco1 are phosphorylated during mitosis (34,49,75). The positions of Cdk1 consensus sites are not precisely conserved beyond the most closely related yeasts, but multiple Cdk1 motifs are present at some location in the N-terminus of most homologs. Given that the phosphorylation of Eco1 seems to serve only as an interaction motif for Cdc4, the exact position of the Cdk1 sites would be under less selective pressure to remain fixed through evolution (33). If the regulation of cohesion establishment in the cell cycle is conserved, it would be interesting to study the effect of

an Eco1 phosphomutant in organisms that use a prophase pathway to remove cohesion from chromosome arms prior to anaphase (98), as these cells may be more sensitive to persistent establishment activity. Additionally, because mutations in human Eco1 homologs have been implicated in certain cancers (58,85), it will also be important to pursue the intriguing possibility that defects in Eco1 regulation generate chromosomal instability and thereby facilitate tumor evolution.

EXPERIMENTAL PROCEDURES

General methods

Yeast strains were derivatives of S288C and are listed in Table S1, along with a list of plasmid constructs. Genetic manipulations were performed using standard techniques (55). Construction of kinase and phosphatase fusion proteins is described in Figure S1B. Cell cycle arrests were done with 20 mg/ml nocodazole, 10 mg/ml alpha factor, 200 mM hydroxyurea, 2 μ M 4-nitroquinoline 1-oxide, or 33 μ g/ml zeocin for 3 h at 30°C unless otherwise stated. All arrests were confirmed by flow cytometric analysis of DNA content. Protein half-lives were analyzed by addition of 100 μ g/ml cycloheximide. To inhibit proteasome activity, 100 mM MG132 was added to cells with a *PDR5* deletion to increase retention of the drug. For the *CDC4* shutoff experiment, cells were grown in YEP media containing 2% raffinose and 0.04% galactose, then treated with nocodazole for 1.5 h before the addition of 2% galactose or dextrose for 4 h to allow for complete turnover of Cdc4. To analyze Eco1 phosphorylation, resolving portions of SDS-PAGE gels were supplemented with 50 mM MnCl₂ and 10 mM Phos-tag reagent (41) made

using standard chemical techniques, with two-fold excess ammonium persulfate and TEMED.

Post-Replication Cohesion Assay

P_{SCC1}-scc1(TEV268)-HA₃:hphNT1:P_{SCC1}:natNT2:P_{MET25}-GFP-SCC1, trp1::TRP1:P_{GALI}-NLS-myc₆-TEV-NLS₂, ura3::lacO₂₅₆:LEU2, his3::P_{CUP1-1}-GFP-LacI:HIS3 strains were grown in YEP media plus 2% raffinose and arrested for 3 h in nocodazole. Cells were then washed and switched to synthetic media lacking methionine (plus nocodazole) for 1 h to induce wild-type Scc1, or kept in complete media to maintain Scc1 repression. Scc1(TEV) was then cleaved by the addition of 2% galactose to induce expression of TEV protease (or 2% dextrose to keep TEV repressed) for 2 h. 100 mM CuSO₄ was also added to fully induce expression of GFP-LacI.

Anaphase Synchrony Assay

ura3::lacO₂₅₆:LEU2, trp1::lacO₂₅₆:TRP1, his3::P_{CUP1-1}-GFP-LacI:HIS3 cultures were grown in synthetic media at room temperature in the presence of 100 mM CuSO₄ to mid-log phase. Cells were then affixed to slides using concanavalin A and imaged using a spinning disk confocal microscope. Images spanning about 4 microns in the z plane were taken every 2.5 s for 10-15 min, except *ECO1-4A esp1-2* images, which were taken every 10 s to allow longer movies (up to 28 min) without photobleaching.

Supplemental Experimental Procedures

Biochemical analyses

Cells were lysed by suspension in urea buffer (20 mM Tris-HCl pH 7.4, 7 M urea, 2 M thiourea, 4% CHAPS, 80 mM β -glycerophosphate, 50 mM NaF) and beadbeating using glass beads. Immunofluorescence microscopy was performed as described (97). Primary antibodies used were α -myc (1:1000, 9E10, Covance), α -PAP (1:5000, P 1291, Sigma), α -HA (1:1000, 12CA5, Roche), α -Cdk1 (1:1000, sc-53, Santa Cruz), α -Clb2 (1:200, y-180, Santa Cruz), and α -tubulin (1:500, YOL1/34, AbCam). Secondary antibodies conjugated to either horseradish peroxidase (GE Healthcare) or fluorophore (Li-Cor) were used at 1:10,000 dilutions. Fluorescent westerns were detected on an Odyssey scanner and quantified using ImageQuant and Prism software.

For analysis of Cdk1 kinase activity toward Eco1, bacterially-purified GST-Eco1 and GST-Eco1-4A were incubated with Clb2-Cdk1 and Clb5-Cdk1, purified as described from yeast (56) and normalized for activity towards the general substrate histone H1, with Clb2-Cdk1 approximately 15-fold less concentrated than Clb5-Cdk1. Reactions were performed in kinase buffer (25 mM HEPES pH 8, 15 mM NaCl, 1 mM MgCl₂) plus γ -³²P-ATP, stopped with SDS sample buffer, and analyzed by SDS-PAGE and autoradiography.

Cohesion Assay

Strains containing *ura3::lacO₂₅₆:LEU2*, *his3::P_{CUP1-1}-GFP-LacI:HIS3* were cultured in YPD media and arrested in metaphase with nocodazole. Temperature-sensitive strains were first arrested at room temperature with alpha factor, then inactivated by raising to

30° for 1 h, and finally released into a metaphase arrest using nocodazole. 100 μ M CuSO₄ was also added to fully induce expression of GFP-LacI. Cells were then fixed in 4% paraformaldehyde for 10 min, washed, and resuspended in PBS for mounting on poly-lysine-coated slides.

Anaphase Synchrony Assay

In our previous studies of anaphase synchrony (32), we used a strain carrying a *lacO*₂₅₆ array, labeled with LacI-GFP, at the *TRP1* locus of chromosome IV (94), plus a *tetO*₃₃₆ array, labeled with TetR-GFP, at the *URA3* locus of chromosome V (66). In otherwise wild-type cells, the TetR-GFP focus separated about 90 seconds after the LacI-GFP focus. Our recent work has revealed that the delayed separation of the TetR-GFP dot is due to abnormally strong cohesion at the *tetO* array (H. Eshleman and D.O.M., unpublished observations). For the current work, we constructed a new strain in which chromosomes were labeled with *lacO*₂₅₆ arrays inserted at both *TRP1* and *URA3* as described (82). Unlike the GFP foci in our previous work, the two foci in this strain separate at about the same time during anaphase.

ACKNOWLEDGEMENTS

We thank L. Holt for ideas and assistance with the phosphomutant fusions, S. Foster, F. Uhlmann, and G. Yaakov for comments on the manuscript, and F. Uhlmann, K. Shokat, D. Toczyski, and S. Gasser for strains and reagents. Spinning disk confocal microscopy

was performed with the valuable assistance of K. Thorn at the UCSF Nikon Imaging Center. This work was supported by funding from the National Institute of General Medical Sciences (GM069901).

FIGURE LEGENDS

Figure 1. Eco1 phosphomutant fusions reveal a phenotype of constitutive phosphorylation

(A) Three-fold serial dilutions of the indicated yeast strains were grown at 30°C on a YPD plate.

(B) Diagram of fusion protein method (see Figure S1B for details). After looping out the stop codon with the Cre recombinase, *ECO1-TAP* is attached to the kinase (*CLN3-1*), as shown here, or phosphatase (*MmCDC14B*).

(C) Three-fold serial dilutions of the indicated strains were grown at room temperature.

Figure 2. Phosphorylation inhibits the cohesion establishment function of Eco1

(A) Cells of the indicated genotype were grown asynchronously at room temperature and examined by immunofluorescence microscopy, staining for tubulin and DAPI. Cells were scored for cell cycle stage, defining a metaphase cell as large-budded with a single DNA mass and short bipolar spindles. Over 200 cells were counted in two independent experiments; error bars represent the standard error of the mean (SEM).

(B) Strains containing a GFP-tagged *URA3* locus were arrested in metaphase at 30°C using nocodazole, and scored for one GFP focus (maintenance of cohesion) or two foci (loss of cohesion). Over 200 metaphase-arrested cells were counted, and an average was calculated from two or three independent experiments; error bars represent SEM.

Figure 3. Phosphorylation in late S phase reduces Eco1 levels

(A) GST-Eco1 or GST-Eco1-4A, purified from bacteria, was incubated for the indicated times with purified Clb2-Cdk1 or Clb5-Cdk1 in the presence of γ -³²P-ATP, and analyzed by SDS-PAGE and autoradiography. Negative controls lacking phosphorylation sites (Eco1-4A), enzyme (–Cdk1), or substrate (–Eco1) were reacted for 30 min. Right panel shows activity toward the general substrate histone H1.

(B) Lysates from *ECO1-TAP* and *ECO1-4A-TAP* cells growing asynchronously (asy) or arrested in G1 with alpha factor (α F) or in mitosis with nocodazole (noc) were analyzed on an SDS-PAGE gel containing Phos-tag reagent to retard the mobility of phosphorylated protein, followed by western blotting for the TAP tag.

(C) Lysates from the indicated cells arrested in mitosis with nocodazole were analyzed on an SDS-PAGE gel containing Phos-tag reagent, followed by western blotting for the TAP tag.

(D) *ECO1-myc₁₃* and *ECO1-4A-myc₁₃* cells were arrested with alpha factor (α F), washed and released. Samples were removed at the indicated times for western blot analysis.

Wild-type Eco1 was also analyzed on a separate gel containing Phos-tag reagent.

Progression through the cell cycle was monitored by western blotting for Clb2, as well as

quantification of budding (entry into S phase) and anaphase binucleate formation (staining DNA with DAPI). Cdk1 was used as a gel loading control.

Figure 4. Eco1 is targeted for proteasomal destruction by SCF^{Cdc4}-mediated ubiquitination

(A) *ECO1-myc13* and *ECO1-4A-myc13* strains were arrested in nocodazole for 3 h, followed by addition of 100 mg/ml cycloheximide (CHX). Lysates were analyzed by western blotting using fluorophore-conjugated secondary antibodies, and the relative amount of protein at each timepoint was quantified and plotted at right.

(B) *ECO1-TAP pdr5Δ* and *ECO1-4A-TAP pdr5Δ* strains were arrested in nocodazole and treated with 100 mM MG132 (+) or DMSO (-) for 1 h before addition of 100 mg/ml cycloheximide. Samples were analyzed by standard western blotting.

(C) *ECO1-myc13* strains in which the endogenous *CDC4* was replaced with *P_{GALS}-HA₃-CDC4* were arrested in nocodazole and then supplemented with 2% dextrose or galactose to repress or activate *CDC4* expression, respectively. Cycloheximide was then added for the indicated time prior to sample removal for western blot analysis using fluorescent secondary antibodies.

(D) Lysates of nocodazole-arrested cells treated as in panels B and C were analyzed by Phos-tag-supplemented SDS-PAGE and western blotting.

Figure 5. Eco1 contains a functional NLS that is necessary for its degradation

(A) Diagram of known Eco1 protein domains; numbers indicate amino acid position. See Figure S1A for sequence of N-terminus.

(B) *ECO1-myc₁₃* strains containing the indicated N-terminal mutations were arrested in metaphase with nocodazole. After addition of cycloheximide (CHX) for the indicated times, lysates were analyzed by western blotting using fluorophore-conjugated secondary antibodies. All N-terminal truncations are *wpl1Δ*. ‘NLS’ indicates that the SV40 Large T antigen nuclear localization signal (PKKKRKVG) was inserted immediately after the start codon. Dark spots on the Cdk1 loading control are due to fluorescence of a molecular weight marker.

(C) Asynchronous *ECO1-myc₁₃* cultures were analyzed by immunofluorescence microscopy using antibodies to Myc and alpha-tubulin, and stained for DNA using DAPI. Images from mitotic cells are shown (based on cell and spindle morphology, and DNA mass separation), and are representative of all cell cycle stages. Bar = 1 μm.

(D) Lysates of nocodazole-arrested cells were analyzed by Phos-tag-containing SDS-PAGE and western blotting.

Figure 6. Unphosphorylated Eco1 can establish cohesion after S phase, and Eco1 is stabilized in the presence of DNA damage

(A) Experimental setup for measurement of cohesion establishment in metaphase.

Cohesion in these strains is established normally in S phase with Scc1(TEV). Cultures are arrested in metaphase, wild-type Scc1 is induced for 1 h, TEV is induced for 2 h, and cohesion of GFP-tagged chromatids is analyzed by microscopy.

(B) Cells were treated as indicated in panel A, and separation of sister chromatids was measured in over 200 metaphase cells in each of two experiments; bars indicate mean +/- SEM. Controls were included in which S-phase cohesion was not cleaved (-TEV) or

wild-type Scc1 was not induced in metaphase ($-Scc1^+$). The difference between WT and *ECO1-4A* is statistically significant ($P=0.004$); for all other differences, $P\leq 0.02$.

(C) Cultures of *ECO1-TAP* (WT) or *ECO1-4A-TAP* (4A) were treated with nocodazole (noc), hydroxyurea (HU), 4-nitroquinoline 1-oxide (4-NQO), or zeocin for 3 h. Lysates were analyzed by western blotting, using Phos-tag reagent to measure phosphorylation state.

(D) *ECO1-TAP* and *ECO1-4A-TAP* strains were arrested by treatment with nocodazole or hydroxyurea, and Eco1 half-life was analyzed by addition of CHX.

Figure 7. Unregulated Eco1 activity perturbs anaphase dynamics

(A) The indicated strains were serially diluted in 3-fold increments onto YPD or YPD plus 10 mg/ml benomyl at room temperature.

(B) Strains containing GFP-tagged *TRP1* and *URA3* loci on chromosomes IV and V, respectively, were grown asynchronously at room temperature, affixed to slides, and live single-cell microscopy movies were taken to monitor sister chromatid separation in cells passing through mitosis. Times between the separation of the two chromosomes were measured. Bars indicate mean \pm SEM. The table lists the values for each parameter. See Figure S5 for details.

Figure S1 (related to Figure 1). Diagrams of Eco1 protein and fusions

(A) Primary structure of Eco1, showing the amino acid sequence of the N-terminal region containing the putative NLS and PIP box (underlined). Positions of the four Cdk1

consensus phosphorylation sites are also shown, with the sequence of phosphorylation site mutants used in this study.

(B) Detailed diagram of fusion strategy and constructs. The integration construct contains homology to the 3' region common to all strains in the TAP library. After Cre induction, *ECO1* is fused in frame with the kinase (*CLN3-1*) or phosphatase (*MmCDC14B*). Fusion constructs were made using previously created Cre and *loxP* plasmids (25). The transcription termination sequence from *CYC1*, along with a *URA3* marker, were cloned between two *loxP* sequences. The *CLN3-1* cyclin allele is truncated at residue 403, before the PEST degradation sequences (72); the fragment of *MmCDC14B* contains residues 44-386 of the parent protein, lacking both nucleolar targeting and nuclear export signals (24). Both fusion ORFs are immediately followed by a termination sequence from the *TEF1* gene. After integration of the fusion construct and selection for *URA3*, a plasmid containing *P_{GALI}-Cre* was transformed into the cells, which were streaked on plates containing galactose to induce the recombinase. These colonies were then streaked on plates containing 5-fluoroorotic acid (5-FOA) to select for cells that recombined out *t_{CYC1}* and *URA3*.

Figure S2 (related to Figure 3). Variations in Eco1 protein level are independent of transcription

Strains with *ECO1-myc₁₃* expressed under its endogenous promoter (*P_{ECO1}*) or a constitutive low-expression promoter (*P_{CYC1}*) were grown asynchronously (asy) or arrested in mitosis with nocodazole (noc). Lysates were analyzed by western blotting for myc.

Figure S3 (related to Figure 4). Eco1 protein stability is affected by high temperature

ECO1-TAP and *ECO1-4A-TAP* strains were grown at room temperature and then arrested in nocodazole at the indicated temperature for 3.5 h. 100 mg/ml cycloheximide (CHX) was added and samples taken at the indicated times for western blotting analysis.

Figure S4 (related to Figure 5). The NLS and PIP box of Eco1 are essential for viability

Diploids heterozygous for both *wpl1Δ* and the indicated *ECO1* allele were sporulated and dissected at 30°C (restrictive temperature for *eco1-1*) to test for viability in a nonsuppressed (*WPL1*) background. Genotypes of representative tetrads are listed at right; gray lettering indicates the inferred genotype of dead spores. All N-terminal mutants also contain a myc₁₃ epitope tag at the C-terminus.

Figure S5 (related to Figure 7B). Timing of chromosome separation in anaphase

Histograms showing the times between separation of two marked chromosomes, in seconds, for the experiment summarized in Figure 7B. Note the difference in time scales in the two panels.

Figure 1

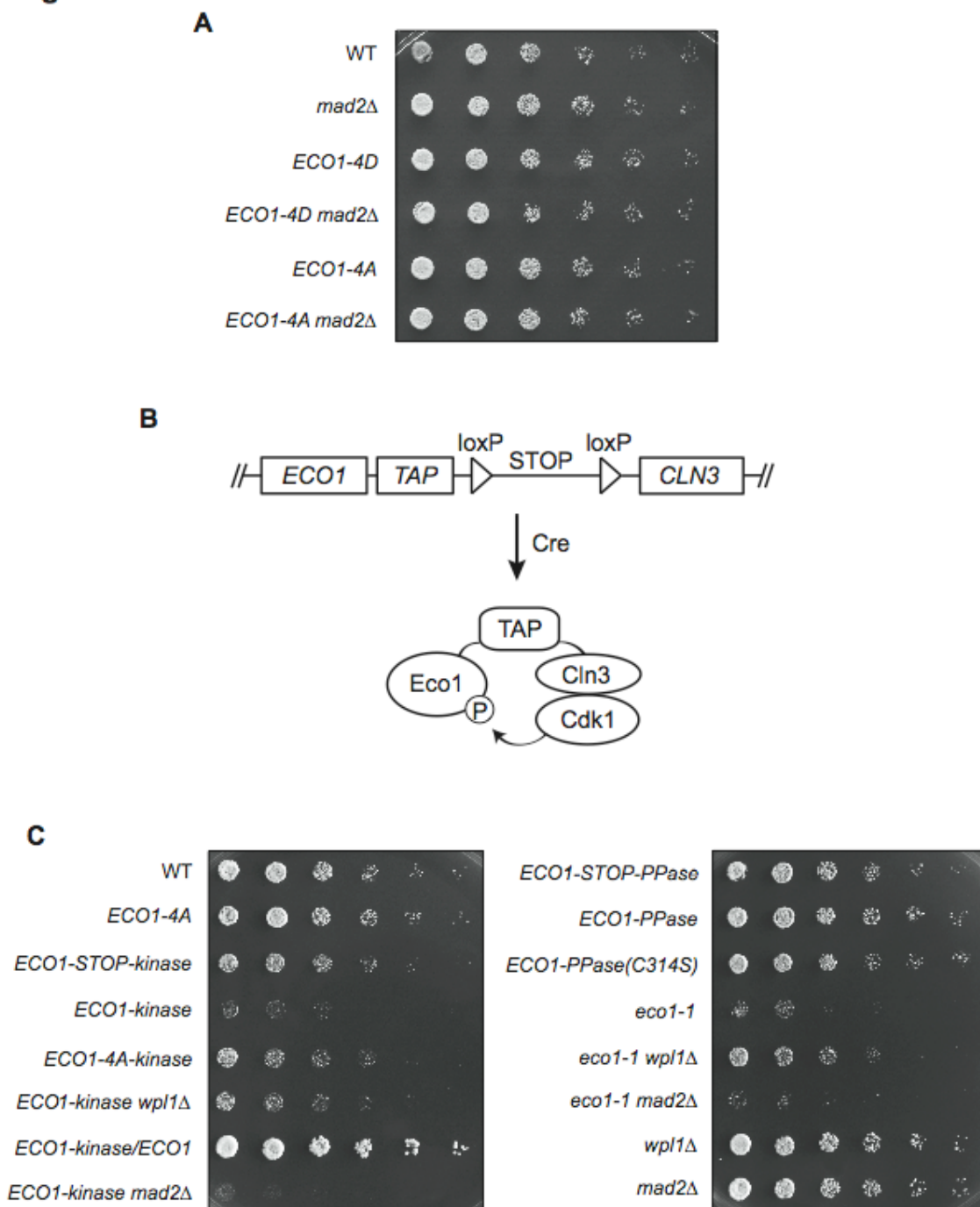
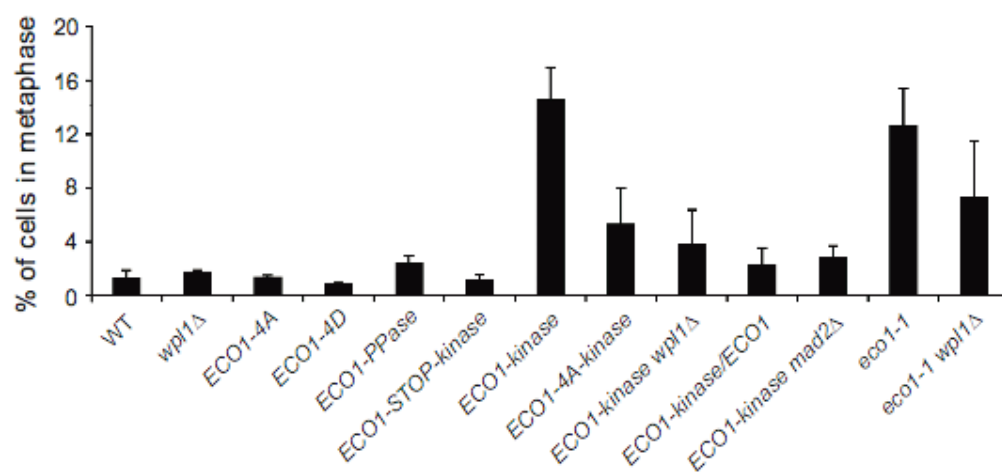


Figure 2

A



B

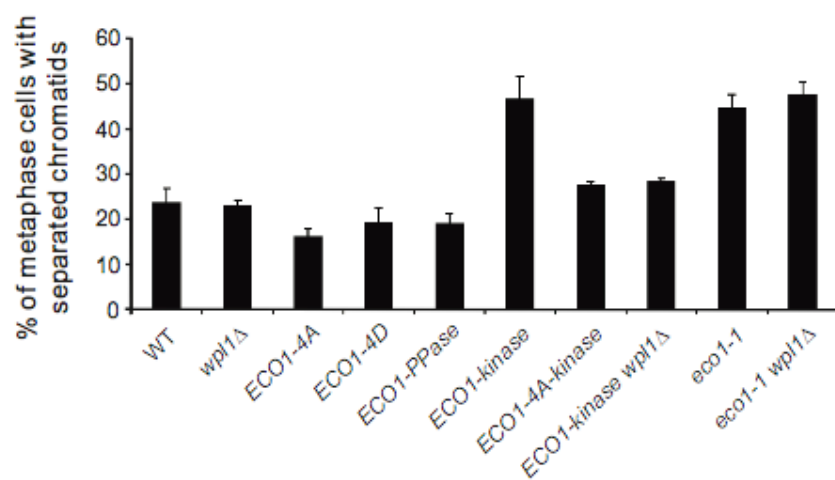


Figure 3

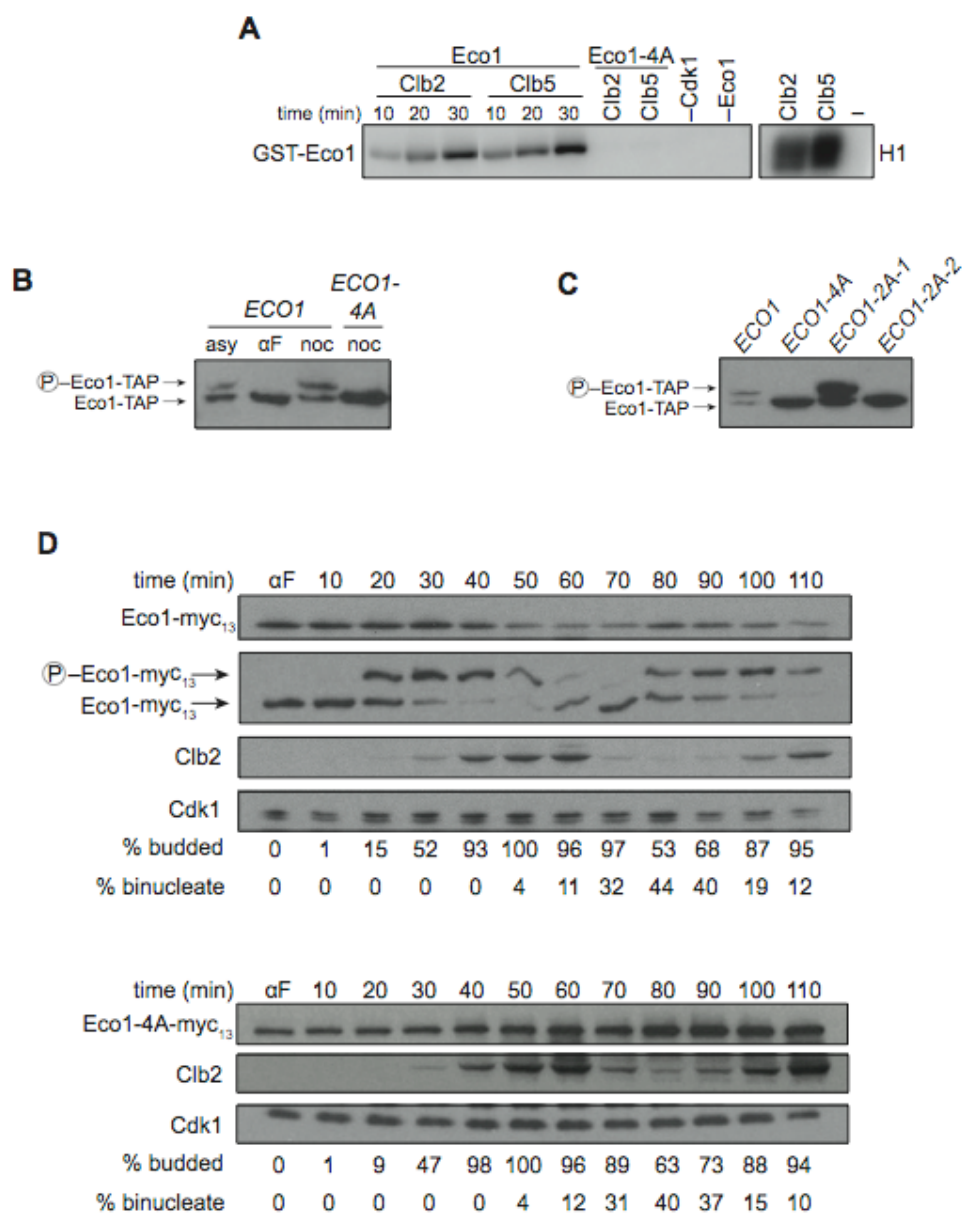


Figure 4

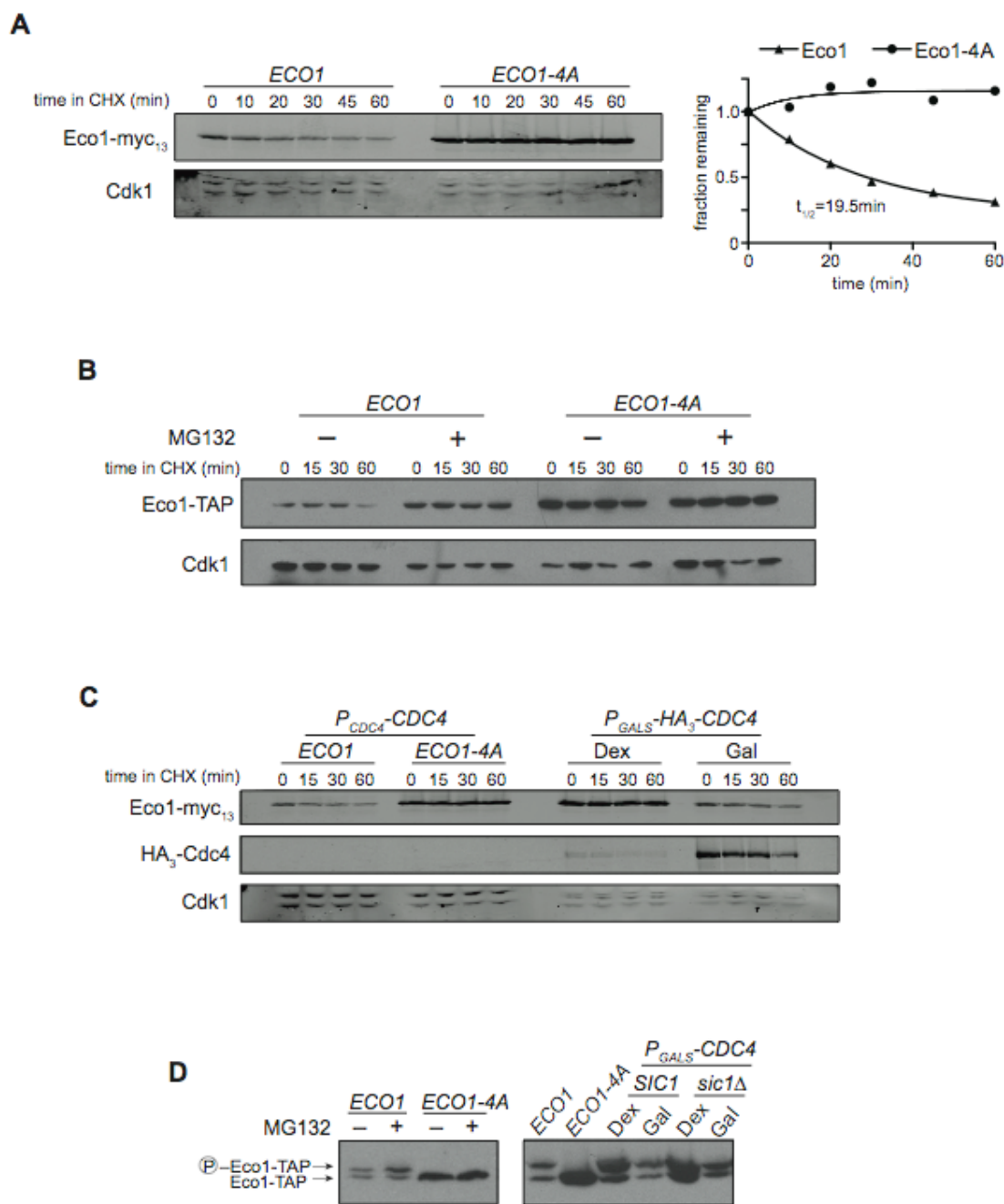


Figure 5

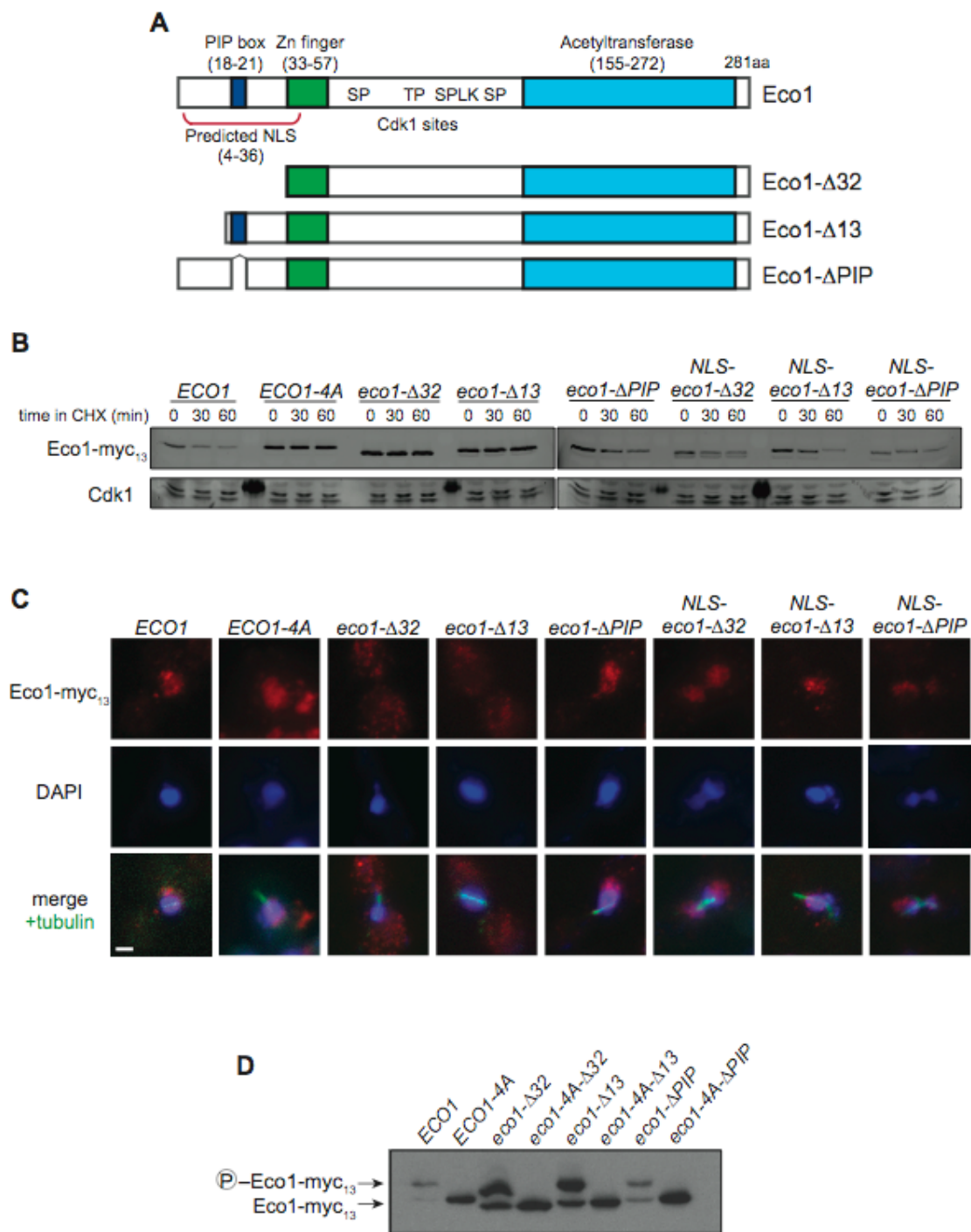


Figure 6

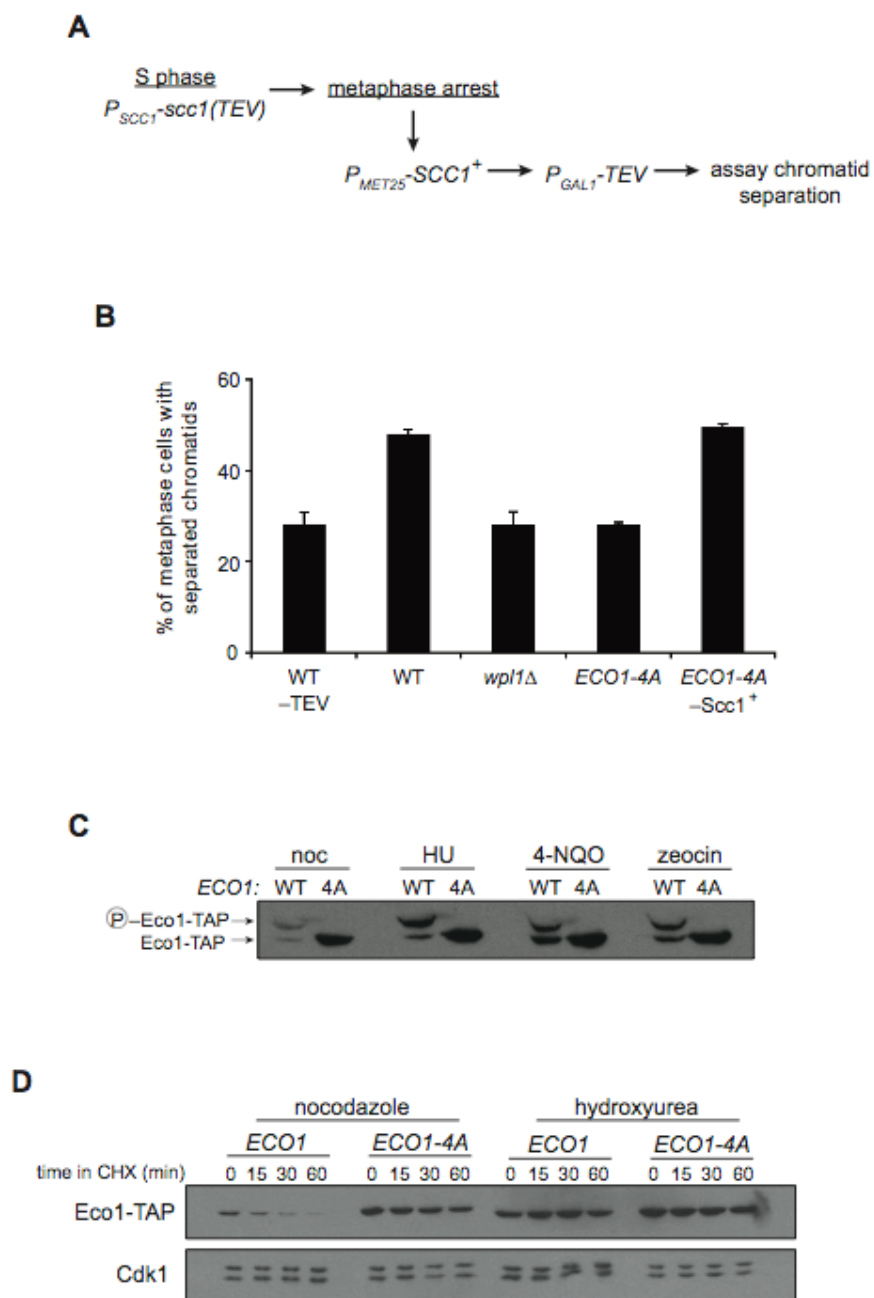
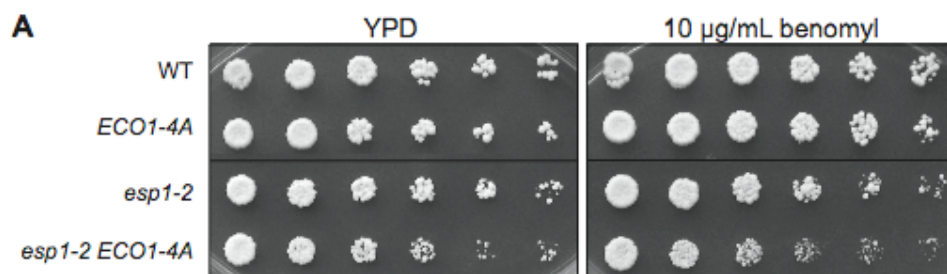
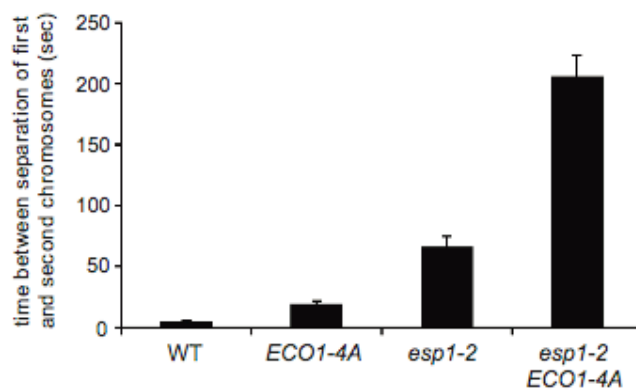


Figure 7

**B**

strain	WT	<i>ECO1-4A</i>	<i>esp1-2</i>	<i>esp1-2 ECO1-4A</i>
n	53	92	45	59
mean	4.8	19.5	66.0	206.2
median	0	15	62.5	180
SEM	1.1	2.1	8.5	17.1
t-test	–	9.0×10^{-6}	5.3×10^{-6}	4.6×10^{-17}

Figure S1

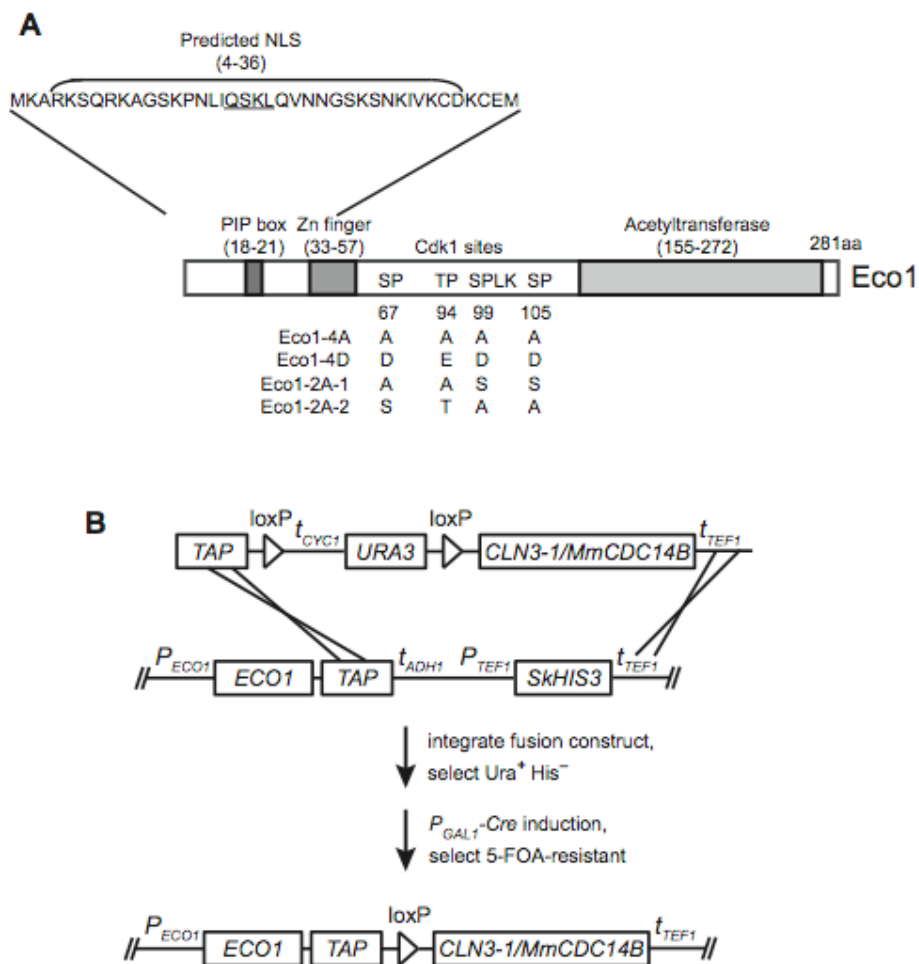


Figure S2

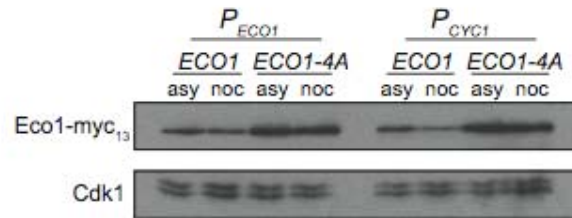


Figure S3

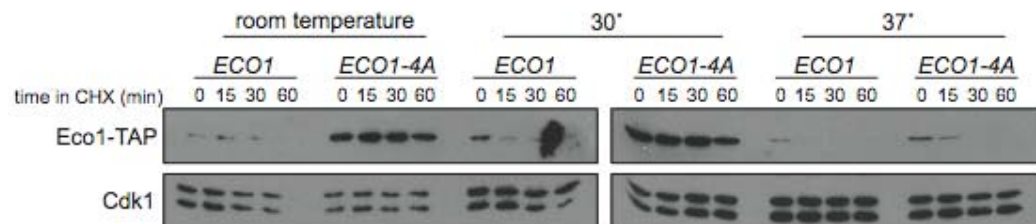


Figure S4


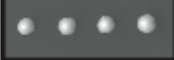





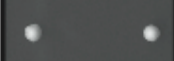








	<i>ECO1</i> <i>WPL1</i>	<i>ECO1</i> <i>WPL1</i>	<i>ECO1-myc₁₃</i> <i>wpl1Δ</i>	<i>ECO1-myc₁₃</i> <i>wpl1Δ</i>
	<i>ECO1-myc₁₃</i> <i>WPL1</i>	<i>ECO1</i> <i>wpl1Δ</i>	<i>ECO1</i> <i>WPL1</i>	<i>ECO1-myc₁₃</i> <i>wpl1Δ</i>
	<i>eco1-1</i> <i>WPL1</i>	<i>ECO1</i> <i>wpl1Δ</i>	<i>ECO1</i> <i>wpl1Δ</i>	<i>eco1-1</i> <i>WPL1</i>
	<i>eco1-1</i> <i>WPL1</i>	<i>ECO1</i> <i>WPL1</i>	<i>ECO1</i> <i>wpl1Δ</i>	<i>eco1-1</i> <i>wpl1Δ</i>
	<i>eco1-Δ32</i> <i>wpl1Δ</i>	<i>ECO1</i> <i>wpl1Δ</i>	<i>eco1-Δ32</i> <i>WPL1</i>	<i>ECO1</i> <i>WPL1</i>
	<i>eco1-Δ32</i> <i>WPL1</i>	<i>eco1-Δ32</i> <i>wpl1Δ</i>	<i>ECO1</i> <i>WPL1</i>	<i>ECO1</i> <i>wpl1Δ</i>
	<i>ECO1</i> <i>WPL1</i>	<i>eco1-Δ13</i> <i>WPL1</i>	<i>ECO1</i> <i>wpl1Δ</i>	<i>eco1-Δ13</i> <i>wpl1Δ</i>
	<i>ECO1</i> <i>wpl1Δ</i>	<i>eco1-Δ13</i> <i>WPL1</i>	<i>eco1-Δ13</i> <i>WPL1</i>	<i>ECO1</i> <i>wpl1Δ</i>
	<i>ECO1</i> <i>wpl1Δ</i>	<i>eco1-ΔPIP</i> <i>WPL1</i>	<i>eco1-ΔPIP</i> <i>WPL1</i>	<i>ECO1</i> <i>wpl1Δ</i>
	<i>ECO1</i> <i>wpl1Δ</i>	<i>eco1-ΔPIP</i> <i>WPL1</i>	<i>ECO1</i> <i>wpl1Δ</i>	<i>eco1-ΔPIP</i> <i>WPL1</i>
	<i>NLS-eco1-Δ32</i> <i>WPL1</i>	<i>ECO1</i> <i>wpl1Δ</i>	<i>NLS-eco1-Δ32</i> <i>WPL1</i>	<i>ECO1</i> <i>wpl1Δ</i>
	<i>NLS-eco1-Δ32</i> <i>WPL1</i>	<i>ECO1</i> <i>wpl1Δ</i>	<i>ECO1</i> <i>wpl1Δ</i>	<i>NLS-eco1-Δ32</i> <i>WPL1</i>
	<i>NLS-eco1-Δ13</i> <i>WPL1</i>	<i>ECO1</i> <i>wpl1Δ</i>	<i>ECO1</i> <i>wpl1Δ</i>	<i>NLS-eco1-Δ13</i> <i>WPL1</i>
	<i>ECO1</i> <i>wpl1Δ</i>	<i>NLS-eco1-Δ13</i> <i>WPL1</i>	<i>NLS-eco1-Δ13</i> <i>WPL1</i>	<i>ECO1</i> <i>wpl1Δ</i>
	<i>ECO1</i> <i>WPL1</i>	<i>NLS-eco1-ΔPIP</i> <i>wpl1Δ</i>	<i>NLS-eco1-ΔPIP</i> <i>WPL1</i>	<i>ECO1</i> <i>wpl1Δ</i>
	<i>NLS-eco1-ΔPIP</i> <i>WPL1</i>	<i>NLS-eco1-ΔPIP</i> <i>WPL1</i>	<i>ECO1</i> <i>wpl1Δ</i>	<i>ECO1</i> <i>wpl1Δ</i>

Figure S5

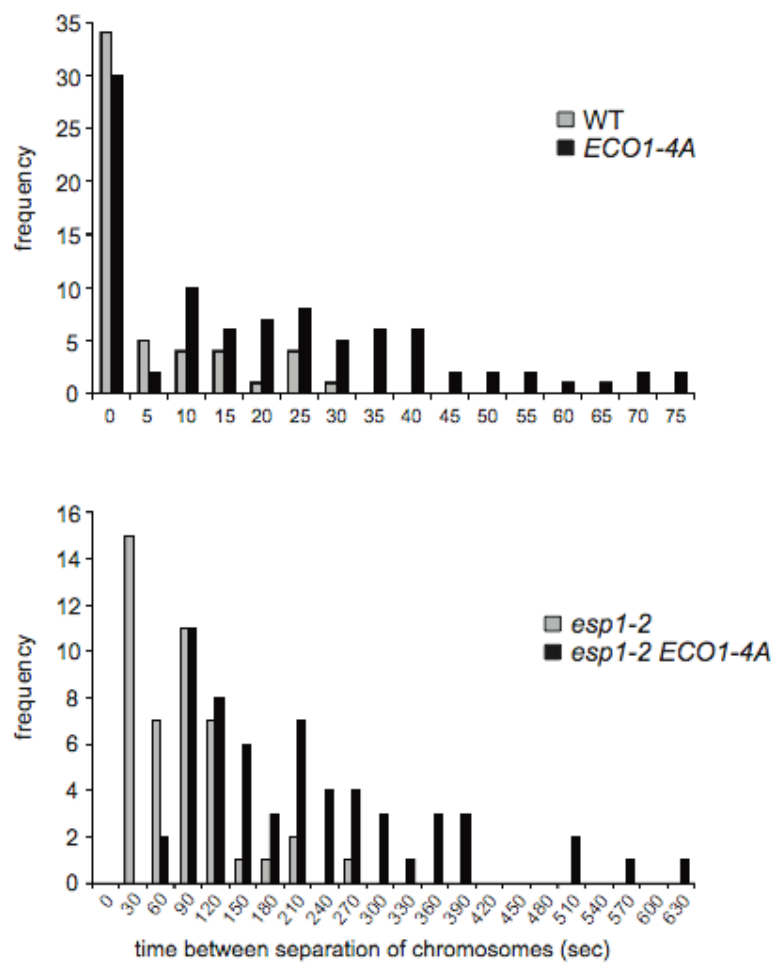


Table S1. List of strains and plasmid constructs.

Strain	Genotype
BY4741	WT S288C (ATCC 201388): his3 Δ 1, ura3 Δ 0, leu2 Δ 0, met15 Δ 0, MATa
8GS6-A2	ECO1-TAP:SkHIS3
MD025	ECO1-myc ₁₃ :HIS3MX6
NL183	URA3:ECO1-4A, MATalpha
NL184	URA3:ECO1-4A-TAP:SkHIS3, MATa
NL186	URA3:eco1-1(G211D), MATalpha
NL187	URA3:eco1-1(G211D), wpl1::kanMX6, MATa
NL188	URA3:eco1-1(G211D), mad2::kanMX6, MATa
NL191	ECO1-TAP-loxP-tCYC1-URA3-loxP-CLN3-1, leu2 Δ 0:pGAL1-Cre:LEU2, MATa
NL192	ECO1-TAP-loxP-tCYC1-URA3-loxP-MmCDC14B, MATa
NL200	ECO1-TAP-CLN3-1, leu2 Δ 0:pGAL1-Cre:LEU2, MATa
NL201	ECO1-TAP-MmCDC14B, [pNL022], MATa
NL214	URA3:ECO1-4A-TAP-CLN3-1, MATa
NL216	URA3:ECO1-4A-myc ₁₃ :HIS3MX6, MATa
NL217	URA3:ECO1-4D, MATalpha
NL218	URA3:ECO1-4A, mad2::kanMX6, MATalpha
NL221	URA3:ECO1-4D, mad2::kanMX6, MATalpha
NL231	ECO1-TAP-CLN3-1, wpl1::kanMX6, leu2 Δ 0:pGAL1-Cre:LEU2, MATa
NL232	ECO1-TAP-CLN3-1, mad2::kanMX6, MATa
NL243	ura3::lacO ₂₅₆ :LEU2, his3::pCUP1-1-GFP-LacI:HIS3, MATa
NL246	NL243, ECO1-TAP-MmCDC14B
NL252	NL243, ECO1-TAP-CLN3-1
NL253	NL243, URA3:ECO1-4A-TAP-CLN3-1
NL254	NL243, ECO1-TAP-CLN3-1, wpl1::kanMX6
NL255	NL243, URA3:eco1-1
NL256	NL243, URA3:eco1-1, wpl1::kanMX6
NL257	NL243, URA3:ECO1-4A
NL258	NL243, URA3:ECO1-4D
NL259	NL243, wpl1::kanMX6
NL293	trp1::lacO ₂₅₆ :TRP1, ura3::lacO ₂₅₆ :LEU2, his3::pCUP1-1-GFP-LacI:HIS3, MATa
NL300	URA3:eco1- Δ 32-myc ₁₃ :HIS3MX6, wpl1::kanMX6, MATa
NL301	URA3:eco1-4A- Δ 32-myc ₁₃ :HIS3MX6, wpl1::kanMX6, MATa
NL304	pdr5::kanMX6, ECO1-TAP:HIS3MX6, MATa
NL305	pdr5::kanMX6, URA3:ECO1-4A-TAP:HIS3MX6, MATa
NL314	pSCC1-sec1(TEV268)-HA ₃ :hphNT1:pSCC1:natNT2:pMET25-GFP-SCC1, trp1::TRP1:pGAL1-NLS-myc ₆ -TEV-NLS ₂ , ura3::lacO ₂₅₆ :LEU2, his3::pCUP1-1-GFP-LacI:HIS3, MATalpha
NL315	NL314, URA3:ECO1-4A
NL320	ECO1-TAP-MmCDC14B(C314S), [pNL022], MATa
NL321	NL293, URA3:ECO1-4A

CHAPTER 3: SEQUENTIAL PRIMED KINASES CREATE A DAMAGE-RESPONSIVE PHOSPHODEGRON ON ECO1 TO CONTROL SISTER-CHROMATID COHESION

This chapter has been submitted to *Nat. Struct. Mol. Biol.* on July 31, 2012.

ABSTRACT

Sister-chromatid cohesion is established during S phase when Eco1 acetylates cohesin. In budding yeast, Eco1 activity falls after S phase due to Cdk1-dependent phosphorylation, which triggers ubiquitination by SCF-Cdc4. We show here that Eco1 degradation requires the sequential actions of Cdk1 and two additional kinases, Cdc7-Dbf4 and the GSK-3 homolog Mck1. These kinases recognize motifs primed by previous phosphorylation, resulting in a precisely ordered sequence of three phosphorylation events on Eco1. Only the latter two phosphorylation sites are spaced correctly to bind Cdc4, resulting in strict discrimination between phosphates added by Cdk1 and Cdc7. Inhibition of Cdc7 by the DNA damage response prevents Eco1 destruction, allowing establishment of cohesion after S phase. This elaborate regulatory system, involving three independent kinases and stringent substrate selection by a ubiquitin ligase, enables robust control of cohesion establishment during normal growth and following stress.

INTRODUCTION

Protein kinases and ubiquitin ligases are key regulators of the cell division cycle, both in normal and perturbed states. The Cyclin-Dependent Kinases (Cdks) in particular are considered the primary drivers of the cell cycle, phosphorylating hundreds of substrates involved in numerous cellular processes(16,33,110). Cdk function is linked to another important regulatory mechanism, protein degradation, by the Skp1-Cullin-F-box (SCF) ubiquitin ligase(78). The F-box subunit of SCF recruits substrates for ubiquitination by interacting with specific sequence motifs (degrons), which usually contain a post-translational modification such as phosphorylation. Phosphodegrons created by Cdks and other kinases tie SCF to many important cell cycle processes. In yeast, for example, phosphorylation of several cell-cycle regulators by Cdk1 leads to their recognition by the F-box protein Cdc4 (Supplementary Table 1). The vertebrate Cdc4 ortholog, Fbw7, also targets many proteins involved in cell proliferation and tumorigenesis(120).

The preferred phosphodegron for Cdc4 and Fbw7 has been studied in considerable detail. Key insights came from phosphopeptide binding experiments, which showed that Cdc4 prefers peptides containing a single phospho-serine or -threonine followed by a proline and preceded by hydrophobic residues: I/L/P-I/L-pS/pT-P-⟨RKY⟩₄ (where ⟨x⟩ refers to disfavored residues)(71). This consensus sequence overlaps partially with the consensus motif of Cdk1 (S/T*-P-x-[K/R], where [K/R] enhances affinity but is not absolutely required). It was subsequently found that Cdc4 has a higher affinity for peptides containing two phosphorylated sites(27), and that local sequence context is less critical than diphosphorylation(3). SCF dimerization might also enhance

binding of a multiply phosphorylated substrate(121), thereby increasing the processivity of ubiquitination(105).

Among its many cell cycle functions, SCF-Cdc4 helps regulate the generation of cohesion between sister chromatids as they are synthesized during S phase(59). Sister-chromatid cohesion is mediated by a protein complex called cohesin, and is established during S phase when the conserved protein Eco1 (also known as Ctf7) acetylates the cohesin subunit Smc3(83,84,100,115). Eco1 levels drop in late S phase due to an increase in degradation rate that requires Cdc4 and Cdk1 consensus sites in Eco1, suggesting that phosphorylation of Eco1 by Cdk1 results in the generation of phosphodegrons that interact with Cdc4(59). The drop in Eco1 abundance prevents cohesion establishment after S phase, as a stabilized, nonphosphorylated Eco1 mutant generates new cohesion in a mitotic arrest. Cdk1 and Cdc4 therefore collaborate to regulate chromosome segregation by preventing excess chromatid cohesion.

Cohesion establishment can also occur after S phase in cells with DNA damage(95,96,116). Reactivation of cohesion establishment is necessary for efficient repair of broken DNA(90) and is dependent on the checkpoint kinase Mec1(95,116) as well as phosphorylation of the cohesin subunit Scc1 (also called Mcd1) by Chk1(29), which is thought to promote acetylation of Scc1-K84 and K210 by Eco1(30). The reactivation of cohesion establishment by DNA damage might also depend on the stabilization of Eco1(59).

Here we present evidence that Eco1 degradation depends on a remarkable cascade of phosphorylation events involving Cdk1 and two additional kinases, Cdc7 and Mck1. We find that after priming by Cdk1 at one site, Cdc7 and Mck1 sequentially

phosphorylate adjacent sites to create a diphosphodegron with high affinity for Cdc4, leading to degradation. We further show that Cdc7 inhibition upon DNA damage stabilizes Eco1, thereby reactivating cohesion establishment. Our experiments highlight the complex regulatory possibilities that can be achieved by multisite phosphorylation of key regulatory proteins.

RESULTS

Eco1 degradation does not depend solely on phosphorylation by Cdk1

Eco1 contains four potential Cdk1 phosphorylation sites clustered in an internal region that is predicted to be disordered (Fig. 1a). Our previous work showed that mutation of all four sites fully stabilized Eco1(59). Here, to assess the contribution of each site, we constructed Eco1 mutants lacking single phosphorylation sites and measured their degradation rates in metaphase-arrested cells treated with the translational inhibitor cycloheximide. We found that the central two sites (T94 and S99) are each absolutely necessary for degradation of Eco1 (Fig. 1b). Mutation of S105 had little effect, while mutation of S67 seemed to increase protein turnover, possibly due to disruption of secondary structure (the zinc finger in Eco1 is only 10 residues upstream of S67).

Eco1 displays a significant mobility shift when analyzed on gels supplemented with a phosphate-binding reagent(41,59). Mutation of S99 resulted in complete loss of the phosphoshift, suggesting that phosphorylation of this residue is solely responsible for the change in mobility (Fig. 1c). We showed previously that this mobility shift occurs

early in S phase, long before Eco1 is degraded, and also following DNA damage, when Eco1 is stabilized(59). Thus, phosphorylation at S99 is not sufficient for Eco1 degradation, suggesting that additional phosphorylation is necessary to create a Cdc4 phosphodegron.

S99 matches the full Cdk1 consensus sequence (S/T*-P-x-R/K), whereas S67, T94, and S105 are only minimal matches (S/T-P). To gain a better understanding of Eco1 phosphorylation by Cdk1, we carried out kinase reactions *in vitro* using purified cyclin-Cdk1 and Eco1. Surprisingly, we found that the S99A mutation blocked all phosphate incorporation by Clb2-Cdk1, to the same degree as mutation of all four sites (Fig. 1d). Similar results were obtained with other cyclin-Cdk1 complexes, including Cln2-Cdk1, Clb3-Cdk1, and Clb5-Cdk1, suggesting that S99 is the only efficient site for phosphorylation *in vitro* by most, if not all, forms of Cdk1 (data not shown).

To fully assess the phosphorylation state of Eco1 in an unbiased manner, we identified sites of phosphorylation *in vivo* by mass spectrometry, using Eco1-Flag₃His₆ purified from proliferating yeast cells. To enrich for phosphorylated Eco1, we purified protein from cells in which *CDC4* was transcriptionally repressed. We identified peptides that contained phosphates on the Cdk1 consensus sites T94 and S99, as well as peptides with phosphates on T94 and the non-Cdk1 site S98 (Fig. 2a, b; Supplementary Fig. 1). We also found phosphates at two other non-Cdk1 sites, S89 and T90. Mutation of these residues had little (T90) or no effect (S89) on Eco1 stability (data not shown), so we focused our efforts on the other novel site, S98.

S98 is the first serine in an SSP motif, which is found at both the third and fourth Cdk1 consensus sites (S99 and S105) (Fig. 1a). Mutation of both upstream serines (Eco1-

S98,104A) fully stabilized Eco1 in a mitotic arrest (Fig. 2c). Stabilization was not due to impaired Cdk1 activity towards the downstream serine, as Eco1-S98,104A still displayed a phosphoshift *in vivo* (Fig. 2d) and was phosphorylated by Cdk1 *in vitro* as efficiently as wild-type protein (Fig. 1d). Mutation of each SSP demonstrated that phosphorylation of S98 was particularly important for Eco1 degradation. The double alanine mutant was slightly more stable than the single S98A mutant, suggesting that S104 might make some minor contribution to turnover (Fig. 2c).

In summary, Eco1 degradation requires three major phosphorylation sites at T94, S98, and S99. Interestingly, only S99 is efficiently phosphorylated by Cdk1 *in vitro*, raising the possibility that other protein kinases are involved.

The kinase Cdc7-Dbf4 is required for Eco1 degradation

Two cell cycle-regulated kinases, Cdc7-Dbf4 and the Polo kinase Cdc5, are known to recognize SSP motifs that are phosphorylated at the second serine. While Cdc5 binds these motifs and phosphorylates a distant site, Cdc7-Dbf4 phosphorylates the S/T immediately upstream(11,54,61,68,80,87,118). Cdc7 was therefore an appealing candidate for the kinase that phosphorylates S98 in Eco1.

Cdc7-Dbf4 is analogous to Cdk1-cyclin, as the catalytic subunit Cdc7 is active only when bound to Dbf4. For this reason, Cdc7-Dbf4 is also called Dbf4-Dependent Kinase (DDK). Like those of Cdk1, Cdc7 levels are constant through the cell cycle, whereas Dbf4 oscillates, rising in late G1 and declining in mitosis(77,97). DDK has known functions in origin firing(48), meiosis(60), and segregation of the chromosomal locus containing the ribosomal DNA(97). However, only a few direct substrates have

been identified, including the replicative helicase subunits Mcm2, 4, and 6(48) and the meiotic proteins Rec8, Mer2, and Sum1(39,54,87,118).

DDK is essential for cell viability but can be deleted in the background of the suppressor mutation *MCM5-P83L*(37). To assess the role of DDK in Eco1 turnover, we measured Eco1 degradation in *dbf4Δ MCM5-P83L* cells arrested in metaphase. Deletion of *DBF4* resulted in full stabilization of Eco1 (Fig. 3a). Thus, both Cdk1 and DDK are necessary, and neither is sufficient, for Eco1 destruction.

The GSK-3 homolog Mck1 is required for Eco1 degradation

As T94 is a poor site for Cdk1-dependent phosphorylation *in vitro* (Fig. 1d), we pursued the possibility that another protein kinase acts at this site. Interestingly, phosphorylation of S98 by DDK is predicted to create a consensus priming site for GSK-3 (glycogen synthase kinase-3), which phosphorylates amino acids four residues upstream of a previously phosphorylated residue (consensus motif: S/T*-x-x-x-pS/pT, where “x” is often proline)(15,18). T94 and phospho-S98 in Eco1 match the consensus motif of the GSK-3 family of kinases, which are the only kinases in yeast primed by +4 phosphorylation(68).

There are four GSK-3 homologs in *S. cerevisiae*: Mck1, Mrk1, Rim11, and Ygk3. Although there is some redundancy in their function, Mck1 has been linked to the broadest range of functions, including centromere integrity, meiotic entry, calcineurin signaling, general stress response, and TOR signaling(31,50,67,74,89). Intriguingly, Mck1 has been implicated in the degradation of three SCF-Cdc4 substrates: Hsl1, Rcn1, and Cdc6(35,42,67).

We analyzed the turnover of Eco1-myc₉ in metaphase-arrested cells individually deleted for each GSK-3 homolog. Strikingly, Eco1 was stabilized in a *mck1Δ* strain to the same extent as the Eco1-T94A mutant (Fig. 3b). Deletions of other GSK-3 paralogs had no effect, revealing a high degree of specificity among the GSK-3 family members.

Phosphorylated Eco1 is a direct target of Cdc7 and Mck1

Our results support a model in which phosphorylation of S99 by Cdk1 primes Eco1 for phosphorylation at S98 by Cdc7, which then primes the protein for phosphorylation at T94 by Mck1. We tested this model directly by measuring kinase activities toward Eco1 peptides carrying phosphates at the predicted priming sites. Synthetic phosphopeptides were used instead of full-length Eco1 to ensure complete phosphorylation of priming sites. Peptides contained residues G91 to K103 of Eco1, plus an extra C-terminal lysine to enhance peptide binding to the anionic filter paper used in the assay. Incubation of Clb2-Cdk1 with an unmodified peptide resulted in robust phosphate incorporation (Fig. 3c). This activity was absent when a phosphate was already present at S99, consistent with our earlier evidence that S99 is the sole major Cdk1 site in the full protein (Fig. 1d). Interestingly, a phosphate on S98 also blocked Cdk1 activity (Fig. 3c). Given that mutation of S99 but not S98 prevents all Cdk1 activity toward Eco1 (Fig. 1d), we suspect that a phosphate at S98 interferes with phosphorylation at S99.

DDK had little activity toward unmodified peptide, but rapidly phosphorylated the peptide with a phosphate at S99 (Fig. 3c), consistent with our hypothesis that phosphorylation of the Cdk1 site at S99 primes Eco1 for phosphorylation by DDK at S98. Similarly, Mck1 was able to phosphorylate an Eco1 peptide only if the peptide

contained a phosphate at S98, and only if it contained T94 (Fig. 3c). These data strongly support our model for the ordered phosphorylation of Eco1 by the three kinases.

Phosphorylation of T94 and S98 creates an efficient Cdc4 recognition site

When we first identified SCF-Cdc4 as the mediator of Eco1 degradation(59), we suspected that a cluster of Cdk1 sites in Eco1 creates a binding site for Cdc4 due to its preference for closely spaced diphosphorylated degrons, often grouped in clusters(3,27,43,106). Our current results, however, prompted us to investigate the contribution of each phosphate to Cdc4 recognition. In those substrates with defined Cdc4 diphosphodegrons, phosphorylated residues are 2 or 3 residues apart, not the 4 residues between T94 and S99 in Eco1 (see Supplementary Table 1). We therefore hypothesized that phosphorylation of S98 brings the phosphate spacing to within the ideal range for Cdc4 binding. To test this idea, we used fluorescence anisotropy to measure the binding of various phosphopeptides to recombinant Cdc4-Skp1 *in vitro* (Fig. 4). Phosphopeptides corresponding to residues G91 to K102 of Eco1 were synthesized and conjugated to a fluorescent small molecule (FITC) at their C-terminus. Peptides were incubated with increasing concentrations of Cdc4, and fluorescence polarization was used to measure bound peptide.

A peptide with phosphates at all three sites (“94-98-99”) bound Cdc4 with an equilibrium dissociation constant of 10.3 μ M (Fig. 4a). Binding affinity was much lower in the absence of phosphate at S98, but was not lower in the absence of a phosphate at S99, consistent with our model that the primary function of S99 phosphorylation is to prime Eco1 for phosphorylation of S98 by DDK.

We observed moderate binding of the Eco1 peptide phosphorylated at T94 alone (Fig. 4a), likely because the sequence around T94 is similar to the consensus Cdc4 binding motif(71). This level of binding appears to be insufficient to mediate degradation *in vivo*, however, as the S98A and S99A mutations completely stabilize Eco1 (Fig. 1b and 2c), and monophosphorylation at T94 is unlikely to occur since Mck1 requires priming at S98 (Fig. 3c). Single phosphates at S98 or S99 had no effect on binding to Cdc4 either individually or together (Fig. 4a). Thus, phosphorylated T94 is the primary binding site whose affinity is supplemented by phosphorylated S98, as seen in other Cdc4 substrates(3,27,53). These results argue that Cdc4-dependent Eco1 degradation requires a specific diphosphorylated degron created by Mck1 and Cdc7.

Precise spacing of diphosphates is important for Cdc4 binding and Eco1 degradation

Our results suggest that phosphates at T94 and S98, but not S99, increase binding of Cdc4 to Eco1 and thereby trigger its destruction. The striking effect of a single extra residue on binding suggested that the distance between phosphates is critical for Cdc4 recognition. To test this, we again used fluorescence anisotropy to measure the binding of peptides containing variations in the distance between phosphates (Fig. 4b). Insertion of isoleucine (an amino acid that does not alter Cdc4 binding *in vitro*(71)) immediately upstream of S98, moving the DDK site to the position of the Cdk1 site (peptide “94-98+I98”), removed the effect of the second phosphate. Additionally, removing a residue between T94 and S98 (N97) made phosphorylation at S98 unnecessary, as peptide “94-99 Δ N97” bound well to Cdc4. The slightly reduced binding of this peptide relative to

“94-98” could be due to local sequence context, although residues at the +2 position are not known to affect Cdc4 binding(71). Thus there is a maximum distance of 3 residues between phosphates that can serve as a Cdc4 diphosphodegron.

We next tested whether there is a minimum distance between phosphates. Removing N97 from a peptide with a phosphate at S98 (the “94-98 Δ N97” peptide) did not reduce the high affinity binding to Cdc4 (Fig. 4b), indicating some flexibility in diphosphate recognition. However, deleting both L96 and N97, leaving only one residue between phosphates (“94-98 Δ LN” peptide), blocked the added effect of the second phosphate. Therefore, Cdc4 binds with high affinity only to substrates with 2 or 3 residues between the two phosphates.

To assess the biological significance of our binding data, we altered the spacing of the phosphorylation sites in Eco1 and monitored protein stability in metaphase-arrested cells. Our model predicted that moving the sites closer by one residue (Eco1-N97 Δ) should remove the requirement for DDK in Eco1 degradation, as the Cdk1 site at S99 would then be the optimal distance from T94 (comparable to the “94-99 Δ N97” peptide in Fig. 4b). Indeed, we found that Eco1-N97 Δ was unstable in a *dbf4 Δ* strain (Fig. 5a), and the S98A mutation did not stabilize Eco1-N97 Δ (Fig. 5b). This mutant was much less stable than the wild-type protein, possibly suggesting that the activity of Cdk1 and Mck1 towards Eco1 is higher than that of DDK. Consistent with this explanation, the small amount of Eco1-N97 Δ protein in the cell did not display a phosphoshift in a metaphase arrest (Supplementary Fig. 2), suggesting that phosphorylation of this mutant by Cdk1 results in immediate degradation, while Cdk1-phosphorylated wild-type Eco1 is more stable due to limited phosphorylation by DDK.

Degradation of the Eco1-N97 Δ mutant is independent of DDK, but our model predicts it should still be dependent on Mck1 activity. We found that Eco1-N97 Δ was highly stabilized in a *mck1* Δ strain (Fig. 5c). While Eco1-N97 Δ was much more stable in *mck1* Δ than in *MCK1* cells, the stabilization was not complete, perhaps indicating that deletion of N97 causes some non-specific protein turnover. However, Eco1-N97 Δ displays a robust phosphoshift in the *mck1* Δ background, indicating that it is still efficiently targeted by Cdk1 *in vivo* (Supplementary Fig. 2). Moreover, additional deletions to this region (see below) fully stabilized the protein, inconsistent with a non-specific effect of removing N97.

Consistent with our Cdc4 binding data *in vitro*, inserting an isoleucine immediately upstream of S98 (Eco1+I98) stabilized the protein in metaphase (Fig. 5d). Deletion of both L96 and N97 (Eco1-L96 Δ N97 Δ) or all three intervening residues (Eco1- Δ 96-98) also completely stabilized the protein (Fig. 5d). The latter is consistent with the amount of binding observed *in vitro* (compare to the “94-98 Δ LN” peptide), again indicating that two phosphates need to be a minimal distance apart to be recognized efficiently. However, Eco1-L96 Δ N97 Δ has spacing of phosphorylation sites similar to the “94-98 Δ N97” peptide that bound well to Cdc4 (Fig. 4b), and might therefore be predicted to be ubiquitinated *in vivo*. Stabilization of this mutant is not due to lack of S99 phosphorylation by Cdk1, as the protein exhibits slower migration on a gel containing phosphate-binding reagent (Supplementary Fig. 2). Instead, the stability is likely due to lack of phosphorylation by Mck1, as removal of L96 and N97 moves T94 out of the -4 position and away from the GSK-3 recognition motif(18). The Eco1-L96 Δ N97 Δ mutant

thus reveals a spacing requirement beyond that of just Cdc4, further supporting our model of Mck1 priming.

DDK determines the timing of Eco1 degradation

To further characterize the DDK-independent degradation of Eco1-N97 Δ , we examined protein levels over the cell cycle. As seen previously(59), wild-type Eco1-TAP protein levels increased during S phase, declined in mitosis, and reappeared after chromosome segregation and cyclin destruction (Fig. 6a). In contrast, Eco1-N97 Δ -TAP levels declined in late G1, 20 minutes earlier than wild-type Eco1 (Fig. 6b). Destruction of Eco1-N97 Δ began at the time that wild-type Eco1 displayed the S99-dependent phosphoshift, but the gel mobility of Eco1-N97 Δ did not change over the entire cycle. Moreover, Eco1-N97 Δ accumulated as cyclin levels dropped in mitosis. Thus, Eco1-N97 Δ levels were inversely related to the amount of Clb-Cdk1 activity in the cell, suggesting that Cdk1 activity determines the timing of Eco1-N97 Δ turnover and that Mck1 activity is constitutive throughout the cell cycle, consistent with a recent report(35). Given that removing the requirement for DDK results in much earlier degradation, it seems likely that the normal timing of Eco1 destruction in late S phase is determined by changes in DDK activity toward S98.

Inhibition of Dbf4 stabilizes Eco1 upon DNA damage

Our data indicate that S98 phosphorylation by DDK is necessary for Eco1 turnover because it is in the correct position to promote Mck1 phosphorylation and Cdc4 binding. Our studies of the Eco1-N97 Δ mutant suggested that the requirement for DDK provides a

mechanism to delay Eco1 degradation until late S phase. We also considered a second important biological rationale for regulation by DDK, based on our previous observation that Eco1 is stabilized by DNA damage(59): DDK activity is thought to be reduced in yeast cells following DNA damage(40,119) (although perhaps not towards all substrates(37,51,77)). In budding and fission yeasts, Dbf4 is extensively phosphorylated after DNA damage, and this phosphorylation depends on the damage response kinase Rad53(20,103,119). Mutations in Dbf4 that block its full phosphorylation by Rad53 lead to inappropriate firing of late replication origins following DNA damage, suggesting that phosphorylation of Dbf4 inhibits DDK function(57,127).

To test if DDK inhibition prevents the degradation of Eco1 in a damage arrest, we used a mutant form of Dbf4 (Dbf4-m25) that lacks many of its Rad53 phosphorylation sites and is therefore refractory to damage-dependent inhibition of late origin firing(57). Treatment of cells with the replication inhibitor hydroxyurea (HU) to activate the DNA damage response led to the stabilization of Eco1-TAP (Fig. 7a), as seen previously(59). However, Eco1 was rapidly degraded in *dbf4-m25* cells treated with HU (Fig. 7a), similar to *mec1Δ* cells that lack the damage response. Maintenance of DDK activity in damage is thus sufficient to destabilize Eco1, further supporting the role of Cdc7 in Eco1 turnover and indicating that Cdk1 and Mck1 activities toward Eco1 are not affected by the damage response.

To further verify that the absence of DDK-dependent phosphorylation is responsible for Eco1 stabilization following DNA damage, we examined the degradation of Eco1-N97Δ, which does not require DDK activity for turnover (Fig. 5a). Consistent with our hypothesis, Eco1-N97Δ-TAP was rapidly degraded in cells subjected to DNA

damage (Fig. 7b). We conclude that Rad53-dependent inhibition of Dbf4 is responsible for the stabilization of Eco1 upon damage.

Stabilization of Eco1 is necessary to establish damage-induced cohesion

Discovering the molecular basis of Eco1 stabilization upon DNA damage allowed us to test whether it is required to establish new cohesion after damage. We used a variation of a previous protocol to measure the generation of damage-induced cohesion in metaphase(116). In this experiment, cells establish normal cohesion in S phase using a version of the Scc1 cohesin subunit containing a TEV protease site (Scc1-TEV). Cultures were then arrested in metaphase, followed by treatment with the UV mimetic 4-nitroquinoline (4-NQO) and induction of wild-type Scc1 lacking the TEV site. This wild-type cohesin was allowed time to establish or not, and then TEV protease was expressed to remove cohesion established during S phase. This left only the cohesin expressed during the damage response to hold the LacI-GFP-tagged sister chromatids together.

In this assay, wild-type cells fail to establish new cohesion and approximately 50% of the cells contain separated LacI-GFP foci. Activation of the establishment machinery lowers this to about 30%(29,59,95,116). As seen previously, we found that DNA damage induced new cohesion in wild-type cells (Fig. 7c). This effect depended on lysines 84 and 210 in Scc1, which are likely Eco1 acetylation sites(30). We found that damage did not induce new cohesion in *dbf4-m25* cells, but this was rescued by mutation of the two DDK consensus sites in Eco1, S98 and S104 (Fig. 7c). Additionally, the Eco1 mutation whose degradation is independent of Dbf4 (Eco1-N97 Δ) did not establish new cohesion after damage, consistent with our model that stabilization in damage is due to

inhibition of DDK. Thus the reactivation of cohesion establishment upon DNA damage depends on the increased levels of Eco1 caused by the reduction of DDK activity.

DISCUSSION

We report the discovery of an intricate series of phosphorylation events that controls the generation of sister chromatid cohesion through the phosphorylation and ubiquitination of the cohesion-promoting enzyme Eco1 (Fig. 7d). Our data suggest that Cdk1-dependent phosphorylation of one Eco1 residue, S99, primes for phosphorylation at the adjacent site, S98, by the cell cycle-regulated kinase Cdc7-Dbf4 (DDK) in late S phase. This then promotes a third phosphorylation at T94 by the GSK-3 homolog Mck1. The result is a precisely spaced pair of phosphates at S98 and T94 that create a high-affinity interaction site for the SCF ubiquitin ligase subunit Cdc4. Because Dbf4 is inhibited by the DNA damage response, full Eco1 phosphorylation is blocked following DNA damage, leading to high Eco1 levels and establishment of new cohesion after S phase.

The participation of Cdc7 in Eco1 degradation adds another layer of regulation to cohesion establishment and permits differential regulation in different cellular states. Regulation by DDK would be inconsequential, however, without the rigorous substrate discrimination we observed for Cdc4 and Mck1. The ability of Cdc4 to distinguish a phosphate attached by DDK from an immediately adjacent phosphate added by Cdk1 is impressive, and will likely be important for other Cdc4 substrates. Likewise, the strict spacing of the GSK-3 consensus sequence means that the distance between phosphates in

GSK-3 targets matches the ideal spacing for Cdc4 binding. These features of Eco1 regulation together impose a set of strict conditions necessary to shut off cohesion establishment, enabling establishment activity to be correctly timed in the cell cycle and responsive to environmental perturbations.

This modularity and convergence of inputs is a common theme in biological regulatory systems. Regulatory proteins that respond only in the presence of multiple upstream inputs are called coincidence detectors and operate as logical ‘AND’ statements. Eco1 degradation represents an unusual case of a triple ‘AND’ statement integrating at least three separate inputs. Changes in any one input—oscillations in Cdk1 activity or DDK inhibition after DNA damage, for example—dramatically influence the output, Eco1 degradation, and the biological process it controls, cohesion establishment. Any proteins that recognize previously-modified targets (e.g. Cdc7, GSK-3, Cdc4, proteasome receptors) have the potential to introduce ‘AND’ gates into a regulatory circuit, making them ideal tools for the integration of cellular inputs.

Critical to the integration of the three Eco1 inputs is our finding that tight Cdc4 binding requires two or three amino acids between phosphates (Fig. 4). In crystallographic structures of Cdc4 bound to phosphopeptides with three residues between phosphates, the anchor phosphothreonine binds the center of the WD40 domain and the C-terminal phosphoserine interacts with R443, S464, T465, and R485, near the edge of the domain(27,106). The C-terminal end of the peptide in these structures forms a small loop, allowing the second phosphoserine to contact the above residues. It is reasonable to predict that a degron with only two residues between phosphates could interact with the same side chains in Cdc4, but perhaps without making a loop. A peptide

with four residues separating phosphates, however, may not be able to make the necessary contortions to align the second phosphate, and a degron with only a single intervening residue is likely not long enough to allow simultaneous interaction with both phosphate-binding sites.

Diphosphorylated Eco1 peptides have an affinity for Cdc4 similar to that of Sic1 phosphopeptides but weaker than the high-affinity substrates Tec1 and Ash1 (Supplementary Table 1). This moderate affinity could represent a selected trait that prevents Eco1 levels from getting too low after S phase, allowing cohesion establishment to be more easily reactivated. An additional possibility is that the peptides do not fully recapitulate all of the binding contacts of the full-length substrate. Upstream residues could make extended interactions with Cdc4, as suggested by recent studies of long peptides from Sic1(106).

It is also possible that additional phosphorylation sites in Eco1 contribute to Cdc4 binding. These sites might include the second SSP motif (S104-S105), as suggested by the slightly additive effect of the S98A and S104A mutations (Fig. 2c), or possibly the more N-terminal phosphates identified by mass spectrometry (S89 and T90). Mck1 may catalyze phosphorylation of T90, since T94 is at the correct priming distance and GSK-3 kinases are known to sequentially phosphorylate substrates by creating their own consensus sites(15,18). Phosphates at T90 and T94 could create another Cdc4 degron, not unlike the phosphodegron in Ash1, which contains three phosphates that create two redundant overlapping Cdc4 binding sites(53). S89 might be phosphorylated by DDK after priming at T90, but this likely does not affect Eco1 degradation. Serine 104 is too far from serine 99 to constitute a diphosphodegron, but might bind to another molecule in

a Cdc4 dimer, as suggested for the interaction of human Fbw7 with its substrate cyclin E(121) and the Pop1/2 homologs in fission yeast(44). The kinase that phosphorylates S89 or S105 remains unknown, however, since we were unable to detect any phosphorylation by Cdk1 at these residues *in vitro* (Fig. 1d and 3c). The finding that Cdk1 only phosphorylates S99 was unexpected, as it shows that some S/T-P sequences are not efficiently targeted by Cdk1, even when they appear accessible to another kinase. Since Cdk1 was unable to phosphorylate T94 even in a short peptide (Fig. 3c), this substrate discrimination could be due to the surrounding primary or secondary sequence, though the exact cause is unclear.

Cdc7 is involved in many different aspects of chromosome biology beyond its essential role in replication initiation. Most notable are its many functions in meiosis, including inhibition of the transcription repressor Sum1 (with Cdk1 and Ime2 kinases) to facilitate progression through meiotic prophase(54), regulation of monopolar spindle attachment (with Polo kinase) likely through phosphorylation of Lrs4(62), as well as initiation of meiotic recombination via Mer2 phosphorylation (after priming by Clb5-Cdk1)(87,118). DDK also phosphorylates the meiotic cohesin subunit Rec8 (with Casein Kinase 1) to promote cohesin cleavage by separase in meiosis I(39). In frog egg extracts, DDK activity is necessary for cohesin loading onto chromatin at sites containing pre-replication complexes, but the substrate is unknown(102). Additionally, a stable mutant form of yeast Dbf4 causes a delay in the segregation of the ribosomal RNA genomic locus in mitosis(97). DDK therefore has pro-cohesion functions in addition to the anti-cohesion function described in this study. All these data demonstrate that DDK often

regulates processes in cooperation with other kinases, highlighting its role as an adaptable kinase that provides an additional layer of regulation.

The regulation of DDK activity by the DNA damage response is not without inconsistencies. Different effects of DNA damage on Cdc7-Dbf4 have been reported, ranging from no effect on kinase activity(37,51,77) to nearly complete inhibition(40,119). DDK activity is unlikely to be completely inhibited in a damage arrest since only late origins of replication are blocked—early origins still fire at the beginning of S phase in the presence of damage(86). Our evidence suggests that the timing of Eco1 degradation in late S phase is determined by DDK (Fig. 6b), which is surprising because Cdc7 activity is thought to be determined solely by binding to Dbf4, which is present throughout S phase(37,77). Moreover, preventing Rad53 phosphorylation of DDK is sufficient to maintain Eco1 degradation in a damage response (Fig. 7a). Thus, there is an intriguing correlation between those DDK events that occur in late S phase (late origin firing, Eco1 degradation) and those inhibited by DNA damage.

The adaptive value of GSK-3 involvement in Eco1 degradation is less clear than that of DDK, but its recognition of primed substrates enables it to serve as a sensor for the activity of other kinases. This prevents attachment of the anchor phosphate at T94 until DDK is active, preventing spurious low-level binding of Cdc4 to the T94 monophosphate. The requirement for Mck1 ensures that Eco1 binding to Cdc4 goes from zero (“99” and “98-99” peptides in Fig. 4) to maximal (“94-98-99” peptide) with no intermediate. The system would not have this property if Cdk1 phosphorylated T94. Additionally, Cdk1 phosphorylation of T94 might require a basic residue at the +3 position, which would weaken Cdc4 binding(71). Given their mutually exclusive

consensus motifs, it will be interesting to see how many of the anchor phosphates in Cdc4 degrons are attached by Cdk1. In contrast, the GSK-3 motif overlaps perfectly with that of Cdc4: both proteins prefer substrates with three residues between phosphorylation sites(18) (Fig. 4). Thus, GSK-3 is ideally suited to provide the N-terminal phosphate in a Cdc4 degron, and metazoan GSK-3 and SCF have many substrates in common(124).

Mck1 is responsive to various cellular stresses(31,42,50,67,74), all of which seem to increase Mck1 activity towards certain substrates, possibly via priming by stress-activated kinases. These stress response pathways may not impinge on cohesion regulation, however, since Mck1 activity does not seem to be limiting for Eco1 degradation (Fig. 6b). The activity profiles of yeast GSK-3 homologs have not been as well characterized as those of their metazoan counterparts, but there are likely to be differences since GSK-3 family members in other eukaryotes tend to be active in cellular resting states and inhibited by growth factors(15), whereas Mck1 is constitutively active(35). Discovery of conditions that inhibit Mck1 activity would reveal new circumstances in which Eco1 could be reactivated, possibly indicating that DNA damage may not be the only stressor to modulate chromatid cohesion.

The results described in this study underscore the utility of post-translational modifications in precisely coordinating essential cell biological processes. To create an exact duplicate of an entire cell, dozens of diverse events must be properly organized and executed faithfully every generation. Just as multicellular development requires an extremely well-orchestrated series of interdependent events, so too must the events of the cell division cycle be exquisitely coordinated. An elegant regulatory system has thus

evolved to ensure the fidelity of cell reproduction, and central to this is the accurate segregation of the genetic material.

ACKNOWLEDGEMENTS

We thank Stephen Bell, David Toczyski, Hiten Madhani, and Kevan Shokat for strains and reagents, Mart Loog for assistance with kinase assays, Amy Ikui for discussion of unpublished results, James Wohlschlegel for advice with mass spectrometry, Jeff Mugridge for assistance with fluorescence anisotropy, and Ellen Edenberg and Scott Foster for critical review of the manuscript. This work was supported by funding from the National Institute of General Medical Sciences (R01-GM069901 to D.O.M. and P41-GM103533 to J.R.Y.) and the National Center for Research Resources (P41-RR011823 to J.R.Y.).

AUTHOR CONTRIBUTIONS

N.A.L. and D.O.M. conceived the experiments, N.A.L. conducted the biological and biochemical experiments, B.R.F. performed mass spectrometry, and B.R.F. and J.K.D.

analyzed mass spectra under the guidance of J.R.Y. N.A.L. and D.O.M. wrote the manuscript.

COMPETING FINANCIAL INTERESTS

The authors declare no competing financial interests.

METHODS

General Methods

All yeast strains are derivatives of the S288C strain BY4741 (see Supplementary Table 2 for a list of strains and plasmids). Genetic manipulations were performed using standard methods(55). Cell cycle arrests were achieved using 15 $\mu\text{g/ml}$ nocodazole, 15 $\mu\text{g/ml}$ alpha-factor, 2 μM 4-nitroquinoline, or 200 mM hydroxyurea for 3 h at 30°C; all arrests were confirmed by flow cytometric analysis of DNA content. Budding index and binucleate formation were counted using cells fixed in 0.02 % sodium azide and either light microscopy or epifluorescence after staining DNA with 1 $\mu\text{g/ml}$ 4',6-diamidino-2-phenylindole (DAPI). Protein degradation experiments were done using 100 $\mu\text{g/ml}$ cycloheximide to inhibit protein synthesis, followed by cell lysis by bead beating in urea buffer (20 mM Tris-HCl pH 7.4, 7 M urea, 2 M thiourea, 4 % CHAPS).

Western blotting

Primary antibodies were anti-myc (9E10, Covance, 1:1000 dilution), anti-PAP (P 1291, Sigma, 1:5000), and anti-Pgk1 (22C5D8, Invitrogen, 1:10,000). Secondary antibodies coupled to horseradish peroxidase from GE Healthcare were used at 1:10,000 dilution. To visualize Eco1-S99 phosphorylation, the resolving portions of SDS-polyacrylamide gels were supplemented with 10 μ M Phos-tag reagent(41) made using standard chemical techniques, 50 μ M MnCl₂, and two-fold excess ammonium persulfate and TEMED.

Mass Spectrometry

Eco1-Flag₃His₆ was purified from *P_{GALS}-HA3-CDC4 sic1 Δ* yeast cells grown overnight in media containing 2% galactose, followed by dilution into 0.033% galactose. Following another day of growth, *CDC4* expression was turned off by the addition of 2% dextrose for 3.5 h at 30°C and 4°C for 45 min. Cells were harvested, frozen in liquid N₂ and mechanically lysed by blending in lysis buffer (50 mM HEPES (pH 7.4), 150 mM NaCl, 0.1% NP-40 plus phosphatase and protease inhibitors). Lysates were spun at 40,000 rpm for 1 h at 4°C and the supernatant incubated with Flag antibody-coupled magnetic beads for 19 h at 4°C. Beads were washed three times in lysis buffer containing 300 mM NaCl. Bound protein was eluted in 1 M arginine-HCl (pH 3.5) at 4°C for 2 h, frozen in liquid N₂ and stored at -80°C.

Tryptic phosphopeptides from Eco1 were analyzed by Multi-dimensional protein identification technology (MudPIT) as previously described(123), with the following modifications. 3-step MudPIT was performed where each step corresponds to 0, 25, and 100% buffer C (500 mM ammonium acetate) being run for 5 min at the beginning of a 2 h reverse phase gradient. Precursor scanning in the Orbitrap XL was performed from 400

to 2000 m/z with the following settings: 5×10^5 target ions, 50 ms maximum ion injection time, and 1 microscan. Data-dependent acquisitions of MS/MS spectra with the LTQ on the Orbitrap XL were performed with the following settings: MS/MS on the 8 most intense ions per precursor scan, 30K automatic gain control target ions, 100 ms maximum injection time, and 1 microscan. Multistage activation (MSA) fragmentation was performed at 35% normalized collision energy on the precursor and then on the expected neutral loss ions with reduced m/z's of 32.70 (+3 ions), 49.00 (+2), and 98.00 (+1). Dynamic exclusion settings were as follows: repeat count, 1; repeat duration, 30 s; exclusion list size, 500; and exclusion duration, 60 s. Protein and phosphopeptide identification and phosphorylation analysis were done with Integrated Proteomics Pipeline (IP2, www.integratedproteomics.com). Tandem mass spectra were extracted to MS2 files from raw files using RawExtract 1.9.9(64) and were searched against a non-redundant UniProt human database with reversed sequences using ProLuCID(125) with the multistage search option(19). The search space included all fully- and half-tryptic peptide candidates. The MSA search option in ProLuCID models both precursor fragment ions and neutral loss fragment ions in the XCorr calculation. Fragment ions from the phosphopeptide precursor were modeled with a mass increase of 79.9663 Da to the original peptide sequence for each phosphate present. The neutral loss fragment ions were modeled with a mass shift of -18.0106 from the loss of water from the original peptide sequence after the neutral loss of phosphate in the first activation step of MSA. Carbamidomethylation (+57.02146) of cysteine was considered as a static modification; phosphorylation (+79.9663) on serine, threonine, and tyrosine were considered as

variable modifications. Peptide candidates were filtered to 0.1% FDR using DTASelect(13,101).

Fig. 2a is the MSA CID fragmentation spectrum of the doubly phosphorylated peptide STGTIpTLNpSSPLKK. From initial unsuccessful attempts with CID fragmentation of the precursor ion only, we found that MSA(88) provided an adequate balance of sequence-specific and phosphorylation site-specific fragment ions for identification of phosphorylation sites on this complex phosphopeptide. The six potential sites of phosphorylation complicated phosphate localization and created multiple phosphate neutral losses (-98 Da) and water losses (-18 Da) during fragmentation. Fortunately, an adequate number of sequence-specific ions for peptide identification were identified with MSA, many with water losses. Additionally, phosphate molecules were detected intact on fragment ions y_9 and y_{10} , yet not on y_5 , unambiguously indicating that T94 and S98 were phosphorylated. Further, preferential cleavage N-terminal of the two proline residues within the sequence due to the *proline effect*(9) conveniently aided generation of both sequence- and phosphorylation site-specific ions. Supplementary Fig. 1 provides additional support of both dual T94 and S98 phosphorylation and singly phosphorylated peptides. Due to co-migration and co-fragmentation of phosphopeptides with LC-MS/MS(14), we also found site-specific fragment ions for individual phosphorylation at S89, T90, and S99, as indicated in Fig. 2b and Supplementary Fig. 1. Ultimately, either the lower abundance of these phosphopeptides, or *proline effect*-favorable fragmentation pathways, may have hindered the identification of other phosphorylation sites.

Kinase Assays

Cib2-Cdk1 and Mck1 were purified from yeast cells overexpressing TAP-tagged versions, as described(56). Overexpressed Cdc7-Dbf4-Flag purified from yeast cells was kindly provided by the lab of Stephen Bell (MIT). Full-length GST-Eco1 protein was purified from bacteria by induction with 0.2 mM IPTG, followed by chemical lysis, ultracentrifugation, and purification on glutathione-sepharose beads. Cdk1 was incubated at room temperature with 1 μ M GST-Eco1 in a 30 μ l reaction consisting of 25 mM HEPES (pH 8.0), 15 mM NaCl, 1 mM MgCl₂, 1 mM DTT, 4 μ Ci γ -³²P-ATP (3000 Ci/mmol), and 100 μ M unlabeled ATP. Reactions were stopped with SDS sample buffer, separated by SDS-PAGE, and visualized by autoradiography.

Peptide kinase assays were performed in duplicate in the same manner except in a 15 μ l total volume with 10 μ M peptide (Cdk1 reactions), 33 μ M peptide (Cdc7 reactions), or 5 μ M peptide (Mck1 reactions) for 45 min (Cdk1), 30 min (Mck1), or 15 min (Cdc7). Reactions were stopped by spotting on P81 phosphocellulose paper (Whatman), washed 5 min in 75 mM phosphoric acid five times, followed by a single 5 min wash in acetone. Air-dried papers were then submerged in scintillation fluid counted on a scintillation counter (Beckman Coulter LS 6500), and converted to moles of total phosphate using a standard curve. For each kinase, values were normalized by subtracting the counts obtained from a control reaction lacking peptide.

Fluorescence Anisotropy

Phosphopeptides containing the Eco1 degron sequence plus a C-terminal tyrosine and cysteine to provide a means of absorbance detection and to conjugate a FITC fluorophore

were synthesized by NeoBioSciences (Cambridge, MA) and purified by HPLC. Lyophilized peptides were resuspended in 1 ml 50 mM Tris-HCl (pH 7.4) to a final concentration of 1-3 mM and stored at -20°C. His₆-Cdc4-LP6DelA GST-Skp1 was purified from bacteria as described(3). Equilibrium binding of FITC-peptides to Cdc4 was measured by fluorescence polarization at room temperature in 96-well plates in triplicate (except the two highest Cdc4 concentrations were done in duplicate) in 40 µl 50 mM Tris-HCl (pH 7.4), 100 mM NaCl, 5 mM BME, 5% glycerol, 0.1 mg/ml BSA, plus 5 nM peptide and varying concentrations of Cdc4-Skp1. An LJL Biosystems Analyst AD plate reader was used with 495 nM excitation and 525 nM emission wavelengths, 10 reads per well, 100 ms integration time, and a z-height of 0.5 mm. Background fluorescence was normalized to a reaction lacking peptide. Data were analyzed using Prism software.

Damage-Induced Cohesion Assay

P_{SCC1}-scc1(TEV268)-HA₃:hphNT1:P_{SCC1}:natNT2:P_{MET25}-GFP-SCC1 trp1::TRP1:P_{GALI}-NLS-myc₆-TEV-NLS₂ ura3::lacO₂₅₆:LEU2 his3::P_{CUP1-1}-GFP-LacI:HIS3 cells were grown overnight in YEP media containing 2% raffinose, then arrested in mitosis using nocodazole for 3 h at 30°C. Cultures were transferred to synthetic media lacking methionine (to induce expression of wild-type Scc1) and containing nocodazole plus either 333 µg/ml zeocin (first experiment) or 2 µM 4-NQO (second experiment) for 1.5 h to establish cohesion or not. Galactose was then added to 2% for 2 h to express TEV protease and cleave the cohesion established during S phase. 100 µM CuSO₄ was added for the last 30 min to fully induce GFP-LacI expression, followed by fixation of cells

with 4% paraformaldehyde for 8 min. Cells were washed, resuspended in dibasic sodium phosphate buffer, affixed to concanavalin A-coated slides, and visualized by epifluorescence microscopy. The *scc1-K84,210R* strain has the two lysines mutated in the copy of *SCC1* under the *MET25* promoter, which is induced concurrent with DNA damage, while *scc1(TEV268)* under the endogenous promoter has these lysines intact.

FIGURE LEGENDS

Figure 1. Analysis of the contribution of individual Cdk1 sites to Eco1 degradation.

(a) Schematic of Eco1 domain structure highlighting the four Cdk1 consensus sites. PIP, PCNA-interacting protein domain; NLS, nuclear localization sequence.

(b) Cultures of the indicated yeast strains were arrested in mitosis with 15 $\mu\text{g/ml}$ nocodazole for 3 h at 30°C, followed by addition of 100 $\mu\text{g/ml}$ cycloheximide (CHX). At the indicated times, urea lysates were prepared for analysis by SDS-PAGE and western blotting, using Pgk1 as a loading control. The Eco1-4A mutant lacks all four Cdk1 consensus sites.

(c) Lysates from the zero time point in (b) were analyzed on an SDS-PAGE gel containing 10 μM Phos-tag reagent to slow the mobility of phosphorylated proteins.

(d) GST-Eco1 protein purified from bacteria was incubated with purified Clb2-Cdk1 and radiolabeled ATP for the indicated times, and analyzed by SDS-PAGE and autoradiography.

Figure 2. Mass spectrometry reveals non-Cdk1 phosphorylation of Eco1.

(a) Eco1-Flag₃His₆ was purified from yeast cultures in which *CDC4* expression was repressed, and then digested with trypsin and subjected to analysis by mass spectrometry (see Methods). A representative phosphopeptide spectrum is shown, with sequence-informative fragmentation ions summarized on the peptide sequence and annotated in blue (b-ions), green (y-ions), orange (c-ions), and purple (a-ions) on the spectra; phosphorylation site-specific ions are in red. Phosphate neutral loss (*), water loss (⁰), and ammonia loss (@) are annotated on b- and y-ions on the spectra. Different combinations of phosphate neutral loss and water and ammonia loss from precursor ions are annotated in black as [M+2H]⁺².

(b) Phosphopeptides identified by tandem mass spectrometry in order of confidence. The number of spectra identified for each phosphopeptide is listed, along with the calculated and measured monoisotopic masses of the phosphopeptides ([M+H]⁺) and the accuracy of the mass measurements in parts per million. *A subset of the HPLC fragment ions from these spectra showed evidence for phosphates on the indicated alternative residues. See Supplementary Fig. 1 for all annotated spectra.

(c) Strains with the indicated mutations were arrested in nocodazole, treated with cycloheximide (CHX) for the indicated times, then lysed in urea buffer and analyzed by western.

(d) Cells containing the indicated *ECO1* mutants were arrested in 15 μg/ml nocodazole for 3 h, and urea lysates were analyzed on an SDS-PAGE gel containing 10 μM Phos-tag reagent to slow migration of phosphorylated proteins, followed by western blotting.

Figure 3. Cdc7-Dbf4 and Mck1 are necessary for full degradation of Eco1 and phosphorylate Eco1 peptides *in vitro*.

(a, b) The indicated strains were arrested in mitosis with nocodazole and treated with cycloheximide (CHX) as in Fig. 1b. At the indicated times, urea lysates were prepared for analysis by SDS-PAGE and western blotting, using Pgk1 as a loading control.

(c) Synthetic peptides based on residues 91-103 of Eco1 (plus an additional C-terminal lysine; sequences at right) were incubated with the indicated purified kinase and γ -³²P-ATP (see Methods for details). For each kinase, phosphate incorporation was normalized to a background control reaction containing no peptide. Values are means from two independent reactions (error bars indicate SEM).

Figure 4. Phosphopeptide binding to Cdc4.

(a,b) FITC-conjugated phosphopeptides derived from Eco1 were incubated with increasing concentrations of Cdc4-Skp1 complex *in vitro*, and the polarization of the fluorescent peptides was used to measure binding. Values are means from two or three experiments (error bars indicate SEM). Data for the “no phosphate”, “94”, and “94-98” peptides in (b) are reproduced from (a). The residues in brackets are for conjugation and purification purposes and are not part of the Eco1 sequence.

Figure 5. Correct phosphate spacing is essential for Eco1 turnover.

(a–d) The indicated strains were arrested with nocodazole, followed by cycloheximide treatment and analysis of protein abundance by western blotting. Both *dbf4Δ* strains contain the *MCM5-P83L* suppressor mutation.

Figure 6. DDK activity limits Eco1 degradation to late S phase.

ECO1-TAP (a) or *ECO1-N97Δ-TAP* cells (b) were arrested in G1 with 15 μg/ml α-factor (αF) for 3 h and then released. At the indicated times, samples were harvested for analysis by western blotting and microscopy. To visualize phosphorylated forms of Eco1, samples were run on separate SDS-PAGE gels containing Phos-tag reagent.

Figure 7. DDK inhibition allows damage-induced cohesion establishment.

(a) The indicated strains were arrested in 15 μg/ml nocodazole plus 200m hydroxyurea, followed by addition of cycloheximide (CHX). At the indicated times, urea lysates were prepared for analysis by SDS-PAGE and western blotting, using Pgk1 as a loading control. The *sml1Δ* deletion is required for viability of *mec1Δ* cells.

(b) The indicated strains were arrested in mitosis with either nocodazole or hydroxyurea, followed by treatment with cycloheximide (CHX). At the indicated times, urea lysates were prepared for analysis by SDS-PAGE and western blotting, using Pgk1 as a loading control.

(c) Separation of GFP-tagged sister chromatids was used to measure sister-chromatid cohesion in mitotic cells treated with DNA damaging agents (see Methods for details). At least 200 cells were counted, and an average taken from two biological repeats; error bars

represent the SEM. The differences between wild-type and *scc1-K84,210R*, *dbf4-m25*, and *ECO1-N97Δ* are each statistically significant ($P=0.004$).

(d) Model of sequential Eco1 phosphorylation and ubiquitination. Beginning in early S phase, Cdk1 catalyzes phosphorylation of S99, which primes Cdc7-Dbf4 to phosphorylate S98 in late S phase through mitosis. This primes Mck1 to phosphorylate T94 and create a high-affinity binding site for SCF-Cdc4, leading to ubiquitination and subsequent destruction by the proteasome. The DNA damage response blocks this sequence of events by inhibiting Cdc7, reactivating cohesion establishment after S phase.

Supplementary Figure 1. Mass spectrometry data.

(a-d) Spectra from all identified phosphopeptides, labeled as in Fig. 2a. Additional phosphorylation site-informative fragment ions are annotated in black with b- or y-ion types circled, and correspond to phosphorylation of the residues in outlined letters. In panel (b), inset is magnification of boxed region.

Supplementary Figure 2. *In vivo* phosphorylation of S99 in Eco1 spacing mutants.

Urea lysates from the zero time points in Figures 5c and 5d were run on a gel containing 10 μ M Phos-tag reagent to slow the migration of phosphorylated proteins, then examined by western.

Figure 2

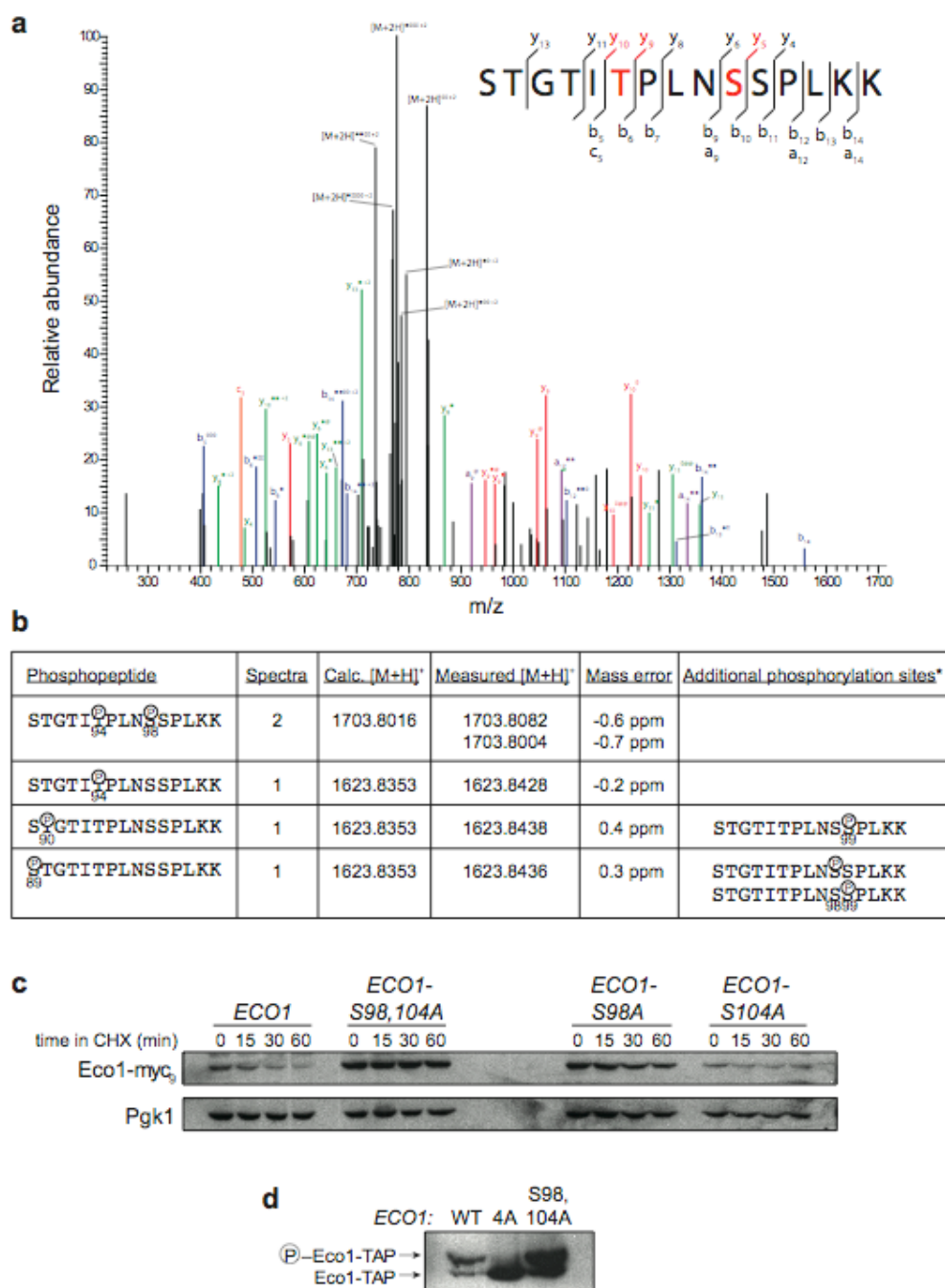


Figure 3

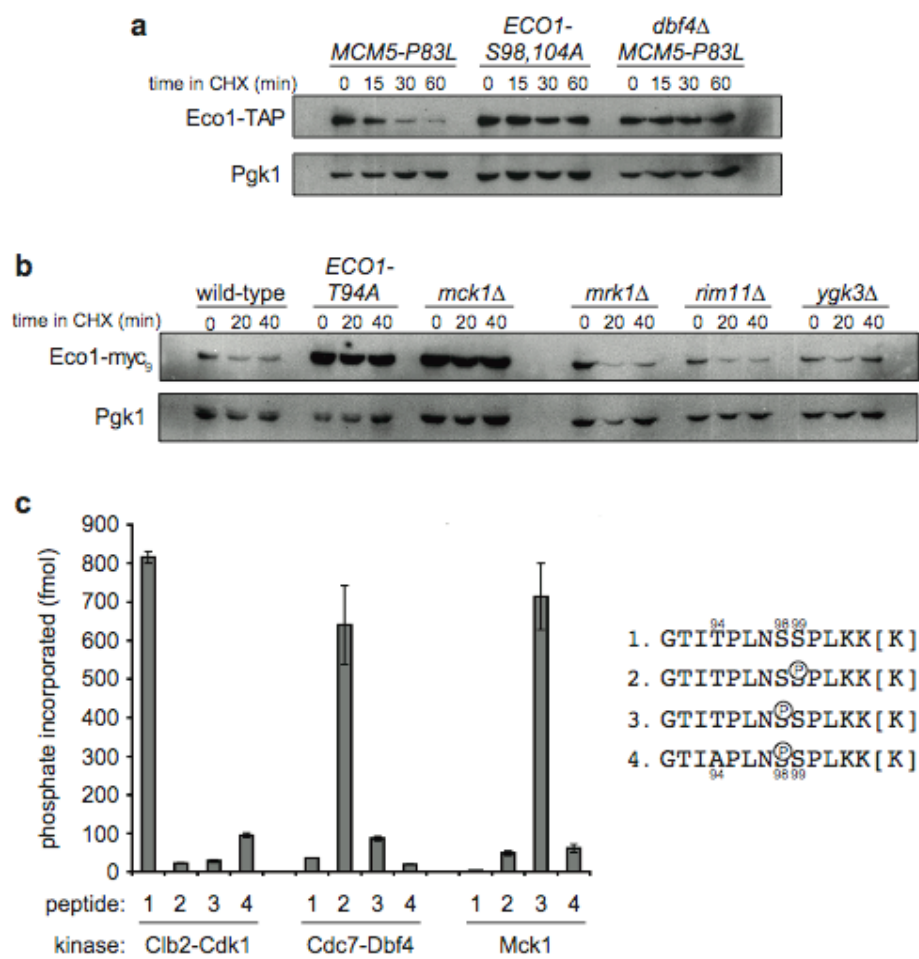


Figure 4

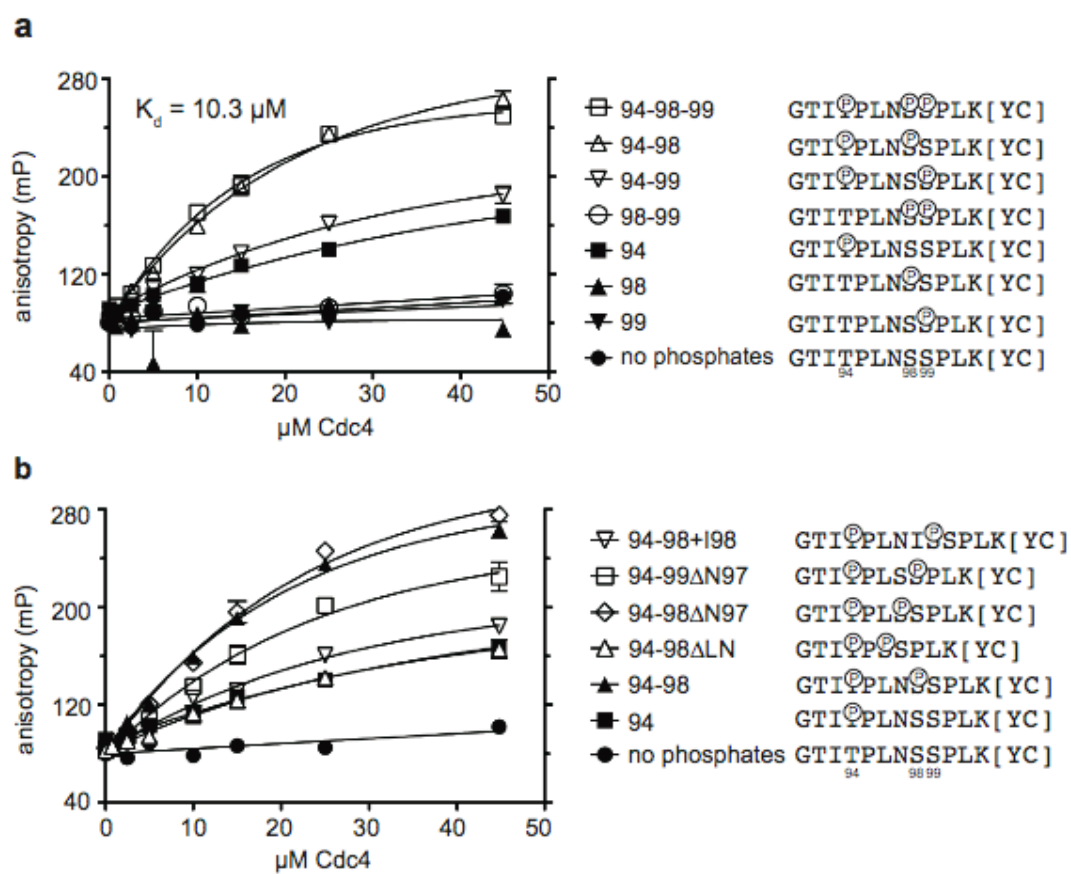


Figure 5

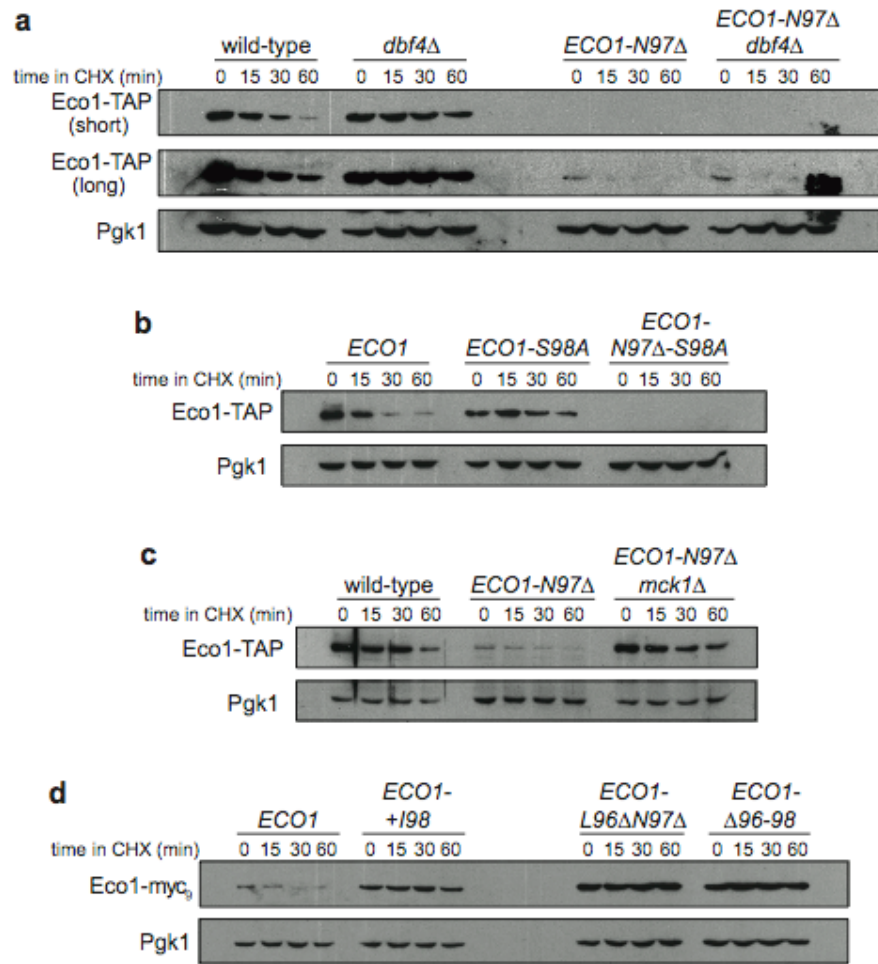


Figure 6

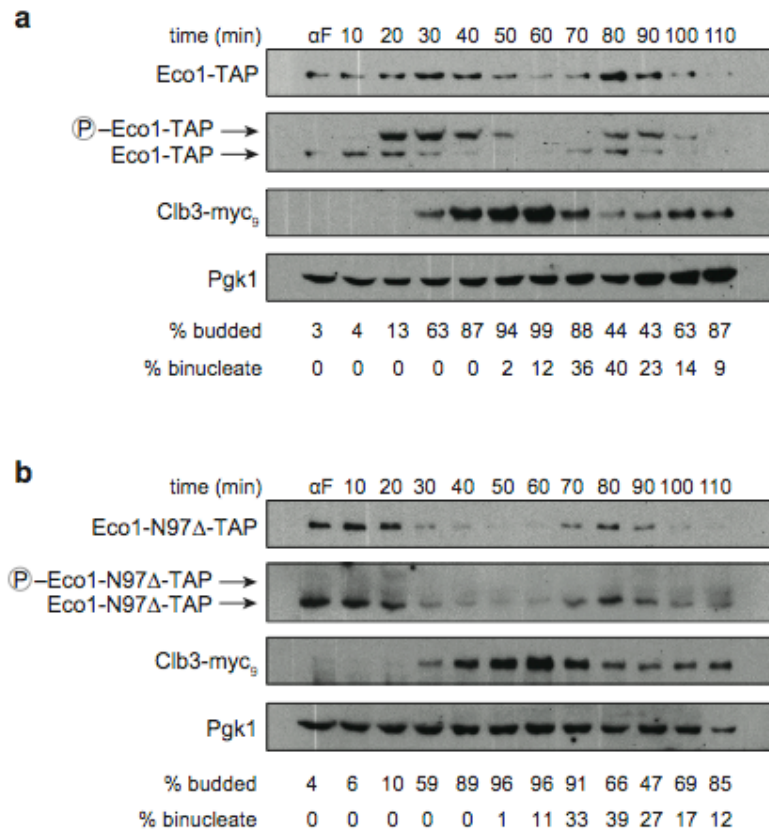
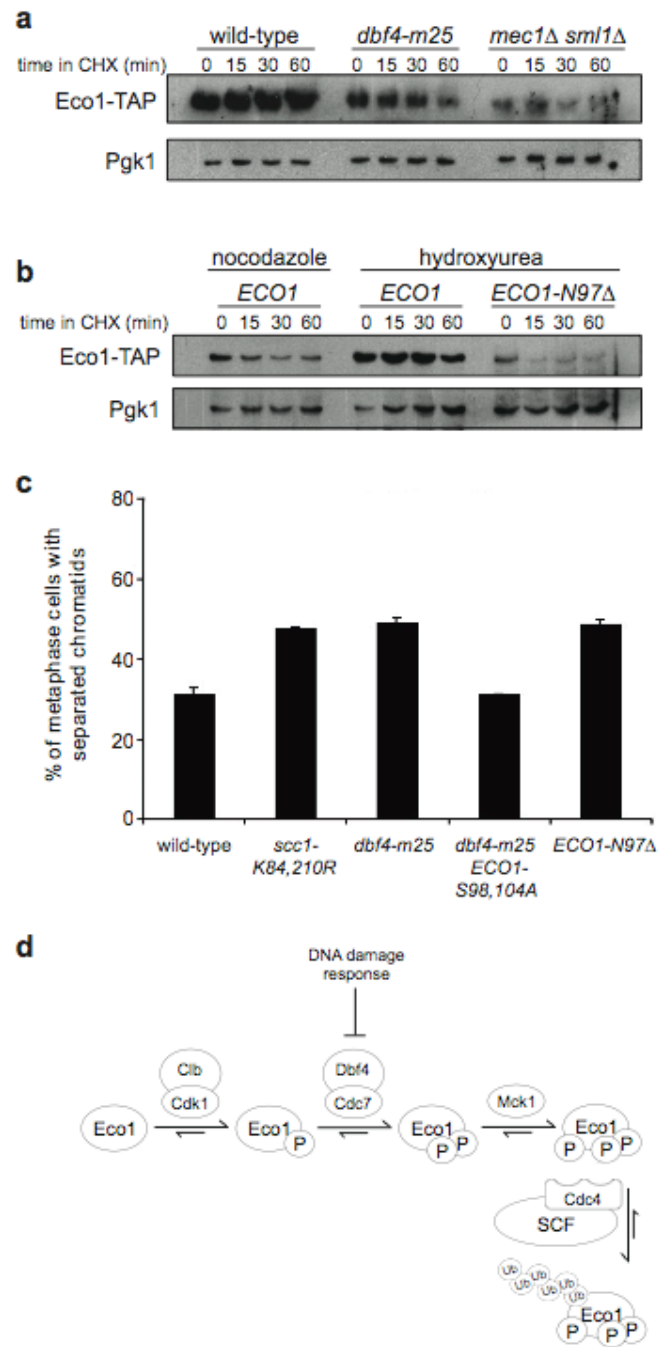
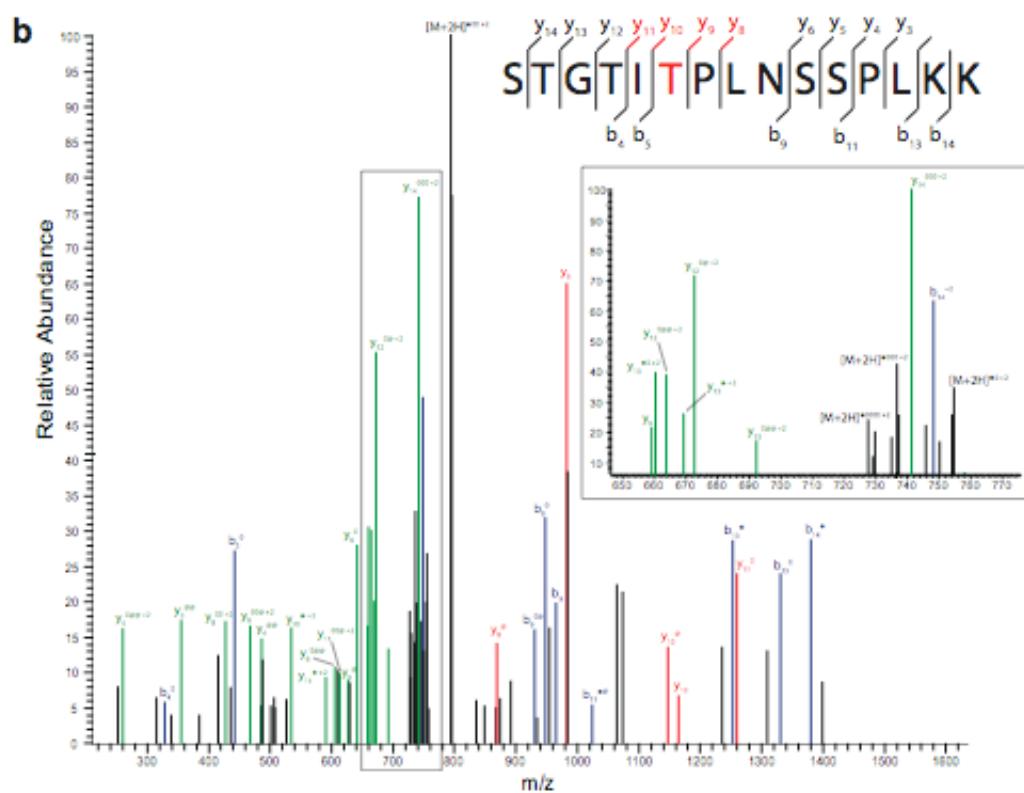
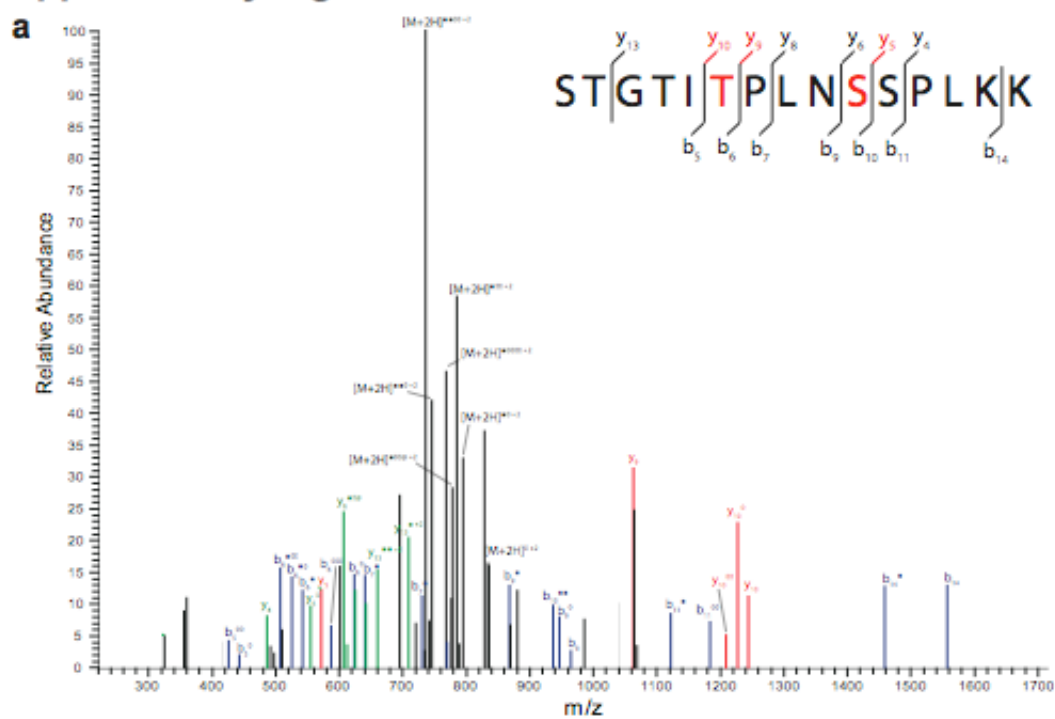


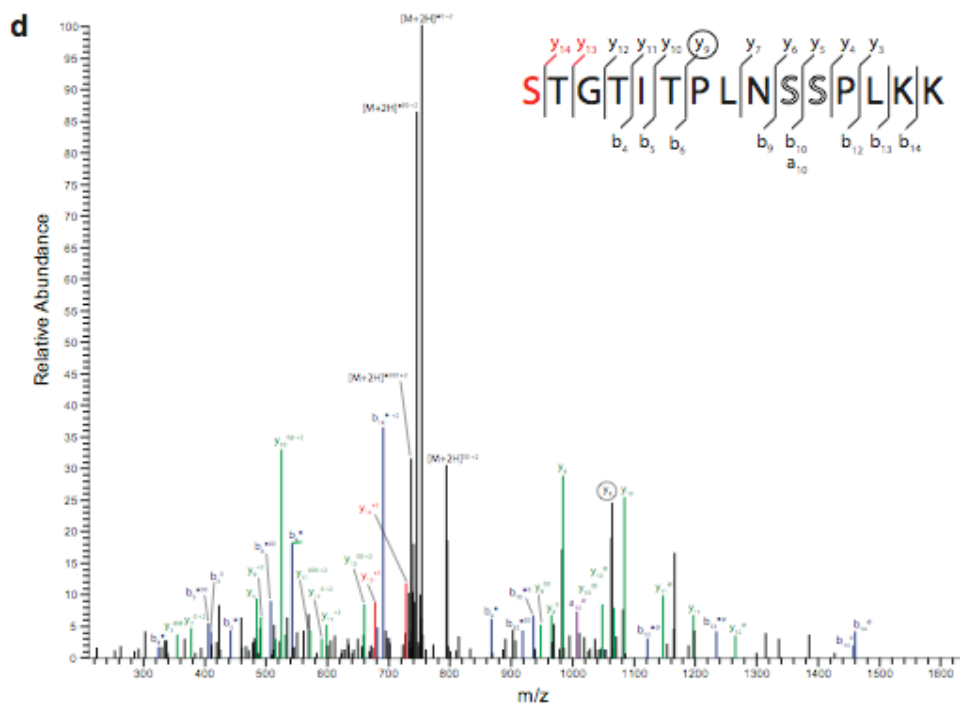
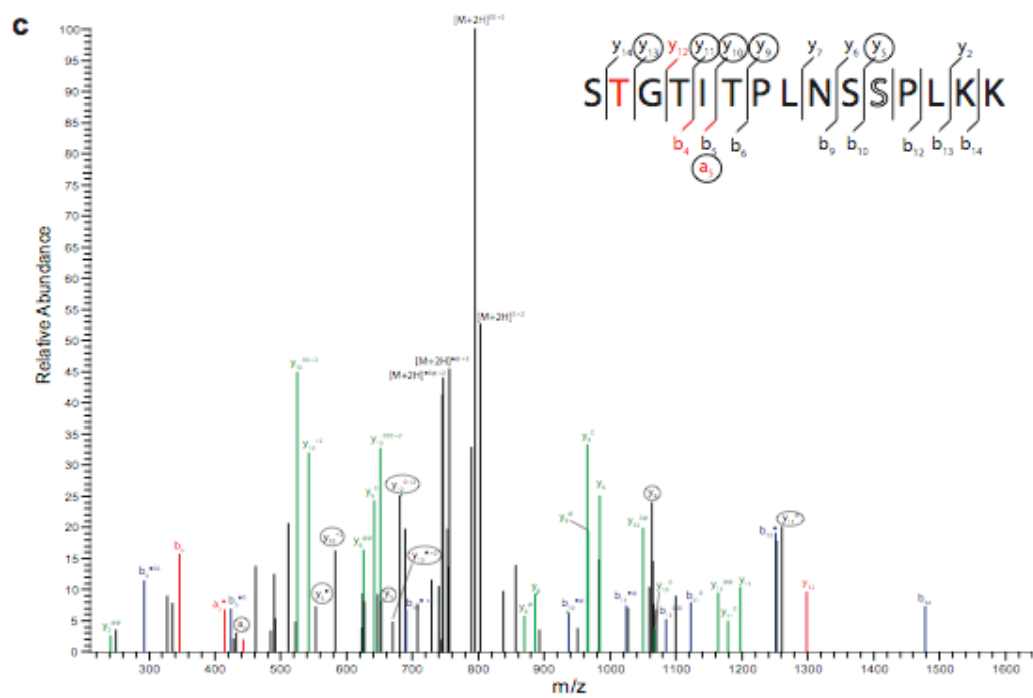
Figure 7



Supplementary Figure 1



Supplementary Figure 1



Supplementary Table 1. Cdc4 substrates in *Saccharomyces cerevisiae*.

Where known, sites of phosphorylation are labeled in red. "Spacing" refers to the number of amino acids between diphosphates in the degron.

Protein	Phosphodegron	Spacing	Kd (μ M)	Reference
Ash1	AWSITPPVTPPMSPPTN	3	0.074	Liu et al, 2011
Cdc6	DVTPESSEPEKL VPLTPTSPVK	3 3		Perkins et al, 2001
Cib6	MNCIPSPISERKIQ ESSINLTPHSTNEKK NYLMDTQSPYHLKSS	unknown unknown unknown		Jackson et al, 2006
Cln3	unknown			Landry et al, 2012
Ctf13	unknown			Kaplan et al, 1997
Eco1	GTITPLNSSPLK	3	10.3	this study
Far1	LNLSPISPPSLKKT	unknown		Gartner et al, 1998
Gcn4	FSSSTDSTPMF VSTTSFLPTPVLED	3 unknown		Kornitzer et al, 1994 Meimoun et al, 2000
Hac1	ATLSPKSMRD	2		Pal et al, 2007
Hsl1	unknown			Mizunuma et al, 2001
Rcn1	FLISPPASPP	3		Kishi et al, 2007
Sic1	MTPSTPPRSRG PVTPSTTKSFK NGLTSPQRSPPFK	3 2 3	4 7 2.6	Hao et al, 2007
Swi5	unknown			Kishi et al, 2008
Ste5	unknown			Garrenton et al, 2009
Tec1	KLLTPITASN	2	0.076	Bao et al, 2010

Supplementary Table 2. Strains and plasmids used in this study.

Strain	Genotype
BY4741	WT S288C (ATCC 201388): MATa, his3Δ1, ura3Δ0, leu2Δ0, met15Δ0
8GS6-A2	ECO1-TAP:HIS3 MATa
NL184	URA3:ECO1-4A-TAP MATa
NL314	pSCC1-SCC1(TEV268)-HA3:hphNT1:pSCC1:natNT2:pMET25-GFP-SCC1 trp1::TRP1:pGAL1-TEV ura3::lacO256:LEU2 his3::pCUP1-GFP-LacI:HIS3 MATalpha
NL358	ECO1-TAP:SkHIS3 mec1::kanMX sml1::LEU2 MATa
NL475	URA3:ECO1-S98,104A-TAP:SkHIS3 MATa
NL546	URA3:ECO1-S98A-TAP:SkHIS3 MATa
NL547	URA3:ECO1-S104A-TAP:SkHIS3 MATa
NL562	ECO1-TAP:HIS3 dbf4-m25:LEU2:dbf4::kanMX MATa
NL563	ECO1-TAP:HIS3 MCM5-P83L MATa
NL569	ECO1-Flag3His6:KIURA3 pCDC4:natNT2:pGALS-HA3-CDC4 sic1::kanMX MATa
NL578	ECO1-TAP:HIS3 dbf4::kanMX MCM5-P83L MATalpha
NL579	dbf4-m25:LEU2:kanMX pSCC1-SCC1(TEV268)-HA3:hphNT1:pSCC1:natNT2:pMET25-GFP-SCC1 trp1::TRP1:pGAL1-TEV ura3::lacO256:LEU2 his3::pCUP1-GFP-LacI:HIS3 MATalpha
NL591	URA3:ECO1-N97Δ-TAP:HIS3 MATa
NL592	URA3:ECO1-N97Δ-S98A-TAP:SkHIS3 MATa
NL593	URA3:ECO1-N97Δ-TAP:SkHIS3 dbf4::kanMX MCM5-P83L MATalpha
NL603	pSCC1-SCC1(TEV268)-HA3:hphNT1:kanMX:pSCC1:natNT2:pMET25-GFP-scc1-K84,210R trp1::TRP1:pGAL1-TEV ura3::lacO256:LEU2 his3::pCUP1-GFP-LacI:HIS3 MATa
NL605	ECO1-myc9:natNT2 MATalpha
NL606	URA3:ECO1-S98,104A-myc9:natNT2 MATa
NL607	URA3:ECO1-S98A-myc9:natNT2 MATa
NL608	URA3:ECO1-S104A-myc9:natNT2 MATa
NL609	URA3:ECO1-4A-myc9:natNT2 MATa
NL610	URA3:ECO1-S67A-myc9:natNT2 MATa
NL611	URA3:ECO1-T94A-myc9:natNT2 MATa
NL612	URA3:ECO1-S99A-myc9:natNT2 MATa
NL613	URA3:ECO1-S105A-myc9:natNT2 MATa
NL619	URA3ECO1+I98-myc9:natNT2 MATa
NL620	dbf4-m25:LEU2:kanMX URA3:ECO1-S98,104A pSCC1-SCC1(TEV268)-HA3:hphNT1:pSCC1:natNT2:pMET25-GFP-SCC1 trp1::TRP1:pGAL1-TEV ura3::lacO256:LEU2 his3::pCUP1-GFP-LacI:HIS3 MATalpha
NL625	URA3:ECO1-L96ΔN97Δ-myc9:natNT2 MATalpha
NL626	URA3:ECO1-Δ96-98-myc9:natNT2 MATalpha

CHAPTER 4: CONCLUSION

One hallmark of life is the ability to self-reproduce, which occurs at all levels of biology: from the first molecules that could catalyze their own synthesis to the elaborate mating rituals of multicellular organisms. At the level of single cells, self-reproduction takes the form of the cell division cycle. The cell cycle is not merely a collection of mechanisms that double the cellular contents, but also the underlying machinery that ensures each event occurs sequentially and faithfully.

In this thesis I have presented data identifying the regulation of sister-chromatid cohesion by the cell cycle machinery. This is achieved through the phosphorylation-mediated degradation of the cohesion-promoting protein Eco1. I have found that degradation of Eco1 in late S phase through M phase prevents cohesion establishment during this time. The regulation of this protein is complicated, as turnover of Eco1 requires three distinct kinases to create a Cdc4 phosphodegron with correctly spaced phosphates. A strict sequence of phosphate-priming events are necessary to fully phosphorylate Eco1, and blocking this sequence by inhibiting one kinase, Cdc7-Dbf4, reactivates cohesion establishment in response to DNA damage. The regulatory scheme uncovered here (see Chapter 3 Figure 6D for pictorial summary) is able to both turn off the generation of new cohesion when it is counter-productive (when cohesin is being proteolyzed by separase in mitosis, Chapter 2), as well as turn on cohesion generation when it is advantageous to do so (to facilitate repair of damaged DNA, Chapter 3).



The experiments in this dissertation point to Eco1 as a hub for regulation of cohesion generation (Figure 1A), analogous to the role of APC in cohesion dissolution. Both Eco1 and APC are the “executors” of cohesion creation/destruction and thus are subject to many forms of regulation that ensure each is active only at the appropriate time in the cell cycle. An interesting feature of Eco1 and APC is that both affect cohesion indirectly: Eco1 acetylates cohesin to inhibit the “anti-establishment” activity of Wpl1 and Pds5, and the APC ubiquitinates securin to activate separase and proteolyze cohesin. Acetylation of Smc3 does not itself affect the affinity of cohesin for chromatin, and the APC has not been reported to directly ubiquitinate Scc1. This is likely because every extra step in a pathway increases the opportunity for additional regulatory inputs, as illustrated by the involvement of Cdc7-Dbf4 in Eco1 degradation allowing cohesion establishment to be reactivated by the DNA damage response (Chapter 3). Another feature of the cohesion creation and destruction pathways is their reciprocal nature—nearly every positive APC input negatively affects Eco1, and vice versa. This makes teleological sense of course, as activation of the DNA damage response, for example, inhibits the APC in order to prevent progression past metaphase until the damage is repaired (1), which is facilitated by cohesion (90).

The discovery of new cohesion establishment after induction of DNA damage in metaphase (95,116) was initially surprising since it had been shown that cohesion establishment is normally strictly limited to S phase (26,30,95,96,112,116). It was subsequently found that the phosphorylation of Scc1-S83 by the checkpoint kinase Chk1 is required to establish damage-induced cohesion (29). This modification is also sufficient to promote establishment independent of DNA damage, as *scc1-S83D* strains

generate new cohesion in an undamaged metaphase arrest (when Eco1 levels are kept low). I have shown that stabilization of Eco1 is necessary to establish damage-cohesion (Chapter 3) and sufficient to generate cohesion in a normal metaphase arrest (Chapter 2). It therefore appears that Scc1 phosphorylation and Eco1 stabilization are each necessary and sufficient to establish cohesion after S phase. It is hard to imagine how damage-induced cohesion requires both factors, while normal S-phase cohesion needs only one. There could be stricter requirements for establishment in a damage arrest than a normal metaphase, though this is counterintuitive since it is beneficial to the cell to generate new cohesion upon damage and harmful in the absence of damage. It is known that a different cohesin subunit is acetylated in damage than in S phase (Scc1 versus Smc3, respectively) (30), but this does not resolve the paradox since the stabilized Eco1-4A mutant also acetylates Scc1-K84 and K210 in an undamaged metaphase (Figure 1B). A better understanding of the mechanics of post-S phase cohesion is needed to fully comprehend its regulation.

A curious feature of cohesion regulation is that the spindle assembly checkpoint (SAC), unlike the DNA damage checkpoint, is only known to affect the cohesion dissolution pathway (via the APC activator Cdc20) and not the cohesion generation pathway (126). This seems odd because the SAC senses lack of tension on the microtubule-attached kinetochores (5) and established cohesion is necessary to create this tension (104). It is reasonable to expect, then, that activation of the SAC would reactivate cohesion establishment since the lack of tension is sometimes due to lack of cohesion. In almost every western blot in this thesis, however, I used an SAC-induced arrest to measure Eco1 degradation in metaphase, and all post-replicative cohesion establishment

assays were also done in an SAC arrest. So the kinetochore biorientation surveillance mechanism does not seem to take advantage of a regulatory pathway very amenable to additional inputs, at least not that has been uncovered. This is either for adaptive reasons (it would be dangerous to activate the establishment machinery with unpaired sister chromatids) or simply for trivial reasons (the mutations required interfere with something else or have just not occurred yet).



Because extra steps in pathways provide extra regulatory opportunities, it is reasonable to predict that there are more undiscovered sources of cohesion regulation. For instance, there is nothing currently known about control of Wpl1's anti-establishment activity. I noticed a small change in mobility of Wpl1-TAP when run on a polyacrylamide gel containing phosphate-binding reagent (Figure 2A). This phosphoshift was present in nocodazole- and damage-arrested cells but not in cells arrested in alpha factor. There also appeared to be two levels of phosphoshift: Wpl1 from a nocodazole arrest displayed a greater shift than Wpl1 from a damage arrest. This may suggest Wpl1 is phospho-regulated in the later stages of the cell cycle and upon DNA damage.

Two plausible kinases responsible for the metaphase super-shift of Wpl1 are Cdc7-Dbf4 and the Polo kinase Cdc5. Wpl1 contains several consensus sites for Cdc7 (S/T-D/E/pS/pT) and Cdc5 (D/E/N-x-S/T), 12 and 23 respectively, which could be due in part to the highly negative character of Wpl1. If Cdc7 and/or Cdc5 do in fact phosphorylate Wpl1, these phosphates might be predicted to promote Wpl1 activity since they are present in metaphase but not in a DNA damage arrest. This hypothesis is attractive for a couple reasons: 1) both kinases are already known to antagonize cohesion

(Figure 1A), Cdc7 through Eco1 degradation (Chapter 3) and Cdc5 through increased separase activity toward phosphorylated Scc1 (2); 2) regulating Wpl1 activity over the cell cycle may make it easier to establish cohesion during S phase, although Wpl1 likely has some anti-establishment activity in S phase since cohesion does not get established in the absence of Eco1 activity (91,108). However, my initial attempts to demonstrate Cdc5 activity toward bacterially-purified Wpl1 gave no result (data not shown). This could either indicate that Wpl1 is not a Cdc5 substrate, or that a priming phosphorylation is required to interact with the Polo-box domain of Cdc5 (which interacts with S-pS-[P] motifs, where [P] is common but not strictly required (92)).

Wpl1 also contains one full Cdk1 consensus site (S/T-P-x-K/R) at T13.

Incubation of recombinant Wpl1 with Cdk1 *in vitro* resulted in robust incorporation of radioactive phosphate, dependent on the presence of the single Cdk1 site (Figure 2B).

Wpl1 was equally phosphorylated by Cdk1-Clb2 and -Clb5, possibly indicating that it is a general Cdk1 substrate that is mostly phosphorylated by Clb2 *in vivo* (56).

Phosphorylation of T13 is not responsible for the observed phosphoshift however, as a Wpl1-T13A mutant displayed the same mobility changes as wild-type (Figure 2A). Some other mitotic kinase that is not inhibited by the DNA damage response, such as the Aurora homolog Ipl1, is therefore responsible for the metaphase shift. Ipl1 is activated by the SAC, so this hypothesis would connect the spindle checkpoint to regulation of cohesion establishment. The nature of this regulation would shed light on whether or not it is advantageous to establish new cohesion when kinetochores are not under tension.

As a preliminary test of Wpl1 regulation, I investigated the effect of Wpl1 overexpression on sister-chromatid cohesion (Figure 2C). Cohesion was assayed visually

by the appearance of one or two GFP dots in a *ura3::lacO LacI-GFP* strain arrested in metaphase with nocodazole (see Chapter 2, Figure 2B). I observed an intermediate loss of cohesion both when Wpl1 overexpression was induced before the metaphase arrest (“Gal into noc” in Figure 2C) and after the arrest (“noc into Gal”), suggesting Wpl1 can oppose cohesion maintenance in addition to establishment. This might be analogous to the removal of arm cohesion in prophase by Wapl in metazoans (21,28,47,65,98,99,117). The data presented here are not conclusive, but do indicate that low Wpl1 levels are crucial to establish and maintain cohesion, and that Wpl1 activity is limiting for counteracting cohesion. One interpretation of this experiment is that Wpl1 overproduction overcomes some inhibitory regulation (or lack of activating regulation), just as overexpressing Eco1 leads to cohesion establishment after S phase (116). Alternatively, a high concentration of Wpl1 may be able to overcome the reduced binding to cohesin thought to be caused by Smc3 acetylation (100). If excess Wpl1 activity does counteract cohesion maintenance, the putative Wpl1 phosphoregulation (Figure 2A) may actually constitute the yeast equivalent of the prophase pathway, which is promoted by Polo kinase (the Cdc5 homolog) in other eukaryotes (28,99).



One key aspect of the Eco1 regulatory system is modularity. By dividing a single task into many highly specialized subroutines that can be shuffled around in a multitude of ways, the capability of the system is increased exponentially. The concept of modularity is found in many biological systems beyond regulatory networks, from language acquisition to the advent of multicellularity (63). The most primitive form of language likely began with extremely simple connections between sounds and meanings

(for example, monkey alarm calls) and has evolved into an intricate grammatical system capable of conveying complex thoughts and intentions (for example, a dissertation). This is attributable in part to the modularity of sentences, which are composed of words with agreed-upon meanings whose exact arrangement conveys meaning. If language was not modular, each intended meaning would require its own unique sound arrangement, limiting the maximum amount of information it can theoretically contain. Multicellular organisms, likewise, began as small groups of cells that stuck together (possibly by incomplete cytokinesis (17,45,81)) and eventually led to the phenotypic and behavioral complexity of the biosphere today. Division of labor among cell types (differentiation) has been critical for this advancement, which greatly expanded the fitness potential of an organism. Similarly, the cell cycle utilizes modular regulatory molecules (see Chapter 1 Figure 1) to precisely coordinate diverse events (such as DNA replication and cohesion establishment) as well as respond to a changing environment.

Modularity also allows a system (such as the cell cycle or human language) to be more “evolvable”—that is, able to adapt more easily. This is partly because it takes fewer mutations to add an additional layer of regulation. Only a single residue (S98) was needed to turn a degron that was Cdk1-dependent and (more or less) timed with the cell cycle—essentially the Eco1-N97 Δ mutant—to a degron that was both better timed with a normal cycle and responsive to DNA damage. Addition of Cdc7 to this regulatory pathway was relatively straightforward because it has a recognition motif capable of binding previously-modified substrates. The same is true of GSK-3 and Cdc4, which have consensus sequences completely dependent on other regulatory proteins, making them great co-regulating “top-players” (Chapter 1 Figure 1). The modularity of these co-

regulatory proteins allowed damage responsiveness to be easily incorporated into the cohesion regulation pathway without having to reinvent the wheel.



There is one final question that needs addressing: why has such a complicated regulatory mechanism evolved for something with such a subtle phenotypic consequence? Why is cohesion generation not just constitutive? I believe it is because chromosome biology is under incredibly strong selective pressure to be precisely regulated—better transmission of the material that actually creates the regulators is inherently highly favored. The level of intricacy uncovered in this thesis illustrates the extremely long timescale that evolution works on, how deep its influence can reach, and the remarkable complexity that natural selection is capable of producing. There is an anthropic principle at work here too: the observation of such regulatory complexity should be expected since the intellectual capacity necessary for such an observation itself requires such elaborate mechanisms.

Figure 1. Diagram of cohesion regulation pathways.

Only post-translational regulations are shown. Not meant to be exhaustive.

Figure 2. Wpl1 regulation *in vivo* and *in vitro*.

A) Cells containing *WPL1-TAP* or *WPL1-T13A-TAP* were grown asynchronously (asynch) or arrested in 20 $\mu\text{g/ml}$ α -factor, 200 mM hydroxyurea HU), or 20 $\mu\text{g/ml}$ nocodazole (noc) for 3 h at 30°C. Urea lysates were made and run on a polyacrylamide gel containing 10 μM Phos-tag reagent (41).

B) Bacterially-prepared GST-TEV-Wpl1 (227 nM) or GST-TEV-Wpl1-T13A (265 nM) was incubated with γ -³²P-ATP and Clb2-Cdk1 or Clb5-Cdk1, whose activities were equalized towards the general substrate histone H1.

C) Strains containing *ura3::lacO pCUP1-GFP-LacI* were arrested in 20 $\mu\text{g/ml}$ nocodazole for 3 h at 30°C. pGAL1-HA₂-Wpl1 was induced in 2% galactose either overnight (“Gal into noc”) or for 50 min after arresting in nocodazole (“noc into Gal”). 100 μM CuSO₄ was added to all cultures for 50 min to fully induce LacI-GFP. At least 100 cells were counted for each strain, and P=0.00000199, 0.00464, and 0.0156 for Eco1-kinase, Gal into noc, and noc into Gal respectively. Right, western blot to verify induction of pGAL1-HA₂-Wpl1. Left two lanes are cell lysates from cultures first arrested in nocodazole in raffinose-containing media before addition of galactose. “WT” strain does not contain the *pGAL1-HA₂-WPL1* construct.

Figure 1

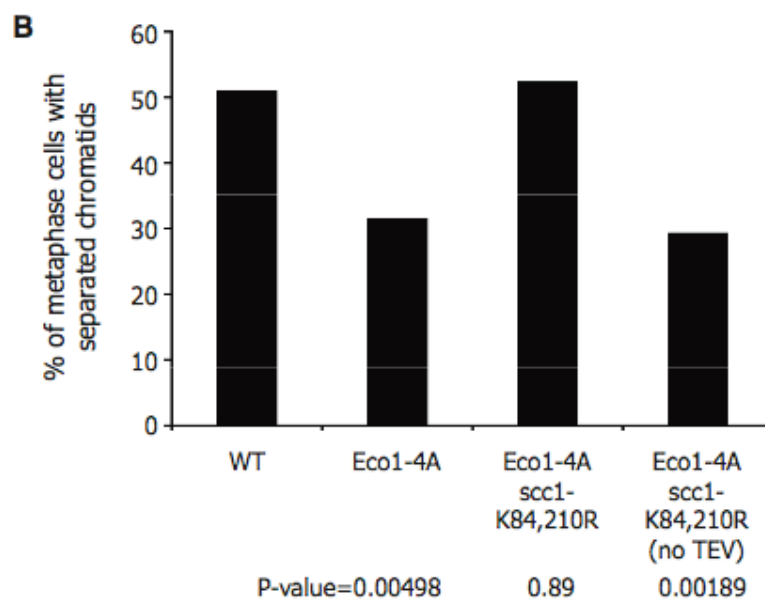
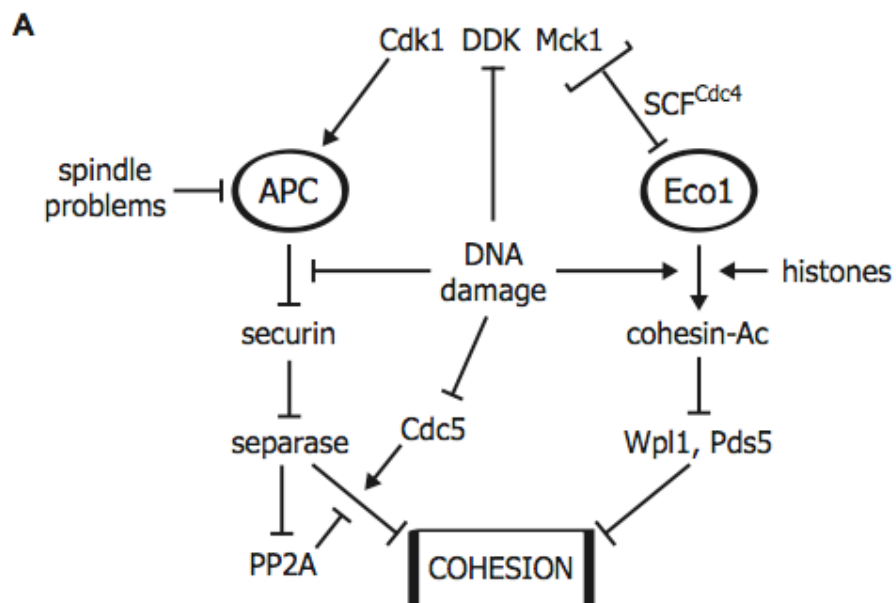
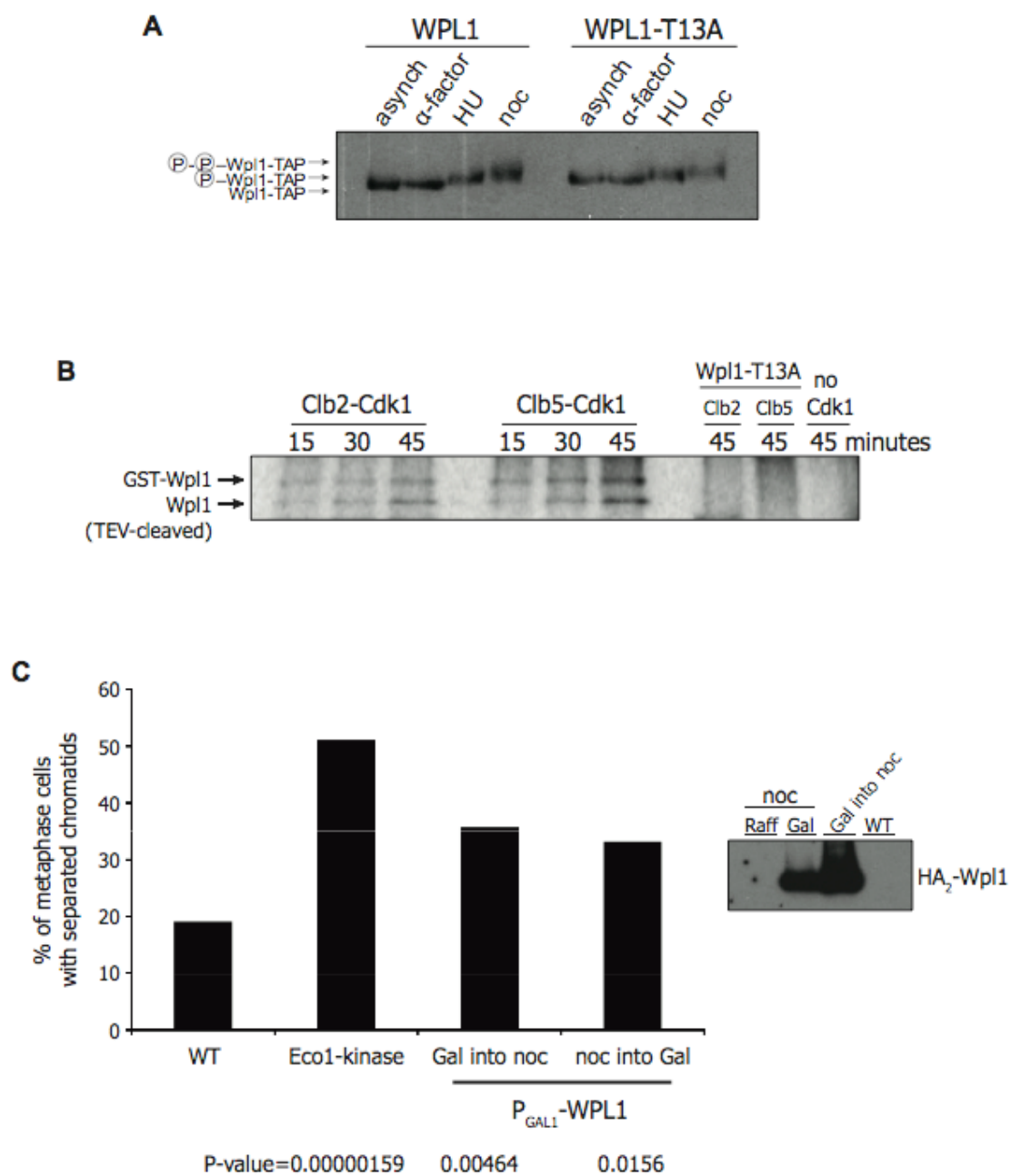


Figure 2



BIBLIOGRAPHY

1. Agarwal, R.; Tang, Z.; Yu, H.; Cohen-Fix, O. Two distinct pathways for inhibiting pds1 ubiquitination in response to DNA damage. *J Biol Chem* 278(45):45027-45033; 2003.
2. Alexandru, G.; Uhlmann, F.; Mechtler, K.; Poupart, M. A.; Nasmyth, K. Phosphorylation of the cohesin subunit Scc1 by Polo/Cdc5 kinase regulates sister chromatid separation in yeast. *Cell* 105(4):459-472; 2001.
3. Bao, M. Z.; Shock, T. R.; Madhani, H. D. Multisite phosphorylation of the *Saccharomyces cerevisiae* filamentous growth regulator Tec1 is required for its recognition by the E3 ubiquitin ligase adaptor Cdc4 and its subsequent destruction in vivo. *Eukaryot Cell* 9(1):31-36; 2010.
4. Beckouet, F.; Hu, B.; Roig, M. B.; Sutani, T.; Komata, M.; Uluocak, P.; Katis, V. L.; Shirahige, K.; Nasmyth, K. An smc3 acetylation cycle is essential for establishment of sister chromatid cohesion. *Mol Cell* 39(5):689-699; 2010.
5. Biggins, S.; Murray, A. W. The budding yeast protein kinase Ipl1/Aurora allows the absence of tension to activate the spindle checkpoint. *Genes Dev* 15(23):3118-3129; 2001.
6. Blondel, M.; Galan, J. M.; Chi, Y.; Lafourcade, C.; Longaretti, C.; Deshaies, R. J.; Peter, M. Nuclear-specific degradation of Far1 is controlled by the localization of the F-box protein Cdc4. *EMBO J* 19(22):6085-6097; 2000.

7. Borges, V.; Lehane, C.; Lopez-Serra, L.; Flynn, H.; Skehel, M.; Rolef Ben-Shahar, T.; Uhlmann, F. Hos1 deacetylates smc3 to close the cohesin acetylation cycle. *Mol Cell* 39(5):677-688; 2010.
8. Brands, A.; Skibbens, R. V. Sister chromatid cohesion role for CDC28-CDK in *Saccharomyces cerevisiae*. *Genetics* 180(1):7-16; 2008.
9. Brechi, L. A.; Tabb, D. L.; Yates, J. R., 3rd; Wysocki, V. H. Cleavage N-terminal to proline: analysis of a database of peptide tandem mass spectra. *Anal Chem* 75(9):1963-1971; 2003.
10. Breslow, D. K.; Cameron, D. M.; Collins, S. R.; Schuldiner, M.; Stewart-Ornstein, J.; Newman, H. W.; Braun, S.; Madhani, H. D.; Krogan, N. J.; Weissman, J. S. A comprehensive strategy enabling high-resolution functional analysis of the yeast genome. *Nat Methods* 5(8):711-718; 2008.
11. Cho, W. H.; Lee, Y. J.; Kong, S. I.; Hurwitz, J.; Lee, J. K. CDC7 kinase phosphorylates serine residues adjacent to acidic amino acids in the minichromosome maintenance 2 protein. *Proc Natl Acad Sci U S A* 103(31):11521-11526; 2006.
12. Ciosk, R.; Shirayama, M.; Shevchenko, A.; Tanaka, T.; Toth, A.; Nasmyth, K. Cohesin's binding to chromosomes depends on a separate complex consisting of Scc2 and Scc4 proteins. *Mol Cell* 5(2):243-254; 2000.
13. Cociorva, D.; D, L. T.; Yates, J. R. Validation of tandem mass spectrometry database search results using DTASelect. *Curr Protoc Bioinformatics Chapter 13:Unit 13 14*; 2007.

14. Courcelles, M.; Bridon, G.; Lemieux, S.; Thibault, P. Occurrence and detection of phosphopeptide isomers in large-scale phosphoproteomics experiments. *J Proteome Res* 11(7):3753-3765; 2012.
15. Doble, B. W.; Woodgett, J. R. GSK-3: tricks of the trade for a multi-tasking kinase. *J Cell Sci* 116(Pt 7):1175-1186; 2003.
16. Enserink, J. M.; Kolodner, R. D. An overview of Cdk1-controlled targets and processes. *Cell Div* 5:11; 2010.
17. Fairclough, S. R.; Dayel, M. J.; King, N. Multicellular development in a choanoflagellate. *Curr Biol* 20(20):R875-876; 2010.
18. Fiol, C. J.; Mahrenholz, A. M.; Wang, Y.; Roeske, R. W.; Roach, P. J. Formation of protein kinase recognition sites by covalent modification of the substrate. Molecular mechanism for the synergistic action of casein kinase II and glycogen synthase kinase 3. *J Biol Chem* 262(29):14042-14048; 1987.
19. Fonslow, B. R.; Niessen, S. M.; Singh, M.; Wong, C. C.; Xu, T.; Carvalho, P. C.; Choi, J.; Park, S. K.; Yates, J. R., 3rd. Single-step inline hydroxyapatite enrichment facilitates identification and quantitation of phosphopeptides from mass-limited proteomes with MudPIT. *J Proteome Res* 11(5):2697-2709; 2012.
20. Gabrielse, C.; Miller, C. T.; McConnell, K. H.; DeWard, A.; Fox, C. A.; Weinreich, M. A Dbf4p BRCA1 C-terminal-like domain required for the response to replication fork arrest in budding yeast. *Genetics* 173(2):541-555; 2006.
21. Gandhi, R.; Gillespie, P. J.; Hirano, T. Human Wapl is a cohesin-binding protein that promotes sister-chromatid resolution in mitotic prophase. *Curr Biol* 16(24):2406-2417; 2006.

22. Gerlich, D.; Koch, B.; Dupeux, F.; Peters, J. M.; Ellenberg, J. Live-cell imaging reveals a stable cohesin-chromatin interaction after but not before DNA replication. *Curr Biol* 16(15):1571-1578; 2006.
23. Ghaemmaghami, S.; Huh, W. K.; Bower, K.; Howson, R. W.; Belle, A.; Dephoure, N.; O'Shea, E. K.; Weissman, J. S. Global analysis of protein expression in yeast. *Nature* 425(6959):737-741; 2003.
24. Gray, C. H.; Good, V. M.; Tonks, N. K.; Barford, D. The structure of the cell cycle protein Cdc14 reveals a proline-directed protein phosphatase. *Embo J* 22(14):3524-3535; 2003.
25. Guldener, U.; Heck, S.; Fielder, T.; Beinhauer, J.; Hegemann, J. H. A new efficient gene disruption cassette for repeated use in budding yeast. *Nucleic Acids Res* 24(13):2519-2524; 1996.
26. Haering, C. H.; Schoffnegger, D.; Nishino, T.; Helmhart, W.; Nasmyth, K.; Lowe, J. Structure and stability of cohesin's Smc1-kleisin interaction. *Mol Cell* 15(6):951-964; 2004.
27. Hao, B.; Oehlmann, S.; Sowa, M. E.; Harper, J. W.; Pavletich, N. P. Structure of a Fbw7-Skp1-Cyclin E Complex: Multisite-Phosphorylated Substrate Recognition by SCF Ubiquitin Ligases. *Mol Cell* 26(1):131-143; 2007.
28. Hauf, S.; Roitinger, E.; Koch, B.; Dittrich, C. M.; Mechtler, K.; Peters, J. M. Dissociation of cohesin from chromosome arms and loss of arm cohesion during early mitosis depends on phosphorylation of SA2. *PLoS Biol* 3(3):e69; 2005.
29. Heidinger-Pauli, J. M.; Unal, E.; Guacci, V.; Koshland, D. The kleisin subunit of cohesin dictates damage-induced cohesion. *Mol Cell* 31(1):47-56; 2008.

30. Heidinger-Pauli, J. M.; Unal, E.; Koshland, D. Distinct targets of the Eco1 acetyltransferase modulate cohesion in S phase and in response to DNA damage. *Mol Cell* 34(3):311-321; 2009.
31. Hirata, Y.; Andoh, T.; Asahara, T.; Kikuchi, A. Yeast glycogen synthase kinase-3 activates Msn2p-dependent transcription of stress responsive genes. *Mol Biol Cell* 14(1):302-312; 2003.
32. Holt, L. J.; Krutchinsky, A. N.; Morgan, D. O. Positive feedback sharpens the anaphase switch. *Nature* 454(7202):353-357; 2008.
33. Holt, L. J.; Tuch, B. B.; Villen, J.; Johnson, A. D.; Gygi, S. P.; Morgan, D. O. Global analysis of Cdk1 substrate phosphorylation sites provides insights into evolution. *Science* 325(5948):1682-1686; 2009.
34. Hou, F.; Zou, H. Two human orthologues of Eco1/Ctf7 acetyltransferases are both required for proper sister-chromatid cohesion. *Mol Biol Cell* 16(8):3908-3918; 2005.
35. Ikui, A. E.; Rossio, V.; Schroeder, L.; Yoshida, S. A yeast GSK-3 kinase Mck1 promotes Cdc6 degradation to inhibit DNA re-replication. in submission; 2012.
36. Ivanov, D.; Schleiffer, A.; Eisenhaber, F.; Mechtler, K.; Haering, C. H.; Nasmyth, K. Eco1 is a novel acetyltransferase that can acetylate proteins involved in cohesion. *Curr Biol* 12(4):323-328; 2002.
37. Jackson, A. L.; Pahl, P. M.; Harrison, K.; Rosamond, J.; Sclafani, R. A. Cell cycle regulation of the yeast Cdc7 protein kinase by association with the Dbf4 protein. *Mol Cell Biol* 13(5):2899-2908; 1993.
38. Jonkers, W.; Rep, M. Lessons from fungal F-box proteins. *Eukaryot Cell* 8(5):677-695; 2009.

39. Katis, V. L.; Lipp, J. J.; Imre, R.; Bogdanova, A.; Okaz, E.; Habermann, B.; Mechtler, K.; Nasmyth, K.; Zachariae, W. Rec8 phosphorylation by casein kinase 1 and Cdc7-Dbf4 kinase regulates cohesin cleavage by separase during meiosis. *Dev Cell* 18(3):397-409; 2010.
40. Kihara, M.; Nakai, W.; Asano, S.; Suzuki, A.; Kitada, K.; Kawasaki, Y.; Johnston, L. H.; Sugino, A. Characterization of the yeast Cdc7p/Dbf4p complex purified from insect cells. Its protein kinase activity is regulated by Rad53p. *J Biol Chem* 275(45):35051-35062; 2000.
41. Kinoshita, E.; Kinoshita-Kikuta, E.; Takiyama, K.; Koike, T. Phosphate-binding tag, a new tool to visualize phosphorylated proteins. *Mol Cell Proteomics* 5(4):749-757; 2006.
42. Kishi, T.; Ikeda, A.; Nagao, R.; Koyama, N. The SCFCdc4 ubiquitin ligase regulates calcineurin signaling through degradation of phosphorylated Rcn1, an inhibitor of calcineurin. *Proc Natl Acad Sci U S A* 104(44):17418-17423; 2007.
43. Koivomagi, M.; Valk, E.; Venta, R.; Iofik, A.; Lepiku, M.; Balog, E. R.; Rubin, S. M.; Morgan, D. O.; Loog, M. Cascades of multisite phosphorylation control Sic1 destruction at the onset of S phase. *Nature* 480(7375):128-131; 2011.
44. Kominami, K.; Ochotorena, I.; Toda, T. Two F-box/WD-repeat proteins Pop1 and Pop2 form hetero- and homo-complexes together with cullin-1 in the fission yeast SCF (Skp1-Cullin-1-F-box) ubiquitin ligase. *Genes Cells* 3(11):721-735; 1998.
45. Koschwanez, J. H.; Foster, K. R.; Murray, A. W. Sucrose utilization in budding yeast as a model for the origin of undifferentiated multicellularity. *PLoS Biol* 9(8):e1001122; 2011.

46. Kosugi, S.; Hasebe, M.; Tomita, M.; Yanagawa, H. Systematic identification of cell cycle-dependent yeast nucleocytoplasmic shuttling proteins by prediction of composite motifs. *Proc Natl Acad Sci U S A* 106(25):10171-10176; 2009.
47. Kueng, S.; Hegemann, B.; Peters, B. H.; Lipp, J. J.; Schleiffer, A.; Mechtler, K.; Peters, J. M. Wapl controls the dynamic association of cohesin with chromatin. *Cell* 127(5):955-967; 2006.
48. Labib, K. How do Cdc7 and cyclin-dependent kinases trigger the initiation of chromosome replication in eukaryotic cells? *Genes Dev* 24(12):1208-1219; 2010.
49. Lafont, A. L.; Song, J.; Rankin, S. Sororin cooperates with the acetyltransferase Eco2 to ensure DNA replication-dependent sister chromatid cohesion. *Proc Natl Acad Sci U S A* 107(47):20364-20369; 2010.
50. Lee, J.; Moir, R. D.; McIntosh, K. B.; Willis, I. M. TOR signaling regulates ribosome and tRNA synthesis via LAMMER/Clk and GSK-3 family kinases. *Mol Cell* 45(6):836-843; 2012.
51. Lei, M.; Kawasaki, Y.; Young, M. R.; Kihara, M.; Sugino, A.; Tye, B. K. Mcm2 is a target of regulation by Cdc7-Dbf4 during the initiation of DNA synthesis. *Genes Dev* 11(24):3365-3374; 1997.
52. Lengronne, A.; McIntyre, J.; Katou, Y.; Kanoh, Y.; Hopfner, K. P.; Shirahige, K.; Uhlmann, F. Establishment of sister chromatid cohesion at the *S. cerevisiae* replication fork. *Mol Cell* 23(6):787-799; 2006.
53. Liu, Q.; Larsen, B.; Ricicova, M.; Orlicky, S.; Tekotte, H.; Tang, X.; Craig, K.; Quiring, A.; Le Bihan, T.; Hansen, C. and others. SCFCdc4 enables mating type

- switching in yeast by cyclin-dependent kinase-mediated elimination of the Ash1 transcriptional repressor. *Mol Cell Biol* 31(3):584-598; 2011.
54. Lo, H. C.; Kunz, R. C.; Chen, X.; Marullo, A.; Gygi, S. P.; Hollingsworth, N. M. Cdc7-Dbf4 is a gene-specific regulator of meiotic transcription in yeast. *Mol Cell Biol* 32(2):541-557; 2011.
55. Longtine, M. S.; McKenzie, A.; Demarini, D. J.; Shah, N. G.; Wach, A.; Brachat, A.; Philippsen, P.; Pringle, J. R. Additional modules for versatile and economical PCR-based gene deletion and modification in *Saccharomyces cerevisiae*. *Yeast* 14:953-961; 1998.
56. Loog, M.; Morgan, D. O. Cyclin specificity in the phosphorylation of cyclin-dependent kinase substrates. *Nature* 434:104-108; 2005.
57. Lopez-Mosqueda, J.; Maas, N. L.; Jonsson, Z. O.; Defazio-Eli, L. G.; Wohlschlegel, J.; Toczyski, D. P. Damage-induced phosphorylation of Sld3 is important to block late origin firing. *Nature* 467(7314):479-483; 2010.
58. Luedeke, M.; Linnert, C. M.; Hofer, M. D.; Surowy, H. M.; Rinckleb, A. E.; Hoegel, J.; Kuefer, R.; Rubin, M. A.; Vogel, W.; Maier, C. Predisposition for TMPRSS2-ERG fusion in prostate cancer by variants in DNA repair genes. *Cancer Epidemiol Biomarkers Prev* 18(11):3030-3035; 2009.
59. Lyons, N. A.; Morgan, D. O. Cdk1-dependent destruction of Eco1 prevents cohesion establishment after S phase. *Mol Cell* 42(3):378-389; 2011.
60. Marston, A. L. Meiosis: DDK is not just for replication. *Curr Biol* 19(2):R74-76; 2009.

61. Masai, H.; Matsui, E.; You, Z.; Ishimi, Y.; Tamai, K.; Arai, K. Human Cdc7-related kinase complex. In vitro phosphorylation of MCM by concerted actions of Cdks and Cdc7 and that of a critical threonine residue of Cdc7 by Cdks. *J Biol Chem* 275(37):29042-29052; 2000.
62. Matos, J.; Lipp, J. J.; Bogdanova, A.; Guillot, S.; Okaz, E.; Junqueira, M.; Shevchenko, A.; Zachariae, W. Dbf4-dependent CDC7 kinase links DNA replication to the segregation of homologous chromosomes in meiosis I. *Cell* 135(4):662-678; 2008.
63. Maynard Smith, J.; Szathmáry, E. The major transitions in evolution. Oxford ; New York: W.H. Freeman Spektrum; 1995.
64. McDonald, W. H.; Tabb, D. L.; Sadygov, R. G.; MacCoss, M. J.; Venable, J.; Graumann, J.; Johnson, J. R.; Cociorva, D.; Yates, J. R., 3rd. MS1, MS2, and SQT- three unified, compact, and easily parsed file formats for the storage of shotgun proteomic spectra and identifications. *Rapid Commun Mass Spectrom* 18(18):2162-2168; 2004.
65. McGuinness, B. E.; Hirota, T.; Kudo, N. R.; Peters, J. M.; Nasmyth, K. Shugoshin prevents dissociation of cohesin from centromeres during mitosis in vertebrate cells. *PLoS Biol* 3(3):e86; 2005.
66. Michaelis, C.; Ciosk, R.; Nasmyth, K. Cohesins: chromosomal proteins that prevent premature separation of sister chromatids. *Cell* 91(1):35-45; 1997.
67. Mizunuma, M.; Hirata, D.; Miyaoka, R.; Miyakawa, T. GSK-3 kinase Mck1 and calcineurin coordinately mediate Hsl1 down-regulation by Ca²⁺ in budding yeast. *EMBO J* 20(5):1074-1085; 2001.

68. Mok, J.; Kim, P. M.; Lam, H. Y.; Piccirillo, S.; Zhou, X.; Jeschke, G. R.; Sheridan, D. L.; Parker, S. A.; Desai, V.; Jwa, M. and others. Deciphering protein kinase specificity through large-scale analysis of yeast phosphorylation site motifs. *Sci Signal* 3(109):ra12; 2010.
69. Moldovan, G. L.; Pfander, B.; Jentsch, S. PCNA controls establishment of sister chromatid cohesion during S phase. *Mol Cell* 23(5):723-732; 2006.
70. Morgan, D. O. *The Cell Cycle: Principles of Control*. London: New Science Press; 2007.
71. Nash, P.; Tang, X.; Orlicky, S.; Chen, Q.; Gertler, F. B.; Mendenhall, M. D.; Sicheri, F.; Pawson, T.; Tyers, M. Multisite phosphorylation of a CDK inhibitor sets a threshold for the onset of DNA replication. *Nature* 414(6863):514-521; 2001.
72. Nash, R.; Tokiwa, G.; Anand, S.; Erickson, K.; Futcher, A. B. The WHI1+ gene of *Saccharomyces cerevisiae* tethers cell division to cell size and is a cyclin homolog. *EMBO J.* 7(13):4335-4346; 1988.
73. Nasmyth, K.; Haering, C. H. Cohesin: its roles and mechanisms. *Annu Rev Genet* 43:525-558; 2009.
74. Neigeborn, L.; Mitchell, A. P. The yeast MCK1 gene encodes a protein kinase homolog that activates early meiotic gene expression. *Genes Dev* 5(4):533-548; 1991.
75. Olsen, J. V.; Vermeulen, M.; Santamaria, A.; Kumar, C.; Miller, M. L.; Jensen, L. J.; Gnäd, F.; Cox, J.; Jensen, T. S.; Nigg, E. A. and others. Quantitative phosphoproteomics reveals widespread full phosphorylation site occupancy during mitosis. *Sci Signal* 3(104):ra3; 2010.

76. Onn, I.; Heidinger-Pauli, J. M.; Guacci, V.; Unal, E.; Koshland, D. E. Sister chromatid cohesion: a simple concept with a complex reality. *Annu Rev Cell Dev Biol* 24:105-129; 2008.
77. Oshiro, G.; Owens, J. C.; Shellman, Y.; Sclafani, R. A.; Li, J. J. Cell cycle control of Cdc7p kinase activity through regulation of Dbf4p stability. *Mol Cell Biol* 19(7):4888-4896; 1999.
78. Petroski, M. D.; Deshaies, R. J. Function and regulation of cullin-RING ubiquitin ligases. *Nat Rev Mol Cell Biol* 6(1):9-20; 2005.
79. Pries, R.; Bomeke, K.; Irniger, S.; Grundmann, O.; Braus, G. H. Amino acid-dependent Gcn4p stability regulation occurs exclusively in the yeast nucleus. *Eukaryot Cell* 1(5):663-672; 2002.
80. Randell, J. C.; Fan, A.; Chan, C.; Francis, L. I.; Heller, R. C.; Galani, K.; Bell, S. P. Mec1 is one of multiple kinases that prime the Mcm2-7 helicase for phosphorylation by Cdc7. *Mol Cell* 40(3):353-363; 2010.
81. Ratcliff, W. C.; Denison, R. F.; Borrello, M.; Travisano, M. Experimental evolution of multicellularity. *Proc Natl Acad Sci U S A* 109(5):1595-1600; 2012.
82. Rohner, S.; Gasser, S. M.; Meister, P. Modules for cloning-free chromatin tagging in *Saccharomyces cerevisiae*. *Yeast* 25(3):235-239; 2008.
83. Rolef Ben-Shahar, T.; Heeger, S.; Lehane, C.; East, P.; Flynn, H.; Skehel, M.; Uhlmann, F. Eco1-dependent cohesin acetylation during establishment of sister chromatid cohesion. *Science* 321(5888):563-566; 2008.
84. Rowland, B. D.; Roig, M. B.; Nishino, T.; Kurze, A.; Uluocak, P.; Mishra, A.; Beckouet, F.; Underwood, P.; Metson, J.; Imre, R. and others. Building sister

- chromatid cohesion: smc3 acetylation counteracts an antiestablishment activity. *Mol Cell* 33(6):763-774; 2009.
85. Ryu, B.; Kim, D. S.; Deluca, A. M.; Alani, R. M. Comprehensive expression profiling of tumor cell lines identifies molecular signatures of melanoma progression. *PLoS One* 2(7):e594; 2007.
86. Santocanale, C.; Diffley, J. F. A Mec1- and Rad53-dependent checkpoint controls late-firing origins of DNA replication. *Nature* 395(6702):615-618; 1998.
87. Sasanuma, H.; Hirota, K.; Fukuda, T.; Kakusho, N.; Kugou, K.; Kawasaki, Y.; Shibata, T.; Masai, H.; Ohta, K. Cdc7-dependent phosphorylation of Mer2 facilitates initiation of yeast meiotic recombination. *Genes Dev* 22(3):398-410; 2008.
88. Schroeder, M. J.; Shabanowitz, J.; Schwartz, J. C.; Hunt, D. F.; Coon, J. J. A neutral loss activation method for improved phosphopeptide sequence analysis by quadrupole ion trap mass spectrometry. *Anal Chem* 76(13):3590-3598; 2004.
89. Shero, J. H.; Hieter, P. A suppressor of a centromere DNA mutation encodes a putative protein kinase (MCK1). *Genes Dev* 5(4):549-560; 1991.
90. Sjogren, C.; Nasmyth, K. Sister chromatid cohesion is required for postreplicative double-strand break repair in *Saccharomyces cerevisiae*. *Curr Biol* 11(12):991-995; 2001.
91. Skibbens, R. V.; Corson, L. B.; Koshland, D.; Hieter, P. Ctf7p is essential for sister chromatid cohesion and links mitotic chromosome structure to the DNA replication machinery. *Genes Dev* 13(3):307-319; 1999.
92. Snead, J. L.; Sullivan, M.; Lowery, D. M.; Cohen, M. S.; Zhang, C.; Randle, D. H.; Taunton, J.; Yaffe, M. B.; Morgan, D. O.; Shokat, K. M. A coupled chemical-genetic

- and bioinformatic approach to Polo-like kinase pathway exploration. *Chem Biol* 14(11):1261-1272; 2007.
93. Spellman, P. T.; Sherlock, G.; Zhang, M. Q.; Iyer, V. R.; Anders, K.; Eisen, M. B.; Brown, P. O.; Botstein, D.; Futcher, B. Comprehensive identification of cell cycle-regulated genes of the yeast *Saccharomyces cerevisiae* by microarray hybridization. *Mol. Biol. Cell* 9(12):3273-3297; 1998.
94. Straight, A. F.; Marshall, W. F.; Sedat, J. W.; Murray, A. W. Mitosis in living budding yeast: anaphase A but no metaphase plate. *Science* 277(5325):574-578; 1997.
95. Strom, L.; Karlsson, C.; Lindroos, H. B.; Wedahl, S.; Katou, Y.; Shirahige, K.; Sjogren, C. Postreplicative formation of cohesin is required for repair and induced by a single DNA break. *Science* 317(5835):242-245; 2007.
96. Strom, L.; Lindroos, H. B.; Shirahige, K.; Sjogren, C. Postreplicative recruitment of cohesin to double-strand breaks is required for DNA repair. *Mol Cell* 16(6):1003-1015; 2004.
97. Sullivan, M.; Holt, L.; Morgan, D. O. Cyclin-specific control of ribosomal DNA segregation. *Mol Cell Biol* 28(17):5328-5336; 2008.
98. Sumara, I.; Vorlaufer, E.; Gieffers, C.; Peters, B. H.; Peters, J. M. Characterization of vertebrate cohesin complexes and their regulation in prophase. *J Cell Biol* 151(4):749-762; 2000.
99. Sumara, I.; Vorlaufer, E.; Stukenberg, P. T.; Kelm, O.; Redemann, N.; Nigg, E. A.; Peters, J. M. The dissociation of cohesin from chromosomes in prophase is regulated by Polo-like kinase. *Mol Cell* 9(3):515-525.; 2002.

100. Sutani, T.; Kawaguchi, T.; Kanno, R.; Itoh, T.; Shirahige, K. Budding yeast Wpl1(Rad61)-Pds5 complex counteracts sister chromatid cohesion-establishing reaction. *Curr Biol* 19(6):492-497; 2009.
101. Tabb, D. L.; McDonald, W. H.; Yates, J. R., 3rd. DTASelect and Contrast: tools for assembling and comparing protein identifications from shotgun proteomics. *J Proteome Res* 1(1):21-26; 2002.
102. Takahashi, T. S.; Basu, A.; Bermudez, V.; Hurwitz, J.; Walter, J. C. Cdc7-Drf1 kinase links chromosome cohesion to the initiation of DNA replication in *Xenopus* egg extracts. *Genes Dev* 22(14):1894-1905; 2008.
103. Takeda, T.; Ogino, K.; Tatebayashi, K.; Ikeda, H.; Arai, K.; Masai, H. Regulation of initiation of S phase, replication checkpoint signaling, and maintenance of mitotic chromosome structures during S phase by Hsk1 kinase in the fission yeast. *Mol Biol Cell* 12(5):1257-1274; 2001.
104. Tanaka, T.; Fuchs, J.; Loidl, J.; Nasmyth, K. Cohesin ensures bipolar attachment of microtubules to sister centromeres and resists their precocious separation. *Nat Cell Biol* 2(8):492-499; 2000.
105. Tang, X.; Orlicky, S.; Lin, Z.; Willems, A.; Neculai, D.; Ceccarelli, D.; Mercurio, F.; Shilton, B. H.; Sicheri, F.; Tyers, M. Suprafacial orientation of the SCFCdc4 dimer accommodates multiple geometries for substrate ubiquitination. *Cell* 129(6):1165-1176; 2007.
106. Tang, X.; Orlicky, S.; Mittag, T.; Csizmok, V.; Pawson, T.; Forman-Kay, J. D.; Sicheri, F.; Tyers, M. Composite low affinity interactions dictate recognition of the

- cyclin-dependent kinase inhibitor Sic1 by the SCFCdc4 ubiquitin ligase. *Proc Natl Acad Sci U S A* 109(9):3287-3292; 2012.
107. Thims, L. *The Human Molecule*: Lulu; 2008.
108. Toth, A.; Ciosk, R.; Uhlmann, F.; Galova, M.; Schleiffer, A.; Nasmyth, K. Yeast cohesin complex requires a conserved protein, Eco1p(Ctf7), to establish cohesion between sister chromatids during DNA replication. *Genes Dev* 13(3):320-333; 1999.
109. Trcek, T.; Larson, D. R.; Moldon, A.; Query, C. C.; Singer, R. H. Single-molecule mRNA decay measurements reveal promoter-regulated mRNA stability in yeast. *Cell* 147(7):1484-1497; 2011.
110. Ubersax, J. A.; Woodbury, E. L.; Quang, P. N.; Paraz, M.; Blethrow, J. D.; Shah, K.; Shokat, K. M.; Morgan, D. O. Targets of the cyclin-dependent kinase Cdk1. *Nature* 425(6960):859-864; 2003.
111. Uhlmann, F. A matter of choice: the establishment of sister chromatid cohesion. *EMBO Rep* 10(10):1095-1102; 2009.
112. Uhlmann, F.; Nasmyth, K. Cohesion between sister chromatids must be established during DNA replication. *Curr Biol* 8(20):1095-1101; 1998.
113. Uhlmann, F.; Wernic, D.; Poupart, M. A.; Koonin, E. V.; Nasmyth, K. Cleavage of cohesin by the CD clan protease separin triggers anaphase in yeast. *Cell* 103(3):375-386; 2000.
114. Unal, E.; Arbel-Eden, A.; Sattler, U.; Shroff, R.; Lichten, M.; Haber, J. E.; Koshland, D. DNA damage response pathway uses histone modification to assemble a double-strand break-specific cohesin domain. *Mol Cell* 16(6):991-1002; 2004.

115. Unal, E.; Heidinger-Pauli, J. M.; Kim, W.; Guacci, V.; Onn, I.; Gygi, S. P.; Koshland, D. E. A molecular determinant for the establishment of sister chromatid cohesion. *Science* 321(5888):566-569; 2008.
116. Unal, E.; Heidinger-Pauli, J. M.; Koshland, D. DNA double-strand breaks trigger genome-wide sister-chromatid cohesion through Eco1 (Ctf7). *Science* 317(5835):245-248; 2007.
117. Waizenegger, I. C.; Hauf, S.; Meinke, A.; Peters, J. M. Two distinct pathways remove mammalian cohesin from chromosome arms in prophase and from centromeres in anaphase. *Cell* 103(3):399-410; 2000.
118. Wan, L.; Niu, H.; Futcher, B.; Zhang, C.; Shokat, K. M.; Boulton, S. J.; Hollingsworth, N. M. Cdc28-Clb5 (CDK-S) and Cdc7-Dbf4 (DDK) collaborate to initiate meiotic recombination in yeast. *Genes Dev* 22(3):386-397; 2008.
119. Weinreich, M.; Stillman, B. Cdc7p-Dbf4p kinase binds to chromatin during S phase and is regulated by both the APC and the RAD53 checkpoint pathway. *EMBO J* 18(19):5334-5346; 1999.
120. Welcker, M.; Clurman, B. E. FBW7 ubiquitin ligase: a tumour suppressor at the crossroads of cell division, growth and differentiation. *Nat Rev Cancer* 8(2):83-93; 2008.
121. Welcker, M.; Clurman, B. E. Fbw7/hCDC4 dimerization regulates its substrate interactions. *Cell Div* 2:7; 2007.
122. Willems, A. R.; Schwab, M.; Tyers, M. A hitchhiker's guide to the cullin ubiquitin ligases: SCF and its kin. *Biochim Biophys Acta* 1695(1-3):133-170; 2004.

123. Wolters, D. A.; Washburn, M. P.; Yates, J. R., 3rd. An automated multidimensional protein identification technology for shotgun proteomics. *Anal Chem* 73(23):5683-5690; 2001.
124. Xu, C.; Kim, N. G.; Gumbiner, B. M. Regulation of protein stability by GSK3 mediated phosphorylation. *Cell Cycle* 8(24):4032-4039; 2009.
125. Xu, T.; Venable, J. D.; Park, S. K.; Cociorva, D.; Lu, B.; Liao, L.; Wohlschlegel, J.; Hewel, J.; Yates, J. R., 3rd. ProLuCID, a fast and sensitive tandem mass spectrometry-based protein identification program. *Mol Cell Proteomics* 5(10):S174; 2006.
126. Yu, H. Cdc20: a WD40 activator for a cell cycle degradation machine. *Mol Cell* 27(1):3-16; 2007.
127. Zegerman, P.; Diffley, J. F. Checkpoint-dependent inhibition of DNA replication initiation by Sld3 and Dbf4 phosphorylation. *Nature* 467(7314):474-478; 2010.
128. Zhang, J.; Shi, X.; Li, Y.; Kim, B. J.; Jia, J.; Huang, Z.; Yang, T.; Fu, X.; Jung, S. Y.; Wang, Y. and others. Acetylation of Smc3 by Eco1 is required for S phase sister chromatid cohesion in both human and yeast. *Mol Cell* 31(1):143-151; 2008.

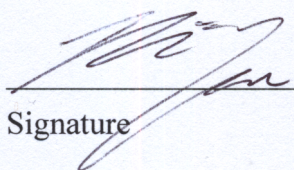
Publishing Agreement

It is the policy of the University to encourage the distribution of all theses, dissertations, and manuscripts. Copies of all UCSF theses, dissertations, and manuscripts will be routed to the library via the Graduate Division. The library will make all theses, dissertations, and manuscripts accessible to the public and will preserve these to the best of their abilities, in perpetuity.

Please sign the following statement:

I hereby grant permission to the Graduate Division of the University of California, San Francisco to release copies of my thesis, dissertation, or manuscript to the Campus Library to provide access and preservation, in whole or in part, in perpetuity.

Nicholas A. Lyons

Author

Signature9/11/12

Date